34e jaargang 2012 nummer 2 issn 1381 - 4842

TIJDSCHRIFT VOOR NUCLEAIRE GENEESKUNDE

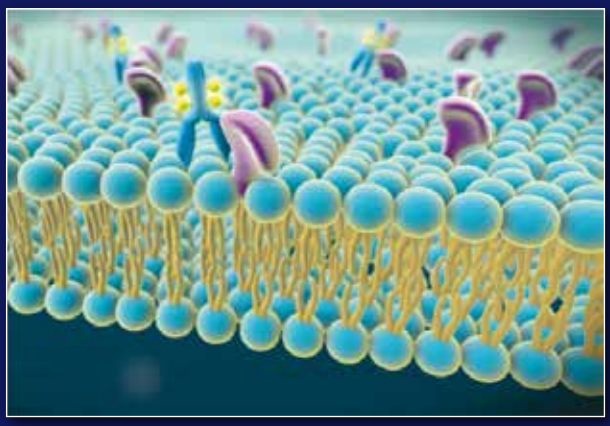

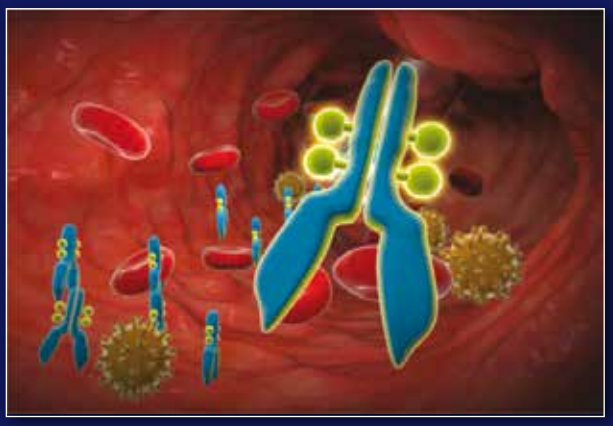

De ORAMED studie

^{226}Ra in een horloge

Radioembolisatie met ^{90}Y-microsferen

COVIDIEN

positive results for life™

Octreoscan™

Your reliable diagnostic tool for diagnosis and staging of Neuro Endocrine Tumours

Experience the impact on your clinical patient management

- When a primary has been resected, SSRS may be indicated for follow up (grade D)[1]
- For assessing secondaries, SSRS is the most sensitive modality (grade B)[1]

1) Guidelines for the management of gastroenteropancreatic neuroendocrine (including carcinoid) tumours, J.K. Ramage et al, UKNET work for neuroendocrine tumours, GUT 2005; 54 Suppl IV:iv1-iv16

For specific prescribing information of your country consult the local COVIDIEN office or its representative.

MALLINCKRODT MEDICAL BV

a Covidien company

Westerduinweg 3

1755 ZG Petten, The Netherlands

Telephone +31(0) 224 567890

Fax +31(0) 224 567008

E-mail info.nucleair@covidien.com

Trade name of the medicinal product: OctreoScan™ | **Qualitative and quantitative composition:** OctreoScan™ is supplied as two vials which cannot be used separately. 1 vial 4920/A with 1.1 ml solution contains at activity reference time: (111)In) Indium(III)chloride 122 MBq 1 vial 4920/B contains: Pentetreotide 10 µg. | **Indications:** 111In-pentetreotide specifically binds to receptors for somatostatin. OctreoScan™ is indicated for use as adjunct in the diagnosis and management of receptor bearing gastro-entero-pancreatic neuroendocrine (GEP) tumours and carcinoid tumours, by aiding in their localisation. Tumours which do not bear receptors will not be visualised. | **Posology and method of administration:** The dose for planar scintigraphy is 110 MBq in one single intravenous injection. Careful administration is necessary to avoid paravasal deposition of activity. For single photon emission tomography the dose depends on the available equipment. In general, an activity dose of 110 to 220 MBq in one single intravenous injection should be sufficient. No special dosage regimen for elderly patients is required. There is limited experience on administrations in paediatric patients, but the activity to be administered in a child should be a fraction of the adult activity calculated from the bodyweight. | **Contraindications:** No specific contra-indications have been identified. Hypersensitivity to the active substance or to any of the excipients. | **Special warnings and special precautions for use:** Because of the potential hazard of the ionising radiation 111In-pentetreotide should not be used in children under 18 years of age, unless the value of the expected clinical information is considered to outweigh the possible damage from radiation. Administration of a laxative is necessary in patients not suffering from diarrhoea, to differentiate stationary activity accumulations in lesions in, or adjacent to, the intestinal tract from moving accumulations in the bowel contents. In patients with significant renal failure administration of 111In-pentetreotide is not advisable because the reduced or absent function of the principal route of excretion will lead to delivery of an increased radiation dose. Positive scintigraphy with 111In-pentetreotide reflects the presence of an increased density of tissue somatostatin receptors rather than a malignant disease. Furthermore positive uptake is not specific for GEP- and carcinoid- tumours. Positive scintigraphic results require evaluation of the possibility that another disease, characterised by high local somatostatin receptor concentrations, may be present. An increase in somatostatin receptor density can also occur in the following pathological conditions: tumours arising from tissue embryologically derived from the neural crest, (paragangliomas, medullary thyroid carcinomas, neuroblastomas, pheochromocytomas), tumours of the pituitary gland, endocrine neoplasms of the lungs (small-cell carcinoma), meningiomas, mamma-carcinomas, lympho-proliferative disease (Hodgkin's disease, non-Hodgkin lymphomas), and the possibility of uptake in areas of lymphocyte concentrations (subacute inflammations) must be considered. Radiopharmaceutical agents should only be used by qualified personnel with the appropriate government authorization for the use and manipulation of radionuclides. | **Interaction with other medicaments and other forms of interaction:** No drug interactions have been reported to date. | **Effects on the ability to drive and use machines:** 111In-pentetreotide does not affect the ability to drive or to use machines. | **Undesirable effects:** Adverse effects attributable to the administration of OctreoScan™ are uncommon. Specific effects have not been observed. The symptoms reported are suggestive of vasovagal reactions or of anaphylactoid drug effects. **MANUFACTURED AND RELEASED BY:** Mallinckrodt Medical B.V., Westerduinweg 3, 1755 LE Petten, The Netherlands **DATE OF PREPARATION:** 17-Feb-2010

INHOUD

VAN DE REDACTIE

Stralenbescherming en stralenbelasting

Een patiënt komt bij u omdat hij last heeft van een pijnlijke rode huid van onder andere zijn handen, na het schoonmaken van twee horloges waarvan de wijzers 'lichtgevend waren gemaakt' met ^{226}Ra-houdende verf. De patiënt spreekt zijn zorg uit dat de radioactiviteit afkomstig van het radium zijn klachten zou hebben veroorzaakt. Wat zou u doen als deze, of een vergelijkbare, situatie zich voordoet? Op pagina 880 kunt u lezen wat collega Dam heeft gedaan.

In deze uitgave van ons Tijdschrift voor Nucleaire Geneeskunde is veel aandacht voor stralenbelasting en stralenbescherming. Vooral de handen van de medewerkers in een hotlab staan frequent bloot aan ioniserende straling. Collega Vanhavere gaat uitvoerig in op de resultaten van het ambitieuze ORAMED project. In dit project, dat in zeven Europese landen is uitgevoerd bij 139 deelnemers in 35 centra, is de handdosis voor ^{99m}Tc, ^{18}F en ^{90}Y nauwkeurig vastgelegd. De uitkomsten van dit project geven handvatten om de dosis op de handen te verminderen zonder dat de kwaliteit van de productie in gevaar komt.
We weten allen dat we verstandig moeten omgaan met ioniserende straling. Enerzijds leidt gebruik ervan tot verbeterde diagnostiek en adequatere behandeling van patiënten, anderzijds kan het juist leiden tot verhoogde gezondheidsrisico's. Het doel van regelgeving rondom het gebruik van ioniserende straling is om de bevolking en werkers in de gezondheidszorg te beschermen tegen de potentiële risico's ervan. In de Nederlandse wetgeving lijken enkele veiligheidslimieten erg streng geformuleerd te zijn. Collega van den Berg vraagt zich af of dit wel zo wenselijk is.

In Utrecht is uitgebreide ervaring opgedaan met radioembolisatie van niet-resectabele primaire of metastatische levermaligniteit. Collega Lam geeft een praktische uiteenzetting van hoe radioembolisatie met ^{90}Y-microsferen het best uitgevoerd kan worden.
Verder aandacht voor radionuclidentherapie met ^{177}Lu-gelabelde liganden. Dit is een belangrijke ontwikkeling in de nucleaire geneeskunde en in Rotterdam is op dit onderzoeksgebied pionierswerk verricht. Zo hebben vele patiënten met een inoperabele of gemetastaseerde neuroendocriene tumor al kunnen profiteren van een behandeling met ^{177}Lu-DOTATATE. Collega de Vries brengt ons op de hoogte van de manieren waarop dit radionuclide succesvol geproduceerd kan worden.

Jan Booij
Hoofdredacteur

Voorplaat: het mechanisme achter het gebruik van beeldvorming met antilichamen, en een ^{89}Zr-trastuzumab PET scan vervaardigd bij een patiënte bekend met HER2 positief, cerebraal gemetastaseerd mammacarcinoom (met dank aan Dr. T.H. Oude Munnink, afdeling Medische Oncologie, Universitair Medisch Centrum Groningen).

Could cleaning of watches with radium painted dials cause erythema?

Drs. A.J. Dam[1], Drs. A.A. Becht[1], Drs. F. Celik[2]

[1] *Department of Medical Technology, Gelre ziekenhuizen, Apeldoorn, The Netherlands*
[2] *Department of Nuclear Medicine, Deventer ziekenhuis, Deventer, The Netherlands*

Abstract

Dam AJ, Becht AA, Celik F. Could cleaning of watches with radium painted dials cause erythema? A patient was referred to the nuclear medicine physician and medical physicist with continuing intermittent complaints of painful and red skin on his hands, arms and nose. The complaints started two weeks after cleaning two watches with radium painted dial and pointers. In order to evaluate potential skin dose contamination due to cleaning a skin dose evaluation is performed, using equipment that is commonly available at a nuclear medicine department. To evaluate the findings of the two radium dials of the patient, some more radium dials were added in this study. In this study twenty different radium dials were used to measure the activity and to calculate the potential hand dose. The maximum hand dose of the patient using the worst-case assumptions was a factor 34 lower than the threshold dose for erythema due to radiation. So, our study showed that radioactive contamination due to cleaning of radium dials cannot lead to erythema. **Tijdschr Nucl Geneesk 2012; 34(2):880-882**

Introduction

A 55-year old male patient was referred to the nuclear medicine physician and medical physicist with intermittent complaints of painful and red skin on his hands, arms and nose. The complaints started two weeks after cleaning two watches containing luminescent painted pointers and dial. Our first contact with the patient was three months after he cleaned his watches without wearing gloves. At that moment the red skin was not visible. However the patient still complained about intermittent painful and red skin on his arms, hands and nose. The patient was very anxious to know whether his complaints were caused by a radium component of the luminescent paint, especially because he had removed the plastic cover of the watches.
In order to answer his question whether his complaints were caused by the radium component of the luminescent paint we performed a skin dose evaluation by using a contamination scintillation detector which is commonly available at a nuclear medicine department.
Luminescent paint containing radioactive isotopes was used until 1950 on dials because of the glowing effect of this paint. Radium-226 (^{226}Ra) with a half life of about 2600 years was a commonly used radioactive isotope in these paints and is a combined alpha, beta and gamma emitter. Radio luminescent paint exists commonly of zinc sulphide mixed with ^{226}Ra. ^{226}Radium itself is not fluorescent, however the alpha particles (due to the decay of ^{226}Ra) interact with zinc sulfide in the paint and therefore emit visible light which glows (figure 1) until the radioactive isotope has decayed. Irradiance of the skin causes excitations and ionizations in atoms and molecules of the skin, at least for a period of time. The epidermis is made of several layers of which the top layer contains dead keratin cells and the deepest layer contains a single layer of basophilic keratinocytes cells who continually divide. The International Commission on Radiological Protection (ICRP) recommends for radiological protection purposes the evaluation of skin dose to the cells of the basal layer. The depth of the basal layer is used in radiological protection as skin thickness. The human body contains a range of skin thickness of 0.02 to 1 mm over all body sites (1). The ICRP recommends for dose calculations to use a skin thickness of 0.07 mm not supposing subcutaneous contamination due to penetration of the skin (2). Acute exposure of radiation with a skin dose of 6 to 8 Gy can lead to erythema, which means reddening of the skin due to inflammatory or immunologic processes. Radiation exposure of more than 50 Gy can even lead to necrosis (3). These effects are all deterministic.
The objective of this article is to answer the following question: could radioactive contamination caused by cleaning radium painted dials and pointers (from now on briefly called radium dials) cause erythema?

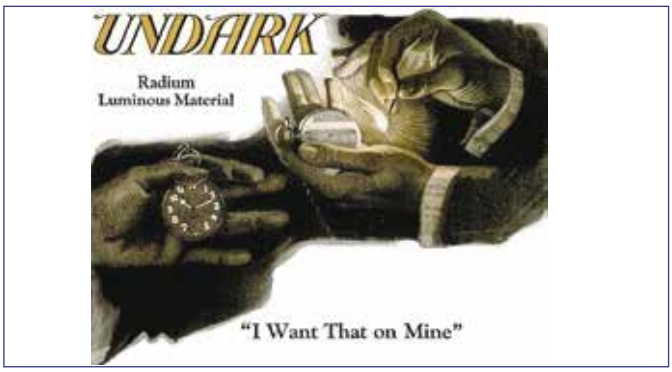

Figure 1. Radium watch advertisement during the years 1910-1920 (5).

Methods

A skin dose evaluation is performed in order to evaluate the potential skin contamination. Measurements are performed to examine the activity of the patient's radium dials, using a CoMo-170 contamination scintillation detector (MED Nuklear-Medizintechnik) at the surface of the radium dial.

In order to calculate the activity the background β/γ counts ($R_{background}$) are subtracted from total β/γ counts (R_{total}) and are compensated for the measurement efficiency factor. The measurement efficiency factor for ^{226}Ra was not mentioned in the manual of the CoMo-170, therefore we calibrated the CoMo-170 with a ^{226}Ra calibration source with a known activity. We found a measurement efficiency factor (η) of 0.86 for the β/γ canal of the CoMo-170, thereby the activity of the watches can be calculated using formula 1:

$$^{1)}activity\ (kBq) = (R_{total} - R_{background}) / \eta = (R_{netto}) / \eta$$

Subsequently, dose calculations are performed to define the worst-case skin dose due to external radiation and skin contamination. The ICRP recommends for non-uniform exposures that the dose should be averaged over the most highly exposed area of 1 cm^2 (2). Using the contamination skin dose constant, i.e. 2.16 mSv.h^{-1}/(kBq/cm^2) for ^{226}Ra including decay products (4), and an assumption of the contamination time, the hand dose can be calculated using formula 2:

$$^{2)}hand\ dose(mSv) = activity\ (kBq) \times 2.16\ mSv.h^{-1}/(kBq/cm^2) \times time\ (h)$$

In order to evaluate our findings and to find out whether or not the activity on the patient's dials was relatively high or low we have collected more watches that contained radium on dials and pointers and added these in our study. To calculate the potential hand dose (mSv) due to potential cleaning of these watches an extra factor 0.5 is added to formula 2, because of a worst-case fifty percent "wipe-off" cleaning factor.

Results

In this study twenty different radium dials were used to measure the activity and to calculate the (potential) hand dose, including the two radium dials of the patient (figure 2).

Table 1 shows the measured R_{netto} for the twenty radium dials, the activity and the calculated skin contamination. The activity of the radium dials ranged from 0.030 to 1.077 kBq with an average

Table 1. Measured counts, activity and calculated (potential) hand dose of the radium dials.

dial	name	R_{netto} (cps)	activity (kBq)	(potential) hand dose (mSv)**
1*	Certina	537	0.624	64.7
2*	Wittnauer	926	1.077	111
3	Remova, Ancre17rubis	169	0.196	10.2
4	Mentor, 4 Jewels	55	0.064	3.32
5	Andre Gourneles	61	0.070	3.63
6	3Entra, Ancre	136	0.158	8.19
7	No Name	113	0.131	6.79
8	Prisma, in cabloc	26	0.030	1.56
9	CiTis, 17 Jewels	187	0.217	11.3
10	Borea, 15 Jewels	69	0.080	4.15
11	Endura	51	0.059	3.06
12	Endura, 21 Rubis	135	0.156	8.09
13	Libell, 21 Jewels	29	0.034	1.76
14	Ancre, Gaupille	660	0.767	39.8
15	Milca, 17 Jewels	745	0.866	44.9
16	Ardito, Andre, 17 Jewels	908	1.056	54.7
17	Kienzle	505	0.587	30.4
18	Kienzle	925	1.076	55.8
19	Ancre, Goupilles	210	0.244	12.7
20	Vito, Ancre, 15 Jewels	750	0.872	45.2

** The two radium dials of the patient (after cleaning by the patient).*
*** The hand dose (in mSv) of the patient due to cleaning of his radium dials (dial 1 and 2) is calculated by the following formula: activity (kBq) x 2.16 mSv.h^{-1} /(kBq/cm^2) x time (h). To calculate the potential hand dose due to potential cleaning of the eighteen other radium dials (dial 3-20) an extra factor 0.5 is added in the formula, because of potential fifty percent "wipe-off" cleaning factor.*

Figure 2. One of the radium dials of the patient, without the plastic cover.

of 0.418 kBq. The activity of the patient's radium dials showed the same order of magnitude as the eighteen other radium dials included in this study.

The following worst-case assumptions were used to calculate the potential hand dose: a contamination time of 48 hours of ^{226}Ra (no thorough washing of the skin during 48 hours) and a hand exposure area of 1 cm^2 (according to ICRP). The (potential) hand dose ranged from 1.56 mSv to 112 mSv with an average of 26.1 mSv. The ratio between the maximum hand dose is minimally a factor 53 lower (6 Gy / 112 mSv) than the threshold dose for erythema due to radiation.

It is likely that the activity of the radium dials of the patient was higher than our measured activity, because the dials were included in our study *after* the patient had cleaned the dials. To calculate the hand dose in worst-case situation we also assumed a ^{226}Ra "wipe off" cleaning factor of 50%, so we calculated a total hand dose of 176 mSv for the patient. The maximum hand dose of the patient, based on the Certina and the Wittnauer, using all the worst-case assumptions is a factor 34 lower (6 Gy / 176 mSv) than the threshold dose for erythema due to radiation.

Discussion

To calculate the hand dose several assumptions were made, such as the ^{226}Ra contamination time of 48 h, the skin contamination area of 1 cm^2 and the wipe-off cleaning factor of 50%. We would like to emphasize that using all these assumptions the calculated skin doses discussed in this study are for a worst-case scenario.

Our study showed that radioactive contamination due to cleaning of radium dials cannot lead to erythema. However, seen from an ALARA principle, it is wise to wear gloves during cleaning watches that possibly contain radioactive luminescent paint.

In this study it is possible to compare sievert and gray directly because the range of the alpha particles is approximately 30 µm which is much less than the nominal skin thickness (6).

Therefore the radiation weight factor of β/γ radiation can be used (radiation weight factor β/γ radiation = 1).

Gamma-ray spectrometry is performed on three radium dials, including the Certina-watch of the patient, in order to check the presence of ^{226}Ra (and decay products) and as an alternative method for estimating the activity. The results of the gamma-ray spectrometry showed the same magnitude as the measurements with the CoMo-170 contamination scintillation detector. So, using equipment that is commonly available at a nuclear medicine department has appeared to be a practical tool not only for measurements of skin contamination but also for calculating a worst-case hand dose.

We discussed our results with the patient and could convince and reassure him that his complaints could not be caused by cleaning his two radium dials. Important in the communication with the patient appeared to be the possibility to perform a measurement with the CoMo-170 himself, showing only background activity. The patient was referred back to his general practitioner for further evaluation of his complaints.

Conclusion

Our study showed that radioactive contamination due to cleaning of radium dials cannot lead to erythema.

Acknowledgements

Authors thank Andre Bloot (senior radiation expert, Delft) for using the ^{226}Ra calibration source and the useful discussions. Furthermore, we would like to thank Bas Vianen (radiation protection expert, Amsterdam), Folkert Draaisma (senior radiation expert, Petten) and Nanno Schreuder (radiopharmacist, Zwolle) for helpful suggestions. Finally, we thank Melgert Spaander for letting us study a part of his watch collection.

References

1. ICRP. International Commission on Radiological Protection, Publication 23. Reference man: anatomical, physiological and metabolic characteristics, 1975
2. ICRP. International Commission on Radiological Protection, Publication 103. The 2007 recommendations of the ICRP, 2007
3. Bos AJJ, Draaisma FS, Okx WJC, Rasmussen CE. *Inleiding tot de stralingshygiëne.* Elsevier, 2007. ISBN: 9789012119054;112
4. Keverling Buisman AS. *Handboek Radionucliden.* BetaText, 2007. ISBN10: 9075541104;230
5. Undark Advertisement. I want that on mine. Popular Sciences.1920;96(5):153
6. Keverling Buisman AS. *Handboek Radionucliden.* BetaText, 2007. ISBN10: 9075541104;12

Implementing PET/CT imaging for head and neck cancer radiotherapy

Dr. R.J.H.M. Steenbakkers

Department of Radiation Oncology, University Medical Center Groningen, Groningen, The Netherlands

Abstract

Steenbakkers RJHM. Implementing PET/CT imaging for head and neck cancer radiotherapy. The prognosis of a patient with locally advanced head and neck cancer is poor. The estimated five year overall survival is approximately 35 percent. Most of these patients are treated with primary (chemo-)radiotherapy. This treatment is correlated with many severe radiotherapy induced toxicities, which have a large impact on quality of life. The challenge of a radiation oncologist is to irradiate the tumor as much as possible and avoid normal tissues at the same time. Critical in order to achieve this challenge is to depict the tumor as accurate as possible. Normally, a CT scan is made to determine the position and extend of the tumor and pathological lymph nodes. Unfortunately, CT is often not very accurate to see the border between tumor and normal tissues. For this purpose, ^{18}F-FDG PET/CT has entered into the way radiation oncologists define (delineate) tumor. Furthermore, FDG PET can help to find pathological lymph nodes which can be easily missed on CT only. The main limitation of using FDG PET is that there is no standard way to set the threshold of the FDG uptake to precisely depict the edge between tumor and normal tissue. The validation of this threshold by pathology correlation is up to now very limited. More research on this issue is warranted.
Another way where PET is promising for radiotherapy purposes is hypoxia imaging. Hypoxic cancer cells are more radio resistant than oxic cancer cells. These hypoxic cells can be imaged with hypoxia PET tracers, like ^{18}F-FMISO of ^{18}F-FAZA. The cure rate of patients with locally advanced head and neck cancer might improve by increasing the radiotherapy dose on these hypoxic cells depicted by these hypoxia PET tracers.
Tijdschr Nucl Geneesk 2012; 34(2):883-888

Head and neck cancer

The tumors considered to be head and neck cancer are located in the nasopharynx, oropharynx, hypopharynx, larynx, oral cavity, nose cavity, sinuses, middle ears and lips. In 2010, in the Netherlands, approximately 2800 patients were registered to have a new head and neck tumor (1). The incidence is slowly increasing with approximately two percent every year. This is mainly due to the increase of incidence of tumors located in the oral cavity and oropharynx, which is probably caused by the increase of human papiloma virus (HPV) induced tumors in the head and neck area. Estimated is that in the next decade the HPV induced head and neck cancer will increase significantly (2). The prognosis of a patient with head and neck cancer is depending on many factors. Important prognostic factors are: tumor stage, tumor location, performance, age, sex, smoking history, HPV status and tumor hypoxia. The estimated 5 and 10 year overall survival rate of a patient with locally advanced (stage III or IV, not nasopharynx) with optimal treatment is about 35 and 25 percent, respectively (3). Indicating the prognosis of these patients is still poor.
The two major treatment options for head and neck cancer is surgery or radiotherapy with or without chemotherapy. Depending on location and tumor stage the appropriate treatment option is chosen for a patient. Usually, small tumors easily accessible are operated upon. Radiotherapy (with or without chemotherapy) is first choice when a tumor is large or a certain organ can not be spared (like larynx) with surgery. Of course, other factors, like age performance and patient wishes, play a role in the decision of treatment choice. Furthermore, combinations of surgery and radiotherapy are also possible.

Head and neck radiotherapy

In about seventy percent of the patients with head and neck cancer, radiotherapy is part of the treatment (primarily of post-operatively). A general principle in radiotherapy is to irradiate the tumor as much as possible to kill all tumor cells and to avoid normal tissues to minimise toxicities. For the head and neck region, many normal tissues which are sensitive to radiation are in the close proximity of the tumor (table 1). When these normal tissues are irradiated too much, patients may face many radiation induced toxicities (table 1) which have large impact on their quality of life (4). Actually, the dose given to normal tissues is the limiting factor on the amount of radiation that can be given to the tumor and pathological lymph nodes. Furthermore, when chemotherapy is concurrently given with radiotherapy, the radiation induced toxicities tend to be more severe.
In the modern era of advanced technology many efforts has been taken to reduce the incidence of severe radiation induced toxicities without compromising the radiation dose delivered to the tumor. Since a few years intensity modulated radiotherapy

Table 1. Normal tissues and their radiation induced toxicities

normal tissue	radiation induced toxicity
spinal cord	myelopathy (Lhermitte's sign) paralysis
mucosa	mucositis lost of taste ulcers
salivary glands	xerostomia sticky saliva speech problems dental problems
eyes	conjunctivitis/keratitis dry eyes cataract blindness
brain	cognitive dysfunction radionecrosis
cochlea	hearing loss deafness
vocal cords	hoarseness
swallowing muscles	dysfagia tube feeding dependence
chewing muscles	trismus speech problems
thyroid gland	hypothyroidism
mandible	osteoradionecrosis
skin	dermatitis ulcers alopecia

(IMRT) is considered to be standard radiotherapy technique. IMRT is based on the way the radiation dose is delivered. Usually multiple radiation beams are used from multiple angles. For the head and neck region normally six to seven different angles. From each angle the beam shape can be changed very fast with a multileaf collimator. This way the intensity of the beam can be modulated. With specialised computer software in a radiotherapy planning system the radiation dose can be computed and optimised. This way it is possible to give a high dose to the tumor and a much lower dose to a normal tissue next to it (figure 1). Another radiotherapy technique is proton therapy, which may probably very suitable to avoid normal structures in the head and neck region. Depending on the energy given to a proton, its maximal energy loss is at a certain depth in tissue. Behind this point hardly any radiation dose is found. In this fashion it is possible to spare normal tissues which are very close to the tumor. Although proton therapy has already been used for several decades, the delivery technique is still in its infancy and not as well developed as IMRT. Besides that, proton therapy is currently not available in the Netherlands.

Head and neck target definition (delineation)

Usually, when a patient with a head and neck tumor is primarily treated with (chemo-) radiotherapy, 70 Gy (i.e. 70.000 mSv) is given in 35 fractions over a period of six to seven weeks. During this period, there are several geometrical uncertainties. The main geometrical uncertainties are setup variation, organ motion and target definition. Although patients are immobilised with a thermoplastic mask during radiotherapy, they cannot be treated exactly the same way every day (setup variation). Patients can shift a few millimeters. For this problem, patients are imaged just before (online verification) or after (off-line verification) with megavolt images or computed tomography (CT) images mounted on the linear accelerator. Using this procedure, the setup variation can be minimised. The same accounts for organ motion. There are two types of organ motion. One is swallowing during treatment and the other one is shape changes during the radiotherapy course due to tumor volume reduction and weight loss.

The largest geometrical uncertainty in the radiotherapy chain is target definition (5, 6). When a patient with a head and neck tumor is referred to the radiotherapy department a CT scan with a thermoplastic mask and intravenous contrast is made. First, the *gross tumor volume* (GTV) is defined on this CT by the treating radiation oncologist (figure 1). The GTV accounts for all visible macroscopic tumor (primary tumor and pathological lymph nodes). The GTV is acquired using visual inspection of the patient and imaging: ultrasound, CT, MRI and/or PET. Secondly, the *clinical target volume* (CTV) is defined. The CTV is a margin around the GTV which accounts for microscopic extension of the tumor (figure 1). Normally, the GTV-CTV margin is 5 to 10 mm, depending on tumor type and characteristics (i.e. perineural growth). Furthermore, in the CTV elective lymph node areas (levels) of the neck are included. These neck levels are defined according to internationally accepted guidelines and atlases (7). Thirdly, the *planning target volume* (PTV) is generated. The PTV accounts for correction of all geometrical uncertainties. The CTV-PTV margin in the head and neck region is generally 5 mm. The delineation of GTV and CTV in the head and neck area is very difficult. One reason is the complex anatomy of the head and neck. Another reason is that on CT it is often difficult to see where the boundaries between tumor and normal tissues are. For these reasons, large variability occurs between radiation oncologists defining the GTV and CTV (6). Several efforts are already made to reduce this observer variation using MRI (6) or FDG PET (8-10). MRI is superior in its soft-tissue contrast compared to CT. FDG PET is a functional imaging modality that identifies tumor areas and pathological lymph nodes which might be missed with CT. Although both MRI and FDG PET showed reduction of observer variation (6, 8-10), target definition still remains the weakest link in the radiotherapy chain.

Target definition using FDG PET

In the Netherlands, treatment of head and neck cancer is

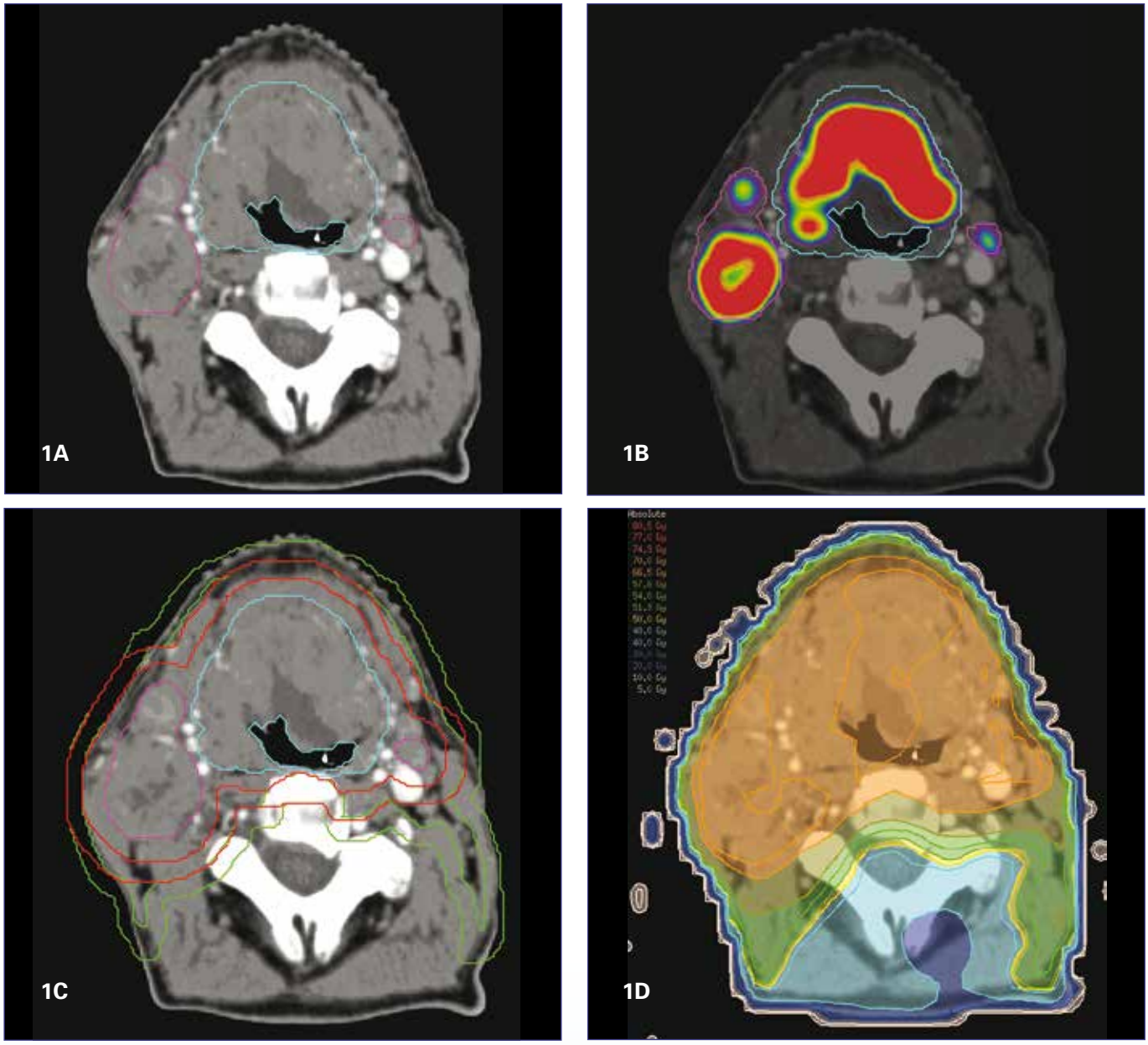

Figure 1. Four identical CT slices of a patient with large cT4N2c oropharyngeal carcinoma. CT slice a) shows the GTV (light blue is the primary tumor and pink the pathological lymph nodes. CT slice b) with a fused FDG PET. CT slice c) shows also the high dose CTV and PTV (red) and the low dose CTV and PTV (green). On CT slice d) iso-contours of the radiotherapy treatment planning are shown based on high and low dose PTV. Iso-contour with color orange, yellow, dark blue represent 70 Gy, 50 Gy and 30 Gy, respectively.

currently centralised in specialised institutions due to its complex treatment. In most of these institutions the FDG PET is incorporated in the treatment planning (figure 1). As stated above, FDG PET combined with CT is useful in target definition and better than CT alone (8-10). Although the sensitivity and specificity in detecting pathological lymph nodes is only slightly better compared to CT, MRI and ultrasound (11-12), FDG PET can be helpful in detecting pathological lymph nodes. Especially pathological lymph nodes in parotid glands and retropharyngeal are easily missed with CT only (figure 2).

The major challenge for radiation oncologists is to depict the edge between tumor and normal tissues. If a tumor is delineated too large, much normal tissue is irradiated as well to a high dose with the risk of excessive toxicities (table 1). If a tumor is delineated to small, the radiotherapy might not cover the entire tumor, risking treatment failure. For this reason, radiation oncologist are afraid to miss tumor and therefore tend to overestimate the real tumor volume (13). FDG PET can help to estimate the tumor edge. The problem is that there is no standard way to set the threshold of the FDG PET images.

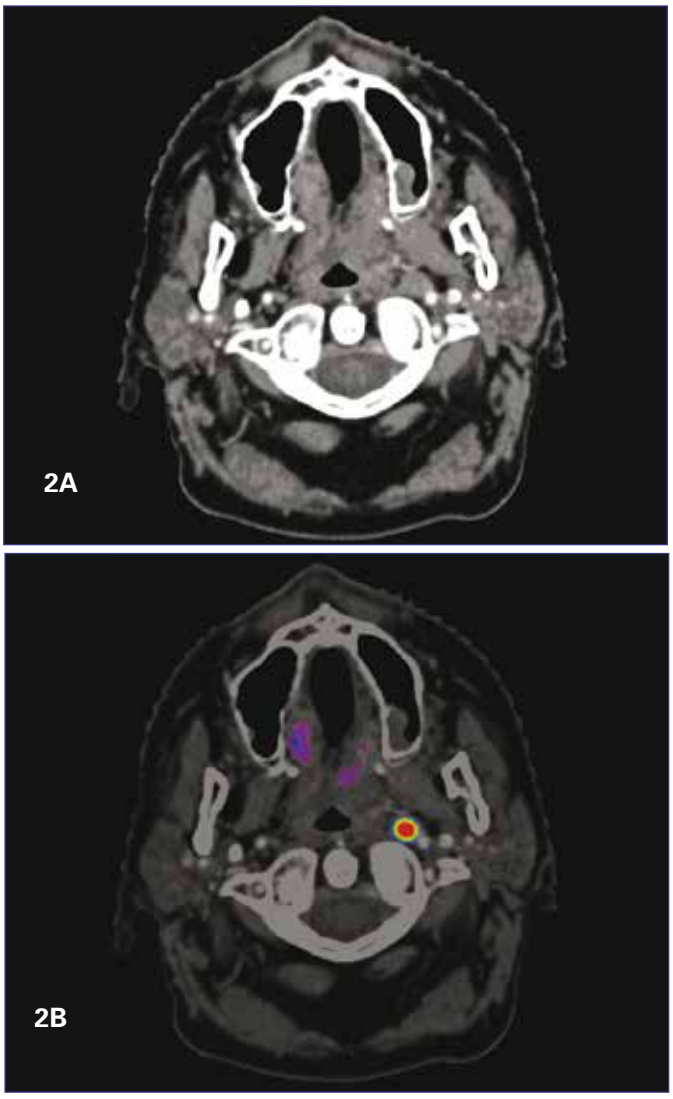

Figure 2. Two identical CT slices of a patient with a cT3N2b oropharyngeal carcinoma. CT slice a) shows a parapharyngeal lymph node at left side which might be easily missed with CT only. CT slice b) with a fused FDG PET shows increased uptake at the parapharyngeal lymph, which can be depicted easily.

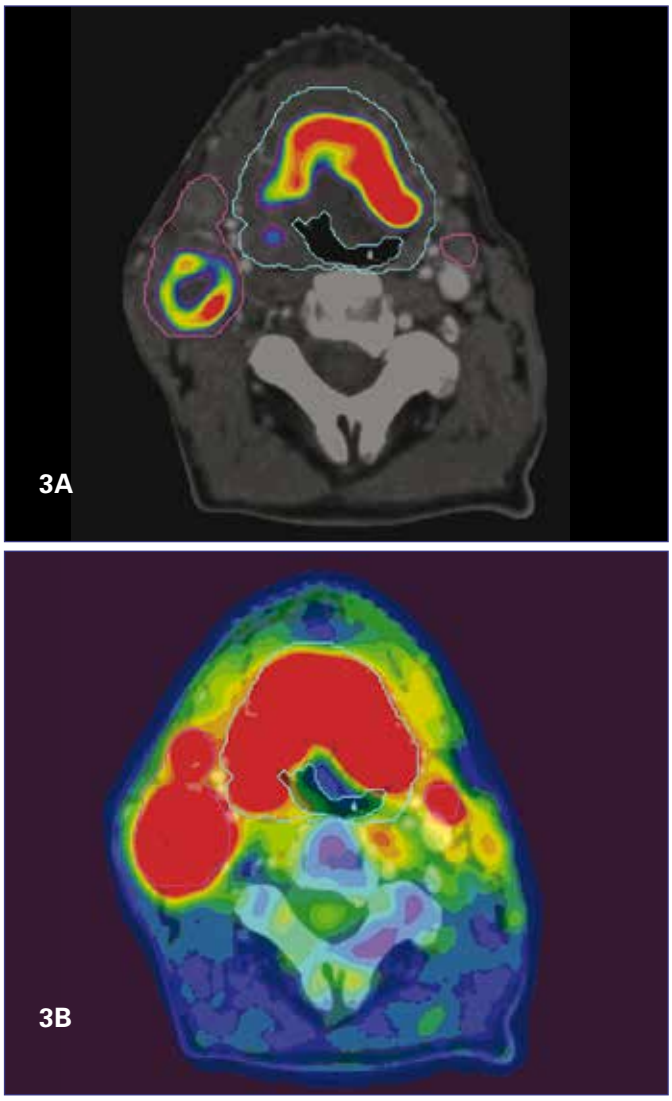

Figure 3. Two identical CT slices of a patient with large cT4N2c oropharyngeal carcinoma (same as figure 1) with a fused FDG PET scan. On CT slice a) and b) the settings of the FDG PET show probably an underestimation and overestimation of the tumor edge, respectively.

Frequently, the threshold is set manually, to match the tumor volume seen on CT. Looking at the amount of FDG uptake seen in the brains can help to set the threshold. The FDG uptake in the brain should be within the skull of the patient. This method is not really a scientific way to look at images and mistakes are easily made. The settings of the threshold can be manipulated with ease. Therefore, overestimation and underestimation of the tumor edge can be made with large consequences as stated before (figure 3). Many efforts are already taken to find a standardised way to set the threshold of the FDG uptake. Numerous automatic methods for setting thresholds have been reported. Most methods are using the standardised uptake value (SUV). Frequently, a percentage of the SUV_{max} is used to set the threshold. This percentages range between 30 and 50 percent (8, 13, 14). Others use a pre-determined absolute SUV (15, 16, 17), which is called $SUV_{cut\ off}$ (SUVCO). The SUVCO rages between 2.5 and 4.0 g/l. Another method, which is not SUV based, is a threshold that is adaptive to the signal-to-background ratio (SBR) (18, 19). Furthermore, other methods like gradient based (20) and halo-edge detections (21) are also not SUV based. The problem with all these methods is that they are depending on the amount of FDG injected, patient characteristics, injection–scan interval, type of PET scanner and many other factors. Therefore, a method found in an institution cannot be exactly duplicated by another institution. Furthermore, the different described methods are quite different from each other, which have a large impact on both volume and shape of the tumor (19). Preferably, all methods to set the threshold of the FDG uptake for finding the edge between tumor and normal tissues should be correlated with pathology. Up to date, for head and neck

cancer, only one study is published correlating pathology with CT, MRI and FDG PET (13). In this study, already published in 2004, nine patients with laryngeal cancer (mainly T4) underwent a CT, MRI and FDG PET just before a total laryngectomy was performed. The threshold settings of het FDG PET for the tumor edge were based on SBR. The mean volume of the surgical specimen was 12.6 cm^3. The mean volumes of the tumor based on CT, MRI and FDG PET were significantly larger: 20.8, 23.8 and 16.3, respectively. Although the mean tumor volume based on the FDG PET was most close to the mean pathology volume, no modality adequately depicted superficial tumor extension. Unfortunately, this study has not been repeated yet for other types of head and neck cancer. Furthermore, the quality of imaging of CT, FDG PET and especially MRI has been the last few years. Probably, the combination of multiple image modalities at the same time would be ideal to accurate delineate the tumor and pathological lymph nodes.

Hypoxia PET for head and neck cancer

As stated before, the prognosis of patients with locally advanced head and neck cancer is poor (3). A major cause of treatment failure is tumor hypoxia. Hypoxic cells are resistant to the cytotoxic effects of both chemotherapy and radiation (22).
In the past, several attempts have been made to overcome tumor hypoxia, such as the use of radiosensitizers, vasodilators, carbogen breathing, or hypoxic cell toxins such as tirapazamine, combined with (chemo) radiation. In general, these combined approaches have come to the expense of increased acute and late radiation induced toxicities (22). Another approach, which may overcome hypoxic tumor resistance, is increasing the radiation dose. However, increasing the radiation dose may also increase toxicities (table 1). Ideally, only hypoxic tumor cells should receive a higher dose. Currently, with modern radiotherapy techniques like IMRT, it has become possible to intensify radiation dose in specific (radio resistant) subvolumes within the tumor (23). For this purpose, imaging of hypoxic tumor subvolumes is essential.
A number of hypoxic specific PET tracers have been developed (24), like ^{18}F-fluoromisonidazole (FMISO), ^{18}F-fluoroazomycin arabinoside (FAZA) and ^{60}Cu-labelled methylthiosemicarbazone (ATSM). Up to date, most frequently used tracer is FMISO (25, 26). Unfortunately, FMISO PET has a low tumor-to-background ratio due to slow accumulation in hypoxic tissues and slow clearance from oxic tissues. Compared to FMISO, the clearance of FAZA from blood and non-target tissues is faster and therefore has a higher tumor-to-background ratio (27). In two experimental studies (28, 29), it has already been demonstrated that FAZA PET/CT is suitable to visualise hypoxic areas in head and neck cancer patients before treatment. Therefore, it is hypothesised that FAZA PET/CT can be used to guide radiotherapy in order to substantially increase the dose to hypoxic tumor subvolumes (28). This might improve local control and subsequent survival of patients with locally advanced head and neck cancer. Until now, limited data is available as to the way and the extent hypoxic areas behave during the radiotherapy course (25, 26).
Hypoxic areas might disappear and appear at different locations during treatment. Furthermore, for most patients it seems that the hypoxic areas disappear in the first few weeks of the radiotherapy course (25, 26) (figure 4). In order to achieve the most optimal hypoxic tumor subvolume dose escalation, several strategies will have to be developed (e.g. gradual dose escalation using IMRT with a simultaneous integrated boost (SIB), intensity modulated arc therapy (IMAT), stereotactic boost (SRT) or proton therapy). Additional information is required with regard to these hypoxia changes during the (chemo-)radiotherapy course before the radiation dose can safely be increased.

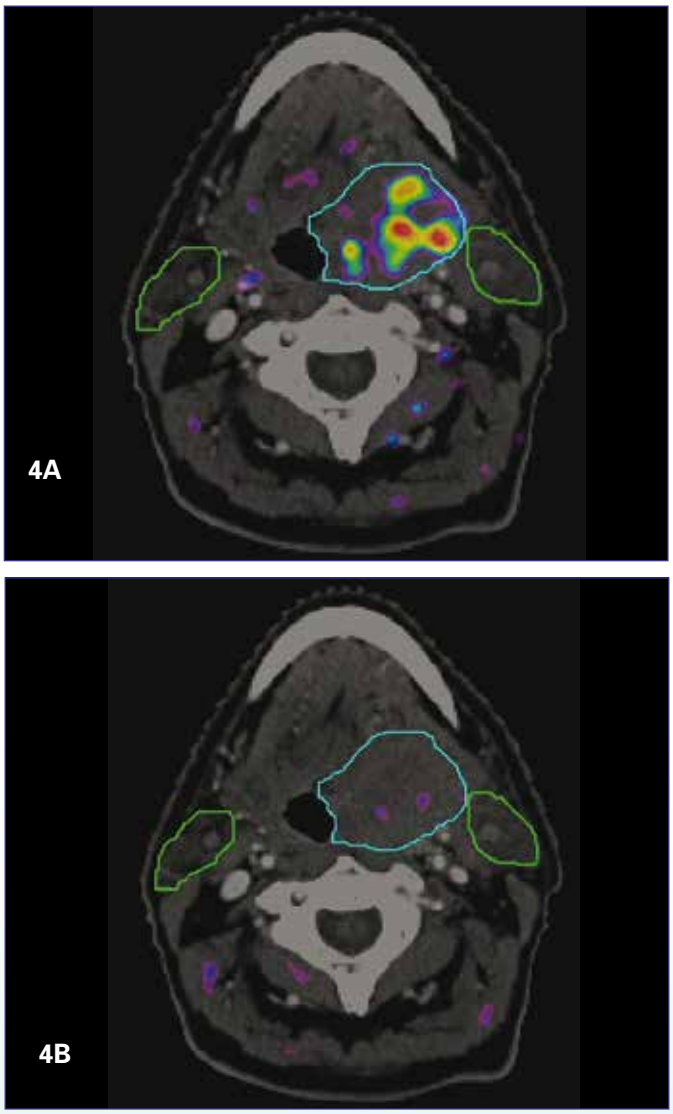

Figure 4. Two identical CT slices of a patient with a cT3N2b oropharyngeal carcinoma with a fused ^{18}F-FAZA PET. CT slice a) shows a fused ^{18}F-FAZA PET made three days before start of chemoradiation with area in the GTV (light blue) probably representing hypoxia. CT slice b) shows a fused ^{18}F-FAZA PET made in the second week (day 12) of chemoradiation, without sign of a hypoxic area in the GTV. The green lines represent the parotid glands.

References:

1. Source: Intergraal Kankercentrum Nederland, www.iknl.nl
2. Marur S, D'Souza G, Westra WH et al. HPV-associated head and neck cancer: a virus-related cancer epidemic. Lancet Oncol. 2010;11:781-9
3. Pignon JP, le Maître A, Maillard E et al. Meta-analysis of chemotherapy in head and neck cancer (MACH-NC): an update on 93 randomised trials and 17,346 patients. Radiother Oncol. 2009;92:4-14
4. Langendijk JA, Doornaert P, Verdonck-de Leeuw IM et al. Impact of late treatment-related toxicity on quality of life among patients with head and neck cancer treated with radiotherapy. J Clin Oncol. 2008;26:3770-6
5. Steenbakkers RJHM, Duppen JC, Fitton I et al. Reduction of observer variation using matched CT-PET for lung cancer delineation: a three-dimensional analysis Int J Radiat Oncol Biol Phys. 2006;64:435-48
6. Rasch CRN, Steenbakkers RJHM Fitton I et al. Decreased 3D observer variation with matched CT-MRI, for target delineation in Nasopharynx cancer. Radiat Oncol. 2010;5:21
7. Grégoire V, Levendag P, Ang KK et al. CT-based delineation of lymph node levels and related CTVs in the node-negative neck: DAHANCA, EORTC, GORTEC, NCIC,RTOG consensus guidelines. Radiother Oncol. 2003;69:227-36
8. Riegel AC, Berson AM, Destian S et al. Variability of gross tumor volume delineation in head-and-neck cancer using CT and PET/CT fusion. Int J Radiat Oncol Biol Phys. 2006;65(3):726-32
9. Ashamalla H, Guirgius A, Bieniek E et al. The impact of positron emission tomography/computed tomography in edge delineation of gross tumor volume for head and neck cancers. Int J Radiat Oncol Biol Phys. 2007;68:388-95
10. Ciernik IF, Dizendorf E, Baumert BG et al. Radiation treatment planning with an integrated positron emission and computer tomography (PET/CT): a feasibility study. Int J Radiat Oncol Biol Phys. 2003;57:853-63
11. Fletcher JW, Djulbegvic B, Soares B et al. Recoomendations on the use of 18FDG PET in oncology. J Nucl Med. 2008;49:480-508
12. Kyzas PA, Evangelou E, Denaxa-Kyza D et al. 18F-fluordeoxyglucose positron emission tomography to evaluate cervical node metastases in patients with head and neck squamous cell carcinoma: a meta-analysis. J Natl Canc Inst. 2008;100:712-20
13. Daisne JF, Duprez T, Weynand B et al. Tumor volume in pharyngolaryngeal squamous cell carcinoma: comparison at CT, MR imaging, and FDG PET and validation with surgical specimen. Radiology. 2004 Oct;233:93-100
14. Paulino AC, Koshy M, Howell R et al. Comparison of CT- and FDG PET-defined gross tumor volume in intensity-modulated radiotherapy for head-and-neck cancer. Int J Radiat Oncol Biol Phys. 2005;61:1385–92
15. Paulino AC, Johnstone PA. FDG PET in radiotherapy treatment planning: Pandora's box? Int J Radiat Oncol Biol Phys. 2004;59:4–5
16. Hong R, Halama J, Bova D et al. Correlation of PET standard uptake value and CT window-level thresholds for target delineation in CT based radiation treatment planning. Int J Radiat Oncol Biol Phys. 2007;67:720–6
17. Moule RN, Kayani I, Moinuddin SA et al. The potential advantages of (18)FDG PET/CT-based target volume delineation in radiotherapy planning of head and neck cancer. Radiother Oncol. 2010;97:189-93
18. Daisne JF, Sibomana M, Bol A et al. Tri-dimensional automatic segmentation of PET volumes based on measured source-to-background ratios: Influence of reconstruction algorithms. Radiother Oncol. 2003;69:247–50
19. Schinagl DA, Vogel WV, Hoffmann AL et al. Comparison of five segmentation tools for 18F-fluoro-deoxy-glucose-positron emission tomography-based target volume definition in head and neck cancer. Int J Radiat Oncol Biol Phys. 2007;69:1282–9
20. Geets X, Lee JA, Bol A et al. A gradient-based method for segmenting FDG PET images: methodology and validation. Eur J Nucl Med Mol Imaging. 2007;34:1427–38
21. Ashamalla H, Guirgius A, Bieniek E et al. The impact of positron emission tomography/computed tomography in edge delineation of gross tumor volume for head and neck cancers. Int J Radiat Oncol Biol Phys. 2007;68:388–95.
22. Hoogsteen IJ, Marres HA, van der Kogel AJ et al. The hypoxic tumour microenvironment, patient selection and hypoxia-modifying treatments. Clin Oncol (R Coll Radiol). 2007; 19:385-96
23. Thorwarth D, Eschmann SM, Paulsen F, Alber M: Hypoxia dose painting by numbers: a planning study. Int J Radiat Oncol Biol Phys. 2007; 68:291-300
24. Grosu AL, Nestle U, Weber WA: How to use functional imaging information for radiotherapy planning. Eur J Cancer. 2009; 45 Suppl 1:461-63
25. Eschmann SM, Paulsen F, Bedeshem C et al. Hypoxia-imaging with (18)F-Misonidazole and PET: changes of kinetics during radiotherapy of head-and-neck cancer. Radiother Oncol. 2007;83:406-10.
26. Lee N, Nehmeh S, Schöder H et al. Prospective trial incorporating pre-/mid-treatment [18F]-misonidazole positron emission tomography for head-and-neck cancer patients undergoing concurrent chemoradiotherapy. Int J Radiat Oncol Biol Phys. 2009;75:101-8
27. Piert M, Machulla HJ, Picchio M et al. Hypoxia-specific tumor imaging with 18F-fluoroazomycin arabinoside. J Nucl Med. 2005;46:106-13
28. Grosu AL, Souvatzoglou M, Roper B et al. Hypoxia imaging with FAZA-PET and theoretical considerations with regard to dose painting for individualization of radiotherapy in patients with head and neck cancer. Int J Radiat Oncol Biol Phys. 2007; 69:541-51
29. Postema EJ, McEwan AJ, Riauka TA et al. Initial results of hypoxia imaging using 1-alpha-D: -(5-deoxy-5-[18F]-fluoroarabinofuranosyl)-2-nitroimidazole (18F-FAZA). Eur J Nucl Med Mol Imaging. 2009; 36:1565-73

Draxmibi® 1mg

Kit for radiopharmaceutical preparation

- Up to 11.1 GBq (300 mCi) of Tc-99m per vial
- 10 hours stability post reconstitution
- 5 vial kit
- Vial of 10 ml

IDB Holland bv

From Atom to Image

Weverstraat 17 5111 PV Baarle-Nassau The Netherlands Tel: +31 (0)13 507 95 58 Fax: +31 (0)13 507 99 12 E-mail: sales@idb-holland.com

www.idb-holland.com

Radioembolisatie voor de behandeling van leverkanker: een praktische handleiding

Dr. M.G.E.H. Lam[1], Drs. J.E. Huijbregts[1], Prof. dr. M.A.A.J. van den Bosch[1], Dr. F.D. van het Schip[1], Dr. J.F. Nijsen[1], Dr. B.A. Zonnenberg[1,2]

[1] Afdeling Radiologie en Nucleaire Geneeskunde, Universitair Medisch Centrum Utrecht
[2] Afdeling Interne Geneeskunde & Infectieziekten, Universitair Medisch Centrum Utrecht

Abstract

Lam MGEH, Huijbregts JE, van den Bosch MAAJ et al. Radioembolization for the treatment of liver cancer: a practical guide. Ytrium-90 radioembolization is a relatively new treatment modality for the treatment of both primary and secondary liver malignancies. It consists of injecting beta-particle emitting yttrium-90 loaded (glass or resin) microspheres into the hepatic artery using a catheter. The clinical results of this form of internal radiation therapy are very promising. The aim of this manuscript is to provide all health care personnel involved in radioembolization information on clinical, procedural and technical aspects of this procedure as a guideline for current or future practise.
Tijdschr Nucl Geneesk 2012; 34(2):890-895

Introductie

Radioembolisatie is een relatief nieuwe behandeling voor levermaligniteiten. Het Universitair Medisch Centrum Utrecht is in 2009 als eerste centrum in Nederland met een radioembolisatie-programma gestart. Inmiddels zijn meer dan honderd patiënten uit het hele land behandeld. Er bestaat in toenemende mate belangstelling voor deze therapie, zowel vanaf de kant van de verwijzers als van potentiële uitvoerders. Verschillende andere centra in Nederland willen de procedure introduceren. Dit stuk focust derhalve op de procedurele en technische aspecten van de behandeling. Het dient als leidraad voor clinici die betrokken zijn bij de introductie van deze nucleaire therapie.

Principe

Radioembolisatie, ook wel selectieve interne radiatie therapie (SIRT) genoemd, betreft een behandeling van primaire of secundaire levermaligniteiten via intra-arteriële toediening van ^{90}Yttrium-microsferen (^{90}Y-microsferen) in de lever. Het betreft een therapie die tot nog toe alleen wordt toegepast als er geen andere therapeutische opties meer zijn. In een grote meta-analyse worden responspercentages genoemd van 79 procent voor colorectale metastasen en 78 tot 89 procent voor het hepatocellulair carcinoom (1). De therapie wordt voorafgegaan door een angiografische procedure waarbij de vaatanatomie in kaart wordt gebracht en collateralen vanuit de arteria hepatica propria/communis worden gecoild. Vervolgens wordt de therapie gesimuleerd door toediening van een testdosis ^{99m}Technetium-macroaggregaten (^{99m}Tc-MAA). Na toediening wordt een scan gemaakt, waarbij wordt gecontroleerd of de toegediende activiteit zich daadwerkelijk in de lever bevindt en niet in de maag, het duodenum, de longen of elders. Indien er sprake is van extrahepatische abdominale depositie kan therapie met ^{90}Y-microsferen niet plaatsvinden. Afhankelijk van de mate van longshunting wordt de dosis aangepast of kan de therapie niet plaatsvinden. Wanneer patiënten na de voorbereidende procedure geschikt worden geacht voor therapie, wordt de therapeutische angiografische procedure met toediening van de ^{90}Y-microsferen gepland. Dosisberekening vindt plaats aan de hand van volumina van lever en tumoren, evenals de body surface area (BSA) van de patiënt.

Radiofarmacon

In Nederland zijn de volgende radiofarmaca beschikbaar (tabel 1):

1. ^{90}Yttrium-SIR-Spheres® (SIRTeX Medical Ltd., Bonn, Duitsland);
2. ^{90}Yttrium-TheraSphere® (MDS Nordion, Ottawa, Canada);
3. ^{166}Holmium-PLLA-microsferen.

In Europa hebben beide ^{90}Yttrium-preparaten een CE-markering als medisch hulpmiddel (Active Implantable Medical Device) voor gebruik bij inoperabele levermaligniteiten zonder gespecificeerde origine. In de Verenigde Staten zijn de SIR-Spheres® microsferen goedgekeurd door de Food and Drug Administration (FDA) als medisch hulpmiddel voor gebruik bij inoperabele levermetastasen van het colorectaal carcinoom (1, 2). TheraSphere® microsferen zijn goedgekeurd voor gebruik bij patiënten met een inoperabel hepatocellulair carcinoom, in de palliatieve setting of als overbrugging naar levertransplantatie (3). ^{166}Holmium-PLLA-microsferen zijn tot nu toe alleen in studieverband in het UMC Utrecht beschikbaar (4).

Inmiddels is het gebruik van ^{90}Yttrium-preparaten bij een hepatocellulair carcinoom door de Nederlandse verzekeraars opgenomen in het zorgpakket. Aan verdere uitbreiding wordt gewerkt.

Tabel 1. Eigenschappen van ^{90}Y-SIR-Spheres® en ^{90}Y-TheraSphere®. Let op de verschillen in specifieke activiteit en aantal microsferen.

	^{90}Y-SIR-Spheres®	^{90}Y-TheraSphere®
matrix	hars	glas
diameter	32 micrometer	25 micrometer
isotoop	^{90}Yttrium	^{90}Yttrium
halveringstijd	64 uur	64 uur
aantal microsferen per dosis	50 miljoen	4 miljoen
gewicht per dosis	1370 mg	110 mg
activiteit per microsfeer	50 Bq	1250-2500 Bq
activiteit per dosis	3 GBq per vial	3-5-7-10-15-20 GBq per vial
beeldvorming	brehmsstrahlung	brehmsstrahlung
testdosis	^{99m}Tc-MAA	^{99m}Tc-MAA

Indicatie

In principe komen patiënten met irresectabele primaire of metastatische levermaligniteit zonder standaard (chemo)-therapeutische opties in aanmerking voor behandeling met ^{90}Y-microsferen (5, 6). Voorwaarden waar de patiënt aan moet voldoen zijn als volgt:

1. ziekte is beperkt tot de lever of tenminste leverdominant;
2. voldoende leverreserve (aanwijzingen voor adequate levertolerantie: geen ascites, normale synthese functie van de lever (albumine > 30 g/L), normaal tot licht verhoogd totaal bilirubine (< 34 µmol/L of < 2 mg/dL);
3. levensverwachting > 12 weken;
4. World Health Organization performance status 0-2.

Contra-indicaties

Absolute contra-indicaties:

1. extrahepatische depositie op de ^{99m}Tc-MAA scintigrafie die niet gecorrigeerd kan worden door embolisatie technieken;
2. pre-therapeutische ^{99m}Tc-MAA scintigrafie met een longshunt van > 20% (SIR-Spheres®) en/of een absolute longshunt van > 610 MBq (>30 Gy longdosis; TheraSphere®)[1];
3. onvoldoende hepatische reserve, al dan niet door excessieve tumorload (> 70% van het levervolume) en/of Child-Pugh classificatie C;
4. nierinsufficiëntie (GFR < 40 mL/min).

Relatieve contra-indicaties:

1. vena porta trombose (portale hypertensie, ascites, splenomegalie);
2. ALAT, ASAT of AF > 5x bovenste limiet van normaal;
3. verhoogd totaal bilirubine (> 34 µmol/l of > 2mg/dL) zonder reversibele oorzaak;
4. nierinsufficiëntie (cave contrastnefropathie);
5. leukocyten < 4.0 10^9/L en/of trombocyten < 150 10^9/L;
6. grote chirurgische ingreep < 4 weken of een niet-geheelde chirurgische wond voor de behandeling;
7. radiotherapie op de bovenbuik (cave levertoxiciteit);
8. chemotherapie < 4 weken voor de geplande behandeling;
9. ernstige comorbiditeit;
10. lichaamsgewicht > 150 kg (i.v.m. tafelcapaciteit);
11. actieve hepatitis;
12. allergie voor contrastmiddel;
13. zwangerschap en het geven van borstvoeding.

Gegevens bij de aanvraag

De aanvrager dient een klinische brief te sturen met het verzoek tot ^{90}Y-radioembolisatie. Deze informatie moet voldoende zijn om de indicatie voor therapie te kunnen stellen. Voor de indicatiestelling vindt overleg plaats met een interventieradioloog en waar nodig met een internist-oncoloog of oncologisch-chirurg. Overleg in multidisciplinair verband strekt tot aanbeveling. Er wordt een beslissing gemaakt of de therapie plaats zal vinden in één sessie (gehele lever) of in twee sessies (rechts en links). Die beslissing is afhankelijk van de vaatanatomie, de kliniek en de uitgebreidheid van de afwijkingen (5,6).

Voor de behandeling is een recente computed tomography (CT) scan van de lever (3-fasen) noodzakelijk (liefst < 2 weken) voor het uitsluiten van extrahepatische ziekte en/of response monitoring. Ook worden het levervolume en de tumorload in de lever berekend met behulp van deze scan. Eventueel kan de beeldvorming aangevuld worden met magnetic resonance imaging (MRI) en/of ^{18}F-FDG PET bij een FDG-avide tumor.

Opname van patiënt

Zowel voor de voorbereidende ^{99m}Tc-MAA procedure als de ^{90}Y-radioembolisatie worden patiënten bij voorkeur opgenomen. Dit in verband met de pre- en posthydratie en om de patiënten

[1]Let op: de fabrikanten adviseren dus een verschillende benadering, zie onder 'berekening van de dosis'

na de therapie te kunnen observeren. Patiënten arriveren de dag voor de procedure en gaan de ochtend na de procedure weer naar huis. De voorbereiding op de afdeling is voor beide procedures gelijk. De angiografische procedures duren gemiddeld tussen de 1 en 3 uur.

De volgende zaken dienen geregeld te worden:
- opname, statusvoering, controle indicatie;
- laboratorium: bloedbeeld, nierfunctie, elektrolyten, leverfunctie, stolling;
- infuus, voor- en nahydreren vanwege contrast: 1.5 L NaCl 0.9% per 24 uur;
- premedicatie:
  - anti-emetica (Ondansetron 8 mg intraveneus 1 uur voor procedure);
  - corticosteroïden (Dexamethason 10 mg intraveneus 1 uur voor procedure);
  - protonpompremmer (start 40 mg Pantozol voor 6 weken, start bij opname voor ^{99m}Tc-MAA scintigrafie.

De corticosteroïden vergroten de tolerantie voor de behandeling en de protonpompremmers worden gegeven om radiatie van ulcera in de tractus digestivus te voorkomen;
- alle patiënten krijgen tijdens de procedure een condoom- of urinekatheter;
- bespreken pijnmedicatie op de afdeling post-embolisatie;
- bespreken van eventuele stralingshygiënische leefregels na ^{90}Y-radioembolisatie (in Utrecht 2 dagen);
- bij behandeling in twee sessies dient een interval tussen de sessies overwogen te worden ter preventie van levertoxiciteit enerzijds en optimale behandeling anderzijds. Een periode van twee tot zes weken wordt aanbevolen (6).

Voorbereidende angiografische ^{99m}Tc-MAA procedure

Deze angiografische procedure heeft als doelen:
1. inspectie van arteriële en veneuze vaatvoorziening van de lever;
2. coilen van relevante vaten (a. gastroduodenalis, a. hepatica dextra);
3. simulatie van de therapie d.m.v. toediening van testdosis ^{99m}Tc-MAA (150 MBq).

Inspectie van arteriële en veneuze vaatvoorziening van de lever

De vaatanatomie van de lever bepaalt de mogelijkheden voor therapie (7). Er zijn globaal drie varianten:
1. De a. hepatica dextra en de a. hepatica sinistra splitsen af van de a. hepatica propria distaal van de a. gastroduodenalis (figuur 1). Behandeling van de gehele lever is mogelijk met katheter in de a. hepatica propria;
2. De a. hepatica dextra en de a. hepatica sinistra splitsen niet af van dezelfde arterie (bijvoorbeeld de a. hepatica dextra komt uit de a. mesenterica superior). Behandeling van de gehele lever vindt plaats vanuit twee afzonderlijke vaten;
3. Een deel van de arteriële vaatvoorziening van de lever is onbereikbaar (bijvoorbeeld de a. hepatica sinistra komt uit de a. gastrica sinistra). Behandeling van slechts een deel van de lever is mogelijk. Als het niet bereikbare deel laesies bevat wordt de behandeling afgeraden.

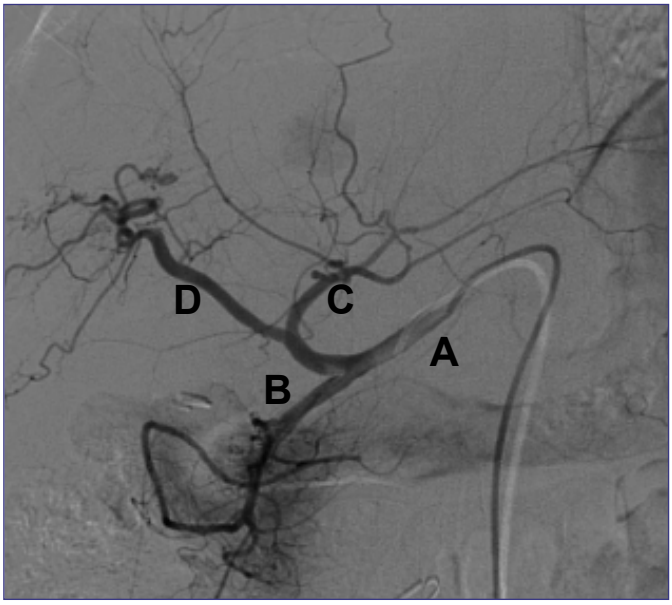

Figuur 1. Angiografie waarbij A=arteria hepatica communis, B=arteria gastroduodenalis, C=arteria hepatica sinistra, D=arteria hepatica dextra.

Coilen van relevante vaten

Bij het gebruik van SIR-Spheres® is coiling van ten minste de a. gastroduodenalis een vereiste. Overige collateralen van de a. hepatica propria/communis worden zo mogelijk eveneens gecoild. Het aantal microsferen (SIR-Spheres® 50 miljoen; TheraSphere® 4 miljoen) zorgt voor embolisatie van de microvasculatuur met mogelijke stasis van de bloodflow, wat risico op backflow -met mogelijk extrahepatische depositie van microsferen- tot gevolg heeft. Bij het gebruik van TheraSphere® is coiling van de a. gastroduodenalis niet strikt noodzakelijk aangezien er minder deeltjes worden toegediend en er daardoor minder kans is op stasis en backflow (7).

Toediening van testdosis ^{99m}Tc-MAA

De positie van de katheter is bepalend voor de distributie van ^{99m}Tc-MAA:
1. In de a. hepatica propria (voordeel: behandeling gehele lever; nadeel: meer kans op extrahepatische depositie en tevens mogelijke preferentiële flow naar links of naar rechts met inadequate dosisdistributie);
2. (Sequentieel) in de a. hepatica dextra en/of sinistra (voordeel: minder kans op extrahepatische depositie). Deze optie is gebruikelijk bij behandeling in twee sessies, maar met verplaatsen van de katheter en twee spuitjes (2 x 75 MBq) ^{99m}Tc-MAA kan ook de hele lever in één sessie bereikt worden;

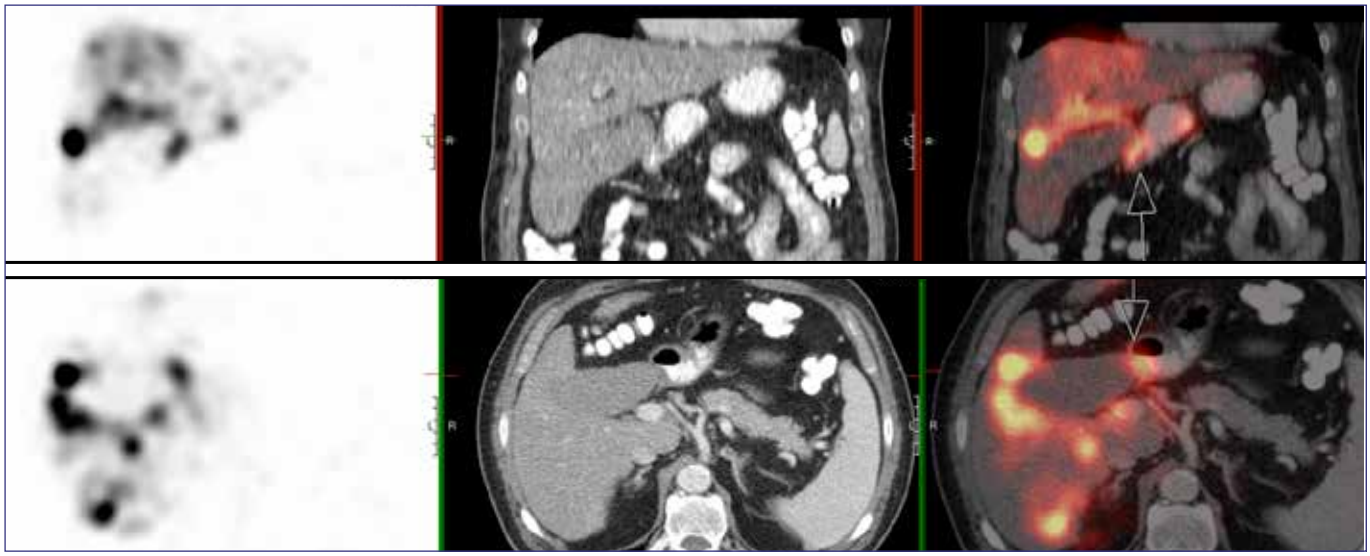

Figuur 2. ^{99m}Tc-SPECT/CT (150 MBq): extrahepatische depositie in de wand van de galblaas (focaal en meer dan de leveractiviteit) of mogelijk het duodenum. In beide gevallen een absolute contra-indicatie voor behandeling.

3. (Sub)segmenteel in een leversegment
   (voordeel: minder kans op extrahepatische depositie;
   nadeel: meer selectief). Bij een beperkt aantal laesies kan deze optie gekozen worden.

In ons centrum heeft optie 2 de voorkeur vanwege de geringere kans op extrahepatische depositie. Als de kliniek het toelaat wordt de gehele lever in één sessie benaderd.

^{99m}Tc-MAA scintigrafie

Na de procedure worden planaire opnamen vervaardigd van thorax en abdomen, evenals single photon emission computed tomography/CT (SPECT/CT) opnamen van het abdomen. In verband met de stabiliteit van ^{99m}Tc-MAA is het belangrijk dat de dosis ^{99m}Tc-MAA zo kort mogelijk tevoren wordt bereid en dat de aansluitende scan zo snel mogelijk na toediening wordt gemaakt. Naarmate het interval tussen bereiding enerzijds en het interval tussen toediening en opnamen anderzijds groter wordt ontstaat er meer vrij ^{99m}Tc-pertechnetaat. Dit kan problemen geven bij het beoordelen van extrahepatische depositie.

Het maken van een SPECT/CT heeft grote meerwaarde boven de planaire opnamen in het beoordelen van extrahepatische depositie in bijvoorbeeld het duodenum (8). Eventueel kan een stand-alone SPECT gefuseerd worden met een recente CT scan. Bij de beoordeling zijn de volgende punten belangrijk:

- Kwaliteit van de opname. Beoordeling vrij ^{99m}Tc-pertechnetaat. Dit is te zien door diffuse uptake in de schildklier, de maag (cave onderscheid met meer focale uptake van ^{99m}Tc-MAA) en de nieren;
- Focale uptake buiten de lever (figuur 2). Dit is een contra-indicatie voor de behandeling met ^{90}Y-microsferen. Een uitzondering is focale uptake in het ligamentum falciforme (relatieve contra-indicatie) (9) en rond de galblaas (geen contra-indicatie indien galblaasuptake < normale leveruptake) (10);
- Shunting naar de longen (berekend op planaire anterior/posterior opnamen, figuur 3);
- Verdeling binnen de lever. Is er focale uptake ter plaatse van de tumoren? Welk deel van de lever wordt behandeld (van belang voor dosisberekening).

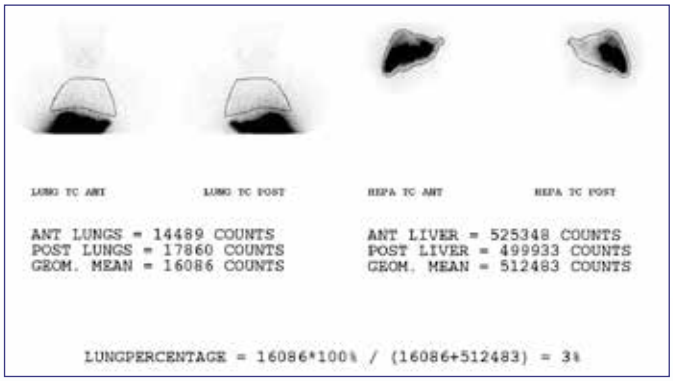

Figuur 3. Berekening van de longshunt. Vanwege scatter zal er altijd activiteit gemeten worden. Grofweg mag de longshunt niet meer bedragen dan 20% (SIR-Spheres®) en/of 610 MBq (TheraSphere®). In deze gevallen moet de dosis worden aangepast of kan de therapie niet doorgaan.

Berekening van de dosis

^{90}Yttrium-SIR-Spheres®

Voor berekening van de dosis op de hele lever wordt in het algemeen de Body Surface Area (BSA) methode gebruikt (5). Deze staat beschreven in de SIRTeX user's manual en is als volgt:

$$A_{gehele\ lever} = BSA - 0.2 + LI$$

Waarin A = dosis in GBq, BSA = Body Surface Area in m^2, LI = Liver Involvement van maligniteit, uitgedrukt in fractie van

het gehele levervolume. De BSA wordt berekend aan de hand van gewicht en lengte:

BSA (m^2) = 0.20247 x lengte $(m)^{0.725}$ x gewicht $(kg)^{0.425}$

LI wordt berekend met behulp van een recente CT of MRI scan:

LI = totale volume maligne laesies/volume totale lever inclusief laesies

In de praktijk betekent dit dat de activiteit die een patiënt krijgt rond de 2 GBq zal zijn, minder dan de 3 GBq die standaard door SIRTeX aangeleverd wordt.

Dosisaanpassing vindt plaats naar aanleiding van eventuele shunting naar de longen. Bij shunting > 10% en < 15% wordt een 20% dosisreductie gehanteerd. Bij shunting > 15% en < 20% wordt een dosisreductie van 40% gehanteerd. Een shuntingspercentage > 20% is voor SIR-Spheres® een absolute contra-indicatie.

Als niet de gehele lever in één keer behandeld wordt, maar bijvoorbeeld maar een deel of twee delen in één sessie, dan moet de dosis (berekend over de gehele lever) verdeeld worden. Daarbij is de fractie van de totale dosis gelijk aan de fractie van het totale levervolume. Als bijvoorbeeld de rechter leverkwab 60% beslaat krijgt de rechter leverkwab 60% van de totaal berekende dosis, onafhankelijk van de tumorload in de betreffende leverhelft.

Op basis van CT wordt het volume berekend van elk deel apart en van de gehele lever. Hieruit volgt de volumefractie. De verdeling van ^{99m}Tc-MAA op SPECT-CT fusiebeelden kan behulpzaam zijn, omdat de anatomische leverkwabben niet altijd overeenkomen met de arteriële vaatvoorziening. De activiteit voor een bepaald deel van de lever wordt berekend door:

A (GBq) = $A_{gehele\ lever}$ (GBq) x volumefractie

^{90}Yttrium-TheraSphere®

Bij de berekening van de dosis wordt uitgegaan van een nominale dosis op de lever, waarbij de aanname gedaan wordt dat 1 GBq ^{90}Yttrium diffuus verdeeld over 1 kg lever een dosis geeft van circa 50 Gy. Omdat de dosis niet diffuus verdeeld is maar zich concentreert rond de laesies, is de dosis op de laesies hoger en de dosis op gezond leverweefsel lager (figuur 4). Bij de berekening van de activiteit wordt derhalve gestreefd naar een nominale dosis van 80 tot 120 Gray.

Dit wordt berekend als:

$A_{targetvolume\ lever}$ = (nominale dosis/50) x levergewicht

Daarbij is $A_{targetvolume\ lever}$ de activiteit in GBq bestemd voor een deel van de lever (kan ook de gehele lever zijn) en is de nominale dosis een gekozen dosis van 80–120 Gy. Het levergewicht (in kg) is

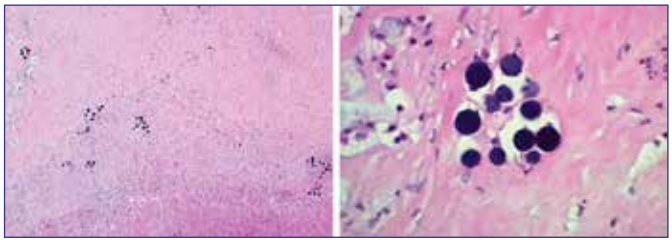

Figuur 4. HE kleuring 40x en 200x vergroot. Microsferen lopen vast in de microvasculatuur van de lever.

gebaseerd op het berekende volume op CT (1 cc = 1 g).

De shunt naar de longen mag bij het gebruik van TheraSphere® niet meer zijn dan 610 MBq. Dit geeft namelijk een dosis op de longen van circa 30 Gy. Eventueel moet de gegeven dosis aangepast worden.

In tegenstelling tot ^{90}Yttrium-SIR-Spheres® is het bij ^{90}Yttrium-TheraSphere® niet mogelijk de dosis na levering aan te passen door middel van optrekken van de benodigde activiteit. Bij bestelling van de activiteit dient de toe te dienen dosis dus al bekend te zijn. De behandeling en de levering moeten dusdanig op elkaar afgestemd worden dat de berekende dosis benaderd wordt.

Bestelling en bereiding van de ^{90}Y-microsferen

Wat betreft ^{90}Y-microsferen is er in Utrecht alleen ervaring met SIR-Spheres®. De bestelling gebeurt via een standaard fax orderformulier aan SIRTeX Medical Europe GmbH waarop het aantal doses (standaard 3 GBq/dosis), behandelingsdatum, het aantal toediensets, toedien V-vials en V-vial houders kunnen worden ingevuld. Bestelling dient altijd vóór woensdag 12 uur te geschieden zodat de ^{90}Y-microsferen de week erna tijdig in huis zijn. Een standaard patiëntendosis bevat een nominale activiteit van 3000 ± 10% MBq, gekalibreerd op 23 uur met een expiratietijdstip 24 uur later. Verder worden een steriele toedienset, toedien V-vial, perspex V-vial houder en perspex delivery box (voor zover besteld) meegeleverd.

Toediening van de dosis ^{90}Y-microsferen

Het toedienen van de dosis gebeurt op de angiokamer door een nucleair geneeskundige in samenwerking met een interventieradioloog. Daarbij is van belang dat de katheter op exact dezelfde plaats ligt als bij de ^{99m}Tc-MAA procedure. Bij een andere ligging van de katheter wordt de voorspellende waarde van de ^{99m}Tc-MAA procedure ondermijnd en bestaat er alsnog een risico op extrahepatische depositie van de microsferen. Tijdens toediening van de dosis wordt herhaaldelijk met contrast gecontroleerd of er geen stasis van de bloodflow en/of backflow is. In dit geval wordt de toediening gestaakt. Na de toediening worden toedienset, katheter en toedienvial teruggemeten, zodat de netto toegediende activiteit kan worden bepaald.

^{90}Y-scintigrafie posttherapie

Om de therapie te evalueren worden de ochtend na de behandeling planaire en SPECT(-CT) bremsstrahlung opnamen vervaardigd (11). In plaats van een SPECT kan ^{90}Y-PET overwogen worden (12). Voor de interpretatie is van belang:

- Focale uptake buiten de lever. Dit is een indicatie voor eventuele behandeling met Amifostine (een organisch thiofosfaat, dat het gezonde weefsel beschermt tegen cytotoxiciteit van ioniserende straling). Overleg met de hoofdbehandelaar is met enige spoed geïndiceerd.
- Shunting naar de longen. Ook dit is een indicatie voor eventuele behandeling met Amifostine. Overleg met de hoofdbehandelaar is met enige spoed geïndiceerd.
- Verdeling binnen de lever. Is er focale uptake ter plaatse van de tumoren? Welk deel van de lever wordt behandeld?
- Zijn er onbehandelde laesies? Is een tweede behandeling noodzakelijk?

Bijwerkingen en follow-up

^{90}Y-radioembolisatie gaat dikwijls gepaard met verschijnselen behorend bij het zogenaamde 'post-embolisatiesyndroom' (6). Dit syndroom bestaat uit vermoeidheid, buikpijn, misselijkheid en/of braken en koorts maar is van tijdelijke aard (tot 14 dagen na de behandeling) en veelal medicamenteus te onderdrukken. Sommige patiënten krijgen direct na het toedienen van de microsferen hevige abdominale pijn, die meestal binnen een aantal uren tot een dag weer verdwijnt. Complicaties die zijn beschreven zijn doorgaans het gevolg van onbedoelde extrahepatische depositie van ^{90}Y-microsferen en behelzen gastritis/duodenitis, gastrointestinale ulcera, pancreatitis, radiatie pneumonitis en cholecystitis (13). Het risico op deze complicaties wordt enorm verminderd door een juiste patiëntenselectie, een nauwgezet uitgevoerde angiografische procedure en goede training van de interventieradioloog en nucleair geneeskundige. Indien een te hoge dosis radioactiviteit in de lever wordt geïmplanteerd, kan dit 'radiation induced liver disease' (RILD) veroorzaken. RILD wordt in het geval van ^{90}Y-radioembolisatie histologisch gekenmerkt door micro-infarcten en portale triaditis, en gaat gepaard met ascites. Deze zeldzame complicatie kan zich tot maanden na de ^{90}Y-radioembolisatie manifesteren en is meestal met corticosteroïden onder controle te brengen. In een aantal in de literatuur beschreven cases heeft dit geleid tot fulminant leverfalen (14). RILD kan worden voorkomen door een correcte patiëntenselectie (leverfunctie) en verlaging van de dosis bij kleine individuen (lichaamsoppervlakte).
Bij de overgrote meerderheid van de patiënten is de morbiditeit laag.

De eerste poliklinische controle vindt circa twee weken na de therapie plaats door een van de artsen betrokken bij de radioembolisatietherapie. Overige controles kunnen weer worden gedaan door de verwijzend arts. Verdere poliklinische bezoeken worden geadviseerd na 4, 8 en 12 weken. Naast de kliniek is controle van de leverfunctie daarbij belangrijk. De respons kan gecontroleerd worden middels CT, MRI en/of ^{18}F-FDG PET. In het algemeen vindt de eerste beeldvorming circa drie maanden na de therapie plaats.

Referenties

1. Vente MA, Wondergem M, van der Tweel I et al. Yttrium-90 microsphere radioembolization for the treatment of liver malignancies: a structured meta-analysis. Eur Radiol. 2009;19:951-9
2. Kennedy A, Salem R. Radioembolization (Yttrium-90 microspheres) for primary and metastatic hepatic malignancies. Cancer J. 2010;16:163-75
3. Sangro B, Salem R, Kennedy A et al. Radioembolization for hepatocellular carcinoma: a review of the evidence and treatment recommendations. Am J Clin Oncol. 2011;34:422-31
4. Smits ML, Nijsen JF, van den Bosch MA et al. Holmium-166 radioembolization for the treatment of patients with liver metastases: design of the phase I HEPAR trial. J Exp Clin Cancer Res. 2010; 29:70
5. Kennedy A, Nag S, Salem R et al. Recommendations for radioembolization of hepatic malignancies using yttrium-90 microsphere brachytherapy: a consensus panel report from the radioembolization brachytherapy oncology consortium. Int J Radiat Oncol Biol Phys. 2007;68:13-23
6. Ahmadzadehfar H, Biersack H-J, Ezziddin S. Radioembolization of liver tumors with Yttrium-90 microspheres. Semin Nucl Med. 2009;40:105-21
7. Lewandowski RJ, Sato KT, Atassi B et al. Radioembolization with 90Y microspheres: angiographic and technical considerations. Cardiovasc Intervent Radiol. 2007;30:571-92
8. Ahmadzadehfar H, Sabet A, Biermann K et al. The significance of 99mTc-MAA SPECT/CT liver perfusion imaging in treatment planning for Y90-microsphere selective internal radiation treatment. J Nucl Med. 2010;51:1206-12
9. Ahmadzadehfar H, Möhlenbruch M, Sabet A et al. Is prophylactic embolization of the hepatic falciform artery needed before radioembolization in patients with 99mTc-MAA accumulation in the anterior abdominal wall? Eur J Nucl Med Mol Imaging. 2011;38:1477-84
10. Lewandowski R, Salem R. Incidence of radiation cholecystitis in patients receiving Y-90 treatment for unresectable liver malignancies. J Vasc Interv radiol. 2004;15:S162
11. Ahmadzadehfar H, Muckle M, Sabet A et al. The significance of bremsstrahlung SPECT/CT after yttrium-90 radioembolization treatment in the prediction of extrahepatic side effects. Eur J Nucl Med Mol Imaging. 2011. Epub ahead of Print
12. Gates VL, Esmail AA, Marshall K et al. Internal pair production of Y-90 permits hepatic localization of microspheres using routine PET: proof of concept. J Nucl Med. 2011;52:72-6
13. Murthy R, Nunez R, Szklaruk J et al. Yttrium-90 microsphere therapy for hepatic malignancy: devices, indications, technical considerations, and potential complications. Radiographics. 2005:25; 41-S55
14. Kennedy AS, McNeillie P, Dezarn WA et al. Treatment parameters and outcome in 680 treatments of internal radiation with resin 90Y-microspheres for unresectable hepatic tumors. Int J Radiat Oncol Biol Phys. 2009;74:1494-500

Extremity dosimetry for nuclear medicine workers

Dr. F. Vanhavere[1], Dr. L. Struelens[1], Dr. A. Carnicer[2], Prof. M. Ginjaume[2], Dr. M. Sans-Merce[3], Dr. L. Donadille[4], I. Barth[5]

[1] *Belgian Nuclear Research Centre (SCK-CEN), Mol, Belgium*
[2] *Universitat Politecnica de Catalunya (UPC), Barcelona, Spain*
[3] *University Hospital Center (CHUV), University of Lausanne, Switzerland*
[4] *Institut de Radioprotection et de Sûreté Nucléaire (IRSN), Fontenay-aux-Roses, France*
[5] *Bundesamt für Strahlenschutz (BfS), Berlin, Germany*

For workers involved in the preparation, labeling or injection of radiopharmaceuticals, radiation exposure is not homogeneous over the whole body, but is mostly localised on the hands. Therefore the monitoring of extremities and skin is required for workers who may receive an annual equivalent dose higher than thirty percent of the limit for hands and skin, that is 150 mSv. The 500 mSv annual dose limit for the extremities applies to the most exposed area of the skin. Even across the hands, the radiation exposure can be very inhomogeneous, so it is important to be able to estimate the maximum local skin dose.
This text provides information on hand doses for nuclear medicine workers and guidance to monitor them, mainly based on the results of the ORAMED project (www.oramed-fp7.eu).

In order to determine the dose distribution across the hands and to supply information on reference dose levels for the most frequent nuclear medicine procedures, a measurement campaign was performed within the ORAMED project.
It included 139 workers from 35 departments in seven European countries (Belgium, France, Germany, Italy, Slovakia, Spain and Switzerland) representing the largest amount of collected data on extremity dosimetry in nuclear medicine up to now (1). The operational personal dose equivalent $H_p(0.07)$ was measured at eleven positions on each hand, considering both the usually expected highest exposed areas (fingertips and fingernails) and the most practical and frequently used positions for routine monitoring (wrist and bases of the fingers). The most frequently employed radionuclides for diagnostics were considered: ^{99m}Tc and ^{18}F. For therapy, ^{90}Y was considered since the handling of this radionuclide is associated with high extremity doses. Measurements were performed separately for each radionuclide and independently for preparation and administration. The experimental data were complemented with Monte Carlo (MC) simulations to better determine the main parameters that influence extremity exposure and the effectiveness of different radiation protection measures. Details on the Monte Carlo protocol and results are described by Ferrari et al (2).

Hand dose distribution

Although hand dose distributions vary between workers and techniques, general trends could be observed. The tips of the fingers of both hands, especially the index and thumb, were identified to be the highest exposed positions. There is general agreement on this issue (3-7). The least exposed positions were found to be the wrists, followed by the bases of the fingers. A clear trend was observed for the non-dominant hand to be more exposed than the dominant hand, in particular for radionuclide preparation. However, this trend was strongly linked to individual working habits. The influence of individual working habits on the most exposed hand and position has also been pointed out in several works (3, 5, 6). For therapy, spatial dose heterogeneity is usually much more pronounced, especially when the radiation protection standard is low. However, in most cases the index tip of the non-dominant hand is still the most exposed position (8, 9).

Maximum skin dose to the hands

For each worker the doses measured at eleven positions on each hand were normalized to the manipulated activity and averaged over the number of measurements he performed. Then, the maximum normalized dose for each worker, $<H_p(0.07)/A>_{max}$, was determined. Table 1 presents the range, median and mean of $<H_p(0.07)/A>_{max}$ over all monitored workers, classified per procedure. It is shown that preparation of radiopharmaceuticals involves higher finger doses per activity than administration because the procedures are longer and there are more steps requiring manipulations of the vials and/or syringes with higher activities, some of them without shielding. Therapy procedures with ^{90}Y involve generally higher mean normalized skin dose to the hands than diagnostics. Within diagnostics ^{18}F involves higher skin doses per activity than ^{99m}Tc because of the different dose rates at contact. Considering typical workloads, preparation of ^{18}F was found to be the most critical of the studied procedures, which is in agreement with other authors' findings (3,4).

Parameters of influence on skin dose to the hands

Shielding was found to be the most important parameter

Table 1. Mean, median, maximum and minimum values of $< H_p(0.07)/A >_{max}$ over all monitored workers per procedure. A stands for administration and P for preparation. Adapted from Sans-Merce et al (1).

	Maximum doses from all workers (mSv/GBq)			
	mean	median	minimum	maximum
P – ^{99m}Tc	0.43	0.25	0.03	2.06
A – ^{99m}Tc	0.23	0.12	0.01	0.95
P – ^{18}F	1.20	0.83	0.10	4.43
A – ^{18}F	0.93	0.64	0.14	4.11
P – ^{90}Y Zevalin	11.0	9.5	1.2	43.9
A – ^{90}Y Zevalin	4.8	2.9	1.0	11.9

affecting skin dose levels, both for diagnostics and especially for therapy. This result is in agreement with the conclusions of ICRP Publication 106 (10) and with other authors' findings (11-13). Even though the use of shielding slows down the whole procedure, increases the difficulty of visualising the required volume and offers less comfort, it results in a dose reduction which cannot be achieved by increasing the working speed. The ORAMED measurement campaign shows that the use of shielding provided a skin dose reduction of a factor from 2 to 5 for diagnostic procedures. Monte Carlo simulations were found to be very useful to decide which was the adequate shielding for each procedure among those most commonly used in the nuclear medicine departments participating to the project. The minimal requirement of shielding for a syringe is 2 mm of tungsten for ^{99m}Tc and 5 mm of tungsten for ^{18}F. For ^{90}Y, 10 mm of PMMA shields completely the beta radiation, but 5 mm of tungsten increases the effectiveness by shielding also the bremsstrahlung photons. The minimal required shielding for a vial is 3 mm of tungsten for ^{99m}Tc and 3 cm of tungsten for ^{18}F. For ^{90}Y, an acceptable shielding is provided with 10 mm of PMMA with an external layer of a few millimeters of lead.
In the ORAMED study only a weak trend was observed for experience to entail lower doses for diagnostic procedures, but it was not statistically significant. When analyzing individual cases of high maximum doses, good working habits were found to be more important than experience.
All practices avoiding direct contact and enlarging distances to the sources can be considered as good practices. Most bad working habits involved direct source contact. Often staff is not aware that near the bottom of a shielded syringe the dose rate is very high. Using tweezers is a very effective means of dose reduction, particularly when vials or syringes have to be held without a shield and during the connection to or separation from the syringe needles or butterflies.

Routine extremity monitoring

As regards detector technical requirements, Carnicer et al (14) demonstrate that for ^{99m}Tc measurements thick standard TLDs (up to 100 mg·cm^{-2}) are appropriate, whereas for ^{18}F and ^{90}Y thin TLDs (up to 10 mg·cm^{-2}) are recommended to avoid potential underestimations (up to 50%) because of the electron and positron radiation. The ratios between the highest dose and the dose at the most common monitoring positions vary from 2 to around 90 for the wrist and from 1 to around 50 for the base of the index. This variability is due to the fact that the dose distribution is strongly operator and technique dependent. The results of the ORAMED project show that the ratio between the maximum dose, considering all positions in both hands, and the dose on the index tip of the non-dominant hand was the lowest one. However, as there are very few dosimetric systems designed to be situated at this position and since it can cause discomfort, a more practical solution is to wear a ring dosemeter placed on the base of the index finger of the non-dominant hand, with the detector facing the palm of the hand. This recommended position is different from that proposed in other works such as ICRP 106 (10). The measured dose at the base of the index finger underestimates the maximum dose for diagnostics and therapy by a factor of about six. Similar correction factors were reported (7,15), but also lower ones, typically of the order of one to four (10,16). ICRP 106 (10) recommends for the estimation of $H_p(0.07)$ a dosemeter placed on the base of the middle finger with the element positioned on the palm side. For this position, ICRP recommends a factor of three to obtain an estimate of the dose to the tip, and of six if the dosemeter faces the back of the hand. ORAMED results show that this correction might be too low in many cases. Finally, it should be noted that there is broad agreement that, in nuclear medicine, the ring dosemeter should be preferred to the wrist dosemeter, which underestimates the maximum dose by a factor of around twenty (1,7).

From the analysis of ORAMED results (4) and other published works on extremity dosimetry in nuclear medicine, recommendations are proposed to improve radiation protection of nuclear medicine staff. These guidelines and training material can be downloaded for free from the website

http://www.oramed-fp7.eu/. In addition, the website provides the instructions to receive an easy tool to estimate hand dose distribution for typical nuclear medicine procedures upon acceptance of freeware license agreement.

References

1. Sans Merce M, Ruiz N, Barth I et al. Recommendations to reduce hand exposure for standard nuclear medicine procedures. Ra¬diat. Meas. 2011;46:1330–3
2. Ferrari P, Sans Merce M, Carnicer A et al. Main results of the Monte Carlo studies carried out for nuclear medicine practices within the ORAMED project. Radiat. Meas. 2011;46(11):1287–90
3. Vanhavere F, Berus D, Buls N et al. The use of extremity dosemeters in a hospital environment. Radiat. Prot. Dosim. 2006;118(2):190–5
4. Covens P, Berus D, Vanhavere F et al. The introduction of automated dispens¬ing and injection during PET procedures: a step in the optimization of extremity doses and whole-body doses of nuclear medicine staff. Radiat. Prot. Dosim. 2010;140(3):250–8
5. Martin C and Whitby M. Application of ALARP to extremity doses for hospital workers. J. Radiol. Prot. 2003;23:405–21
6. Mebhah D, Djeffal S, Badreddine A et al. Extremity dosimetry in nuclear medicine services using thermoluminescent detectors. Radiat. Prot. Dosim. 1993;47:439–43
7. Jankowski J, Olszewski J and Kluska K. Distribution of equivalent doses to skin of the hands of nuclear medicine personnel. Radiat. Prot. Dosim. 2003;106:177–80
8. Carnicer A, Sans Merce M, Baechler S et al. Hand exposure in diagnostic nuclear medicine with ^{18}F and ^{99m}Tc -labelled radio-pharmaceuticals - results of the ORAMED project. Radiat. Meas. 2011;46:1277–82
9. Rimpler A, Barth I, Ferrari P et al. Extremity exposure in nuclear medicine therapy with 90Y-labelled substances - Results of the ORAMED project. Radiat. Meas. 2011;46:1283–6
10. International Commission on Radiological Protection. Radiation dose to patients from radiopharmaceuticals - Addendum 3 to ICRP Publication 53. ICRP Publication 106. Ann. ICRP 38 (1-2), Annex E. International Commission on Radiological Protection (2008)
11. Montgomery A, Anstee D, Martin C and Hilditch T. Reductions in finger doses for radiopharmaceutical dispensing afforded by a syringe shield in an automatic dose dispenser Nucl. Med. Commun. 1999;20:89–94
12. Tsopelas C, Collins P and Blefari C. A simple and effective technique to reduce staff exposure during the preparation of radiopharmaceuticals. J. Nucl. Med. Technol. 2003;31:37–40
13. Whitby M and Martin CA. Multi-centre study of dispensing methods and hand doses in UK hospital radiopharmacies. Nucl. Med. Commun. 2005;26:49–60
14. Carnicer A, Ginjaume M, Duch M et al. The use of different types of thermoluminescent dosemeters to measure extremity doses in nuclear medicine. Radiat. Meas. 2011;46:1835–8
15. Wrzesien M, Olszewski J and Jankowski J. Hand exposure to ionising radiation of nuclear medicine workers. Radiat. Prot. Dosim. 2008;130:325–30
16. Covens P, Berus D, Buls N et al. Personal dose monitoring in hospitals: global assessment, critical applications and future needs. Radiat. Prot. Dosim. 2007;124:250-9

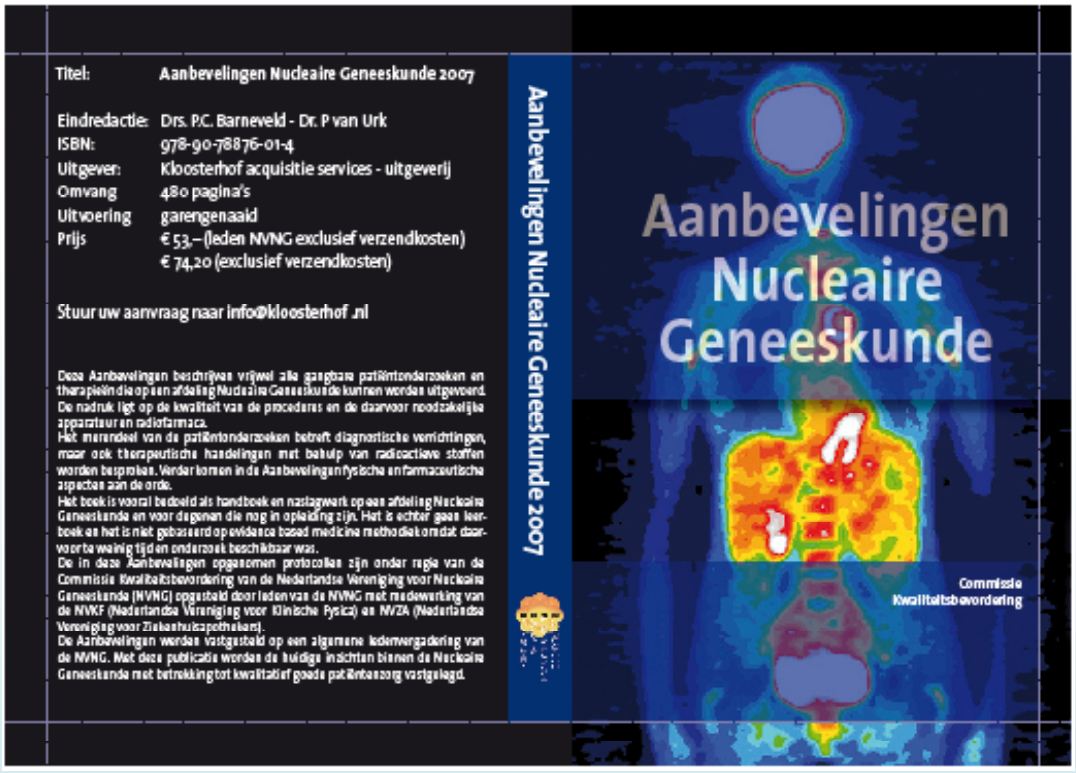

The production of medicinal ^{177}Lu and the story of ^{177m}Lu: detrimental by-product or future friend?

Dr. D.J. De Vries*
Dr. H.T. Wolterbeek

Radiation and Isotopes for Health (RIH), Department of Radionuclides, Radiation & Reactors (R3), Delft University of Technology, Delft, The Netherlands

** Corresponding author: Daniel.DeVries@tudelft.nl*

Abstract

De Vries DJ, Wolterbeek HT. The production of medicinal ^{177}Lu and the story of ^{177m}Lu: detrimental by-product or future friend? The radionuclide ^{177}Lu has become essential in various types of radiotherapy. In the Netherlands alone, more than 400 patients per year are treated with this radionuclide. To date, many scientific publications have concerned themselves with the variety of uses for ^{177}Lu. However, relatively few have aimed to explain the separate production routes or address the reasons why the vast majority of ^{177}Lu, produced for medical use, comes from the irradiation of enriched ^{176}Lu targets in high flux nuclear reactors. This work describes the thought processes involved in deciding which production route is best and details the complexities involved in calculating specific activity, total activity, and quantifying radioactive impurities. Additionally, the amount (and potential impact) of ^{177m}Lu is discussed with respect to total patient dose. The authors also suggest a potential use for this long-lived radionuclide.
Tijdschr Nucl Geneesk 2012; 34(2):899-904

Introduction

Late in the twentieth century, researchers at the National Institutes of Health (Bethesda, Maryland, USA) reported the first use of a ^{177}Lu labeled immunoconjugate as a therapy for a human carcinoma (1). Since these first promising results, ^{177}Lu has grown in application and production. In fact, ^{177}Lu radionuclide has recently become one of the work-horse radionuclides for peptide-receptor radionuclide therapy (PRRT). In the Netherlands alone, more than ten patients per week, ~9.25 GBq per patient, are treated with some form of ^{177}Lu. In fact, one major ^{177}Lu supplier (located in the Netherlands) produces ~750 GBq of ^{177}Lu per week. These figures do not necessarily include production or use of ^{177}Lu in research activities.
Given the growth in use and production over the past two decades, and the projected growth over the coming decades, the importance of ^{177}Lu gives clear motivation for this article. This work will provide an explanation and evaluation of the current, most probable production routes; to include charged particle reactions, the use of high energy neutron generators, and production in nuclear reactors. Since it is widely known that the majority of ^{177}Lu is produced by nuclear reactors, this production route will be further scrutinised by examining the following; reaction cross-sections, target composition, specific activity (SA), irradiation time, and radionuclide purity. Finally, since the development of a radioisotope production scheme is a never-ending process, the problem and potential of ^{177m}Lu will be discussed.
The following is a very brief explanation concerning the basics of radionuclide production. In order to facilitate greater understanding, the terms cross-section and flux are defined as they pertain to the simplified equation for radionuclide production:

$$N_t = \sigma \Phi N_0 (1-e^{-\lambda t})$$

where:
N_t = the number of product atoms at time (t)
σ = the reaction cross section in barns (b)
Φ = the incident particle flux (e.g. ^{1}n, ^{1}H, or ^{2}H)
N_0 = the number of target atoms at time (t = 0)
λ= the decay constant of the product radionuclide ($\lambda=\ln(2)/t_{½}$)
t = the duration of exposure to the incident particle flux

The neutron capture cross section is the effective cross-sectional area of a target nucleus and is expressed in barns (abbreviated b), where one $b=10^{-24}$ cm^2. This proportionality constant means that a large σ equates to a large interaction probability. The flux is simply the number of incident particles (neutrons, protons, etc.) that pass through an area of the sample per unit time. For example, a neutron irradiation flux is expressed in units of $n \cdot cm^{-2} \cdot s^{-1}$. This simplified production equation becomes rapidly more complicated when accounting for a heterogeneous target that produces significant quantities of yet more potential target nuclei. These calculations are further complicated by radioactive decay which, over long irradiation times, leads to even more and different product nuclei.

The production routes (charged particle, neutron generators and reactors)

Charged particle reactions

The use of linear accelerators or cyclotrons for the production of proton rich radioisotopes (especially of low atomic number) is quite common. Examples of this include most of the radioisotopes associated with PET imaging (e.g. ^{13}N, ^{15}O, ^{18}F, ^{68}Ge, ^{124}I, and many others). However, the use of charged particle reactions for the production of neutron rich radionuclides is less common. As the atomic number increases, the number of protons in the nucleus increases, requiring higher and higher particle energies in order to overcome the Coulomb barrier, and cause a nuclear reaction. As a consequence of the increased energies, the resulting nuclear reactions begin to knock out more and more nucleons. For instance, ^{A}X(p,pxn)^{A}Y, where ^{A}X is the target, ^{A}Y is the product, and x is the number of neutrons knocked out in the reaction. Though the incident particle energy remains rather constant, the number of neutrons knocked free during this type of reaction may be quite high. The resulting distribution of products further complicates this production route.

Recently, a group of researchers at the Brookhaven National Laboratory (Upton, NY, USA) explored the feasibility of using high energy protons, impinging on hafnium and tantalum targets, in order to produce medically relevant quantities of ^{177}Lu (2). To summarise their results, they found that for relatively high energy protons (100 – 200 MeV) the largest cross-section for producing ^{177}Lu was only 19.9±2.0 mb (Hf target with 195 MeV protons); the smallest of any of the lutetium isotopes between A=169-172 (the production cross-section for natural $^{175/176}$Lu was not measured). In fact, the production cross-section for the ^{171}Lu ($t_{½}$=8.24 d) was found to be 86.9±8.7 mb. Additionally, in order to reduce the co-production of unwanted lutetium isotopes, the target would have to be significantly enriched in ^{177}Hf.
Production of ^{177}Lu using deuteron irradiations of ytterbium targets was studied by a recent international collaboration at the cyclotron department (VrijeUniversiteitBrussel) (3). This group irradiated natural ytterbium targets and investigated the production cross-sections using deuteron energies between ~3 MeV and ~20 MeV. They found that the main route of ^{177}Lu production is from the ^{176}Yb(d,p)^{177}Yb followed by β- decay, rather than by direct production via the ^{176}Yb(d,n)^{177}Lu reaction. Furthermore, they set an upper limit on the ^{176}Yb(d,n)^{177m}Lu reaction cross-section of 0.1 mb. Ultimately, this group concluded that the use of highly enriched targets would still result in the co-production of several stable or radioactive isotopes which would negatively influence the specific activity of ^{177}Lu. However, under optimal condition they believe that batches of 60 GBq of ^{177}Lu could be produced in 72 hour irradiations (maximum beam intensity of 100 μA). This route would still require the chemical separation of lutetium from the bulk ytterbium target and the specific activity would depend greatly on the time between irradiation and chemical separation.

There remain many difficulties to overcome in the production of ^{177}Lu by charged particle reactions. These include relatively low reaction cross-sections for production, co-production of a variety of lutetium radionuclides (some with half-lives comparable to ^{177}Lu), and complex post-irradiation chemical separation (Lu product from a bulk Hf target). These difficulties lead most to conclude that cyclotron (accelerator) production is not currently a viable route for the large total ^{177}Lu activities required for medical use.

Neutron generators

There are two general types of small neutron generators used for the production of radionuclides: D-D and D-T neutron generators. In each case, deuterium gas is ionised and accelerated to a tritium or deuterium target (usually present as a metal deuteride or tritide). These generator systems have three main advantages over nuclear reactor produced neutrons in that they can be easily (and quickly) switched on and off, they produce relatively monoenergetic neutrons (2.5 MeV and 14.1 MeV; D-D and D-T respectively), and they are small enough that any hospital or production facility could possess one. However, the main disadvantage is that their typical flux is relatively low: on the order of 10^{10} n·cm^{-2}·s^{-1}. Generally speaking, the D-D neutron generator is of limited utility in radionuclide production because of typically small reaction cross-sections at ~2.5 MeV.

There are relatively few ways to produce ^{177}Lu with neutron generators: 181Ta(n,nα)^{177}Lu, ^{180}Ta(n,α)^{177}Lu, and ^{177}Hf(n,p)^{177}Lu. For each of these reactions the production cross-sections for 2.5 MeV neutrons are <<1μb. For 14 MeV neutrons the cross-sections are approximately 15 μb, 1 mb, and 1 mb respectively (4). Each of these routes has at least one significant disadvantage. The ^{181}Ta(n,nα)^{177}Lu reaction actually favors production of ^{177m}Lu, with a cross-section of 51 mb (5). The natural abundance of ^{180}Ta is only 0.012%, which would require a very expensive, and significantly enriched isotopic target for the ^{180}Ta(n,α)^{177}Lu reaction. For the ^{177}Hf(n,p)^{177}Lu reaction, competition from the ^{176}Hf(n,p)^{176}Lu (σ=~1.6 mb) would also require the use of an isotopically enriched target. A one week irradiation (14.1 MeV neutrons) of a 100% enriched ^{177}Hf target would produce <247 kBq of ^{177}Lu. Therefore, the combination of low total neutron flux, low reaction cross-section, the potential expense of enriched isotopic targets, and co-production of stable lutetium make ^{177}Lu production via neutron generators less than viable.

High flux reactor (HFR) production (direct and indirect)

The use of nuclear reactors to produce ^{177}Lu has many advantages over the previously discussed routes; chief among these are the neutron flux and maximum target mass. Today's high flux production reactors typically have thermal neutron fluencies of at least 10^{14} n·cm^{-2}·s^{-1} (epithermal and fast neutron fluencies are typically on the order of 10^{14} n·cm^{-2}·s^{-1} as well), and the ability to irradiate samples weighing from micrograms

to hundreds of grams (depending on sample densities). Nuclear reactor production of ^{177}Lu, almost exclusively, follows one of the following two routes; ^{176}Lu(n,γ)^{177}Lu or ^{176}Yb(n,γ)^{177}Yb→^{177}Lu. These are known as the ´direct´ and ´indirect´ routes respectively (figure 1). These routes will be discussed with respect to the following: reaction cross-sections, target composition, specific radioactivity, irradiation time, and radionuclide purity.

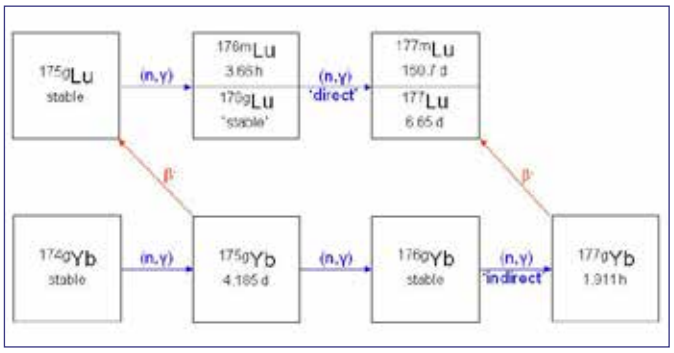

Figure 1. Selected portion of the chart of the nuclides showing neutron activation reactions (blue) and radioactive decay (red). Type of neutron reaction is shown in parentheses. Direct and indirect production routes for ^{177}Lu are shown in blue.

Reaction cross-sections

Perhaps the most important factor influencing reactor production of ^{177}Lu via the direct route is the neutron reaction cross-sections; typically measured in barns (1 b=10^{-24} cm^2). Values for the production cross-section of the ^{176}Lu(n,γ)^{177}Lu reaction are widely quoted, and may include 2043±50 b(6) or 2093±135 b (7) for thermal neutrons. However, epithermal neutron activation, with cross-sections ranging from 1069±41 b (6) to 1013±46 b (7), is quite important and sometimes overlooked. Another very important, and relatively recently published, cross-section influencing lutetium production is for the ^{177}Lu(n,γ)^{178}Lu reaction. The values for this burn-up reaction include 1000±300 b (8) and 880±75 b (9). These values significantly influence the maximum amount of ^{177}Lu that can be produced.

Production of ^{177}Lu via the indirect route is also very dependent on the reaction cross-sections. Typically, these values are 2.4±0.2 b (6) and 5.75±0.50 b (6) for the thermal and epithermal neutron activation of ^{176}Yb. These values are several orders of magnitude lower compared to production via the direct route. This means that the maximum ^{177}Lu activity produced will be much lower (same sample mass and irradiation time). Also significant is the ^{174}Yb(n,γ)^{175}Yb reaction cross-section: 65±5 b (6) and 37.7±1.3 b (6) for thermal and epithermal neutron activation respectively. These values are important because this reaction forms stable ^{175}Lu, leading to a reduction in the specific activity of ^{177}Lu in the final product; further discussed in the specific activity and radionuclide purity sections.

Target composition

Natural lutetium is composed of two stable isotopes, ^{175}Lu and ^{176}Lu, each occurring 97.41% and 2.59% respectively. Natural ytterbium is composed of seven stable isotopes, with ^{174}Yb and ^{176}Yb being the most important concerning the production of ^{177}Lu. In natural ytterbium, the ^{174}Yb and ^{176}Yb species occur 31.83% and 12.76% respectively. Because natural lutetium is only 2.59% ^{176}Lu and natural ytterbium is only 12.76% ^{176}Yb, most producers utilise an enriched isotopic target, to maximise ^{177}Lu production. Enriched stable isotopes can be quite expensive, sometimes costing tens or hundreds of thousands of dollars for a single gram. Table 1 compares the cost, total activity, and specific activity for each production route. Though costly, enriched targets are often seen as a necessity because they produce a correspondingly high specific activity product. The direct route will often employ a target enriched to >80% in ^{176}Lu, while the indirect route may utilise a target enriched to >95% in ^{176}Yb. The effect of enrichment on specific activity will be discussed in the following section.

Specific radioactivity

There is some contention about the definition of specific activity as it pertains to radioisotope production. The following definition comes from the glossary of terms in quantities and units in clinical chemistry, IUPAC-IFCC Recommendations 1996, page 993: for the activity of a material divided by the mass of material, for a specific isotope or mixture of isotopes. For a radiochemist, the specific activity of ^{177}Lu would then be the activity of ^{177}Lu (Bq) in a sample divided by the total mass of lutetium present in the sample; whether it is radioactive

Table 1. Sample characteristics, pre- and post-irradiation. TA: theoretical activity, SA: specific activity, EOI: end of irradiation.

chemical form	enrichment assay	enriched isotope	price per 100 mg ($)	^{177}Lu TA EOI (TBq)	^{177}Lu SA EOI (TBq/100mg)	^{177}Lu cost ($/TBq)
Lu_2O_3	natural		9,31	3,02	3,3	3,08
Lu_2O_3	83,31%	^{176}Lu	34455,00	71,90	80,3	479,21
Yb_2O_3	97,79%	^{176}Yb	2025,00	0,27	35400,0	7500,00

or stable. This explicitly means that co-production of any lutetium isotope, other than that of ^{177}Lu, will lower the resulting specific activity.

The relationship between enriched target materials and the resulting specific activity should now be apparent. The specific activity of ^{177}Lu resulting from the irradiation of natural target, because it is only 2.59% ^{176}Lu, will always be much less than that produced by the irradiation of >80% enriched ^{176}Lu. Production via the direct route, using an enriched target, can theoretically yield a ^{177}Lu specific activity of ~800 TBq/gram of target (~21.6 kCi/gram). This value is approximately 20% of the theoretical maximum specific activity. The use of a natural lutetium target will lower this amount by at least a factor of twenty (~33 TBq/gram). These values represent the maximum specific activities calculated at the end of irradiation and are summarised in table 2. The decay of ^{177}Lu will cause the specific activity to drop as a function of time (table 2). However, because the mass of ^{177}Lu is also changing, this is not always a simple relationship.

In the case of the indirect route, utilising anisotopically enriched target has two purposes. First, the total ^{177}Lu activity produced is directly proportional to how much ^{176}Yb is present in the sample. The second purpose is to reduce the amount of ^{174}Yb present. Neutron capture in ^{174}Yb leads to the production of ^{175}Lu, which reduces the resulting specific activity of ^{177}Lu. Irradiation of a >95% enriched ytterbium target can theoretically produce a specific activity of ~354 PBq/gram (table 2). This value is approximately 86% of the theoretical maximum specific activity. Again, the decay of ^{177}Lu will cause the specific activity to drop as a function of time. This relationship is more complicated than in the direct route because ^{177}Yb (t½=1.911 h) decays to form more ^{177}Lu and ^{175}Yb (t½=4.185 d) decays to produce more ^{175}Lu.

Irradiation time

The duration of irradiation is the most direct way of controlling the amount of radioactivity created by neutron activation. The total activity of ^{177}Lu as a function of irradiation time is shown in figure 2. These activities are calculated for a 100 mg sample and represent the maximum amount of ^{177}Lu present at the end of irradiation (EOI).

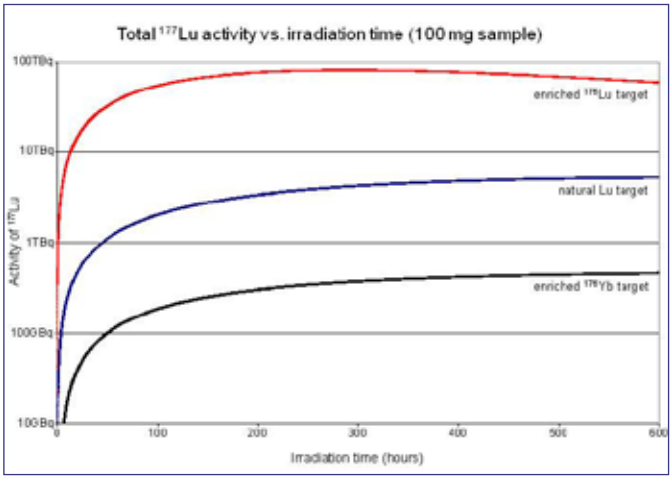

Figure 2. Total ^{177}Lu activity as a function of irradiation time. Calculated total activities are for 100 mg samples; enriched ^{176}Lu target (red), natural Lu target (blue), and enriched ^{176}Yb target (black).

The direct route produces the highest total activity of ^{177}Lu (figure 2) for a given sample mass. This is true for both natural and enriched lutetium. For an enriched target, there is clearly an optimal irradiation time. This is because after a certain point (~290 hours or 12.1 days), burn-up of the ^{177}Lu product begins to overtake production. This maximum is also due to the continuously shrinking number of ^{176}Lu atoms available for activation. However, in 600 hours the ^{177}Lu produced from a natural target has not reached a maximum value. This is because of the relatively large cross-section for the ^{175}Lu(n,γ)^{176}Lu reaction. In effect, a natural target is continuously producing more ^{176}Lu, which is then available for activation. The total activity of ^{177}Lu will continue to rise (although quite slowly) until such time that the supply of ^{175}Lu atoms begins to dwindle.

The indirect route produces significantly less ^{177}Lu activity for a given sample mass (figure 2). In fact, for identical sample masses, the product activity is more than two orders of magnitude lower than for an enriched target via the direct route. For longer irradiation times, the indirect route will continue to produce more total ^{177}Lu activity (and all its by-products) until the number of ^{176}Yb atoms begins to dwindle; at which point the burn-up of ^{177}Lu becomes significant.

Table 2. Specific activity of ^{177}Lu and total Lu mass per injection.

production route	^{177}Lu TA/injection (GBq)	^{177}Lu SA at EOI (TBq/100mg)	Lu mass/injection at EOI (µg)	^{177}Lu SA at 1 wk (TBq/100mg)	Lu mass/injection at 1wk (µg)
natural Lu	9,25	3,3	279,74	1,62	572,15
enriched Lu	9,25	80,3	11,52	43,07	21,37
enriched Yb	9,25	35400,0	2,60	247,71	3,70

Radionuclide purity

Despite the initial purity of the target used to produce ^{177}Lu, many other (radio)nuclides are created during irradiation. Transmutation is an inevitable process that directly depends on the composition of the target, irradiation duration, and decay time following irradiation. The growth of several by-products is shown in figure 3 (for an enriched ^{176}Lu target). The main products of transmutation are by far the stable isotopes of hafnium (^{176}Hf, ^{177}Hf, and ^{178}Hf). In fact, hafnium accounts for more than 10% of the sample mass at the EOI, and grows continually with the decay of lutetium. However, since these by-products are not species of lutetium, they do not impact the specific activity of ^{177}Lu. It is important to note that the relatively large mass of hafnium could negatively impact the chemical processes that follow irradiation (e.g. chemical purification, peptide bonding, etc.). Additionally, two important lutetium radioisotopes are also co-produced; ^{176m}Lu and ^{177m}Lu.

Following a seven day irradiation (enriched ^{176}Lu target in a HFR), there are approximately three atoms of ^{176m}Lu per thousand atoms of ^{177}Lu (figure 3). This may not seem like a large amount, but because of the much shorter half-life (t½=3.66 hour), the activity at the EOI is only a factor of eight lower than ^{177}Lu. The total ^{176m}Lu activity falls dramatically after an appropriate cooling time. However, in many cases this cooling time is approximately 24 hours; only 6.6 half-lives (reduction by a factor of 94). The remaining ^{176m}Lu will continue to produce ^{176}Hf until it has completely decayed. Because of its relatively short half-life, and the time between production and injection, it is doubtful that ^{176m}Lu could play any significant role in the end-use of the ^{177}Lu product.

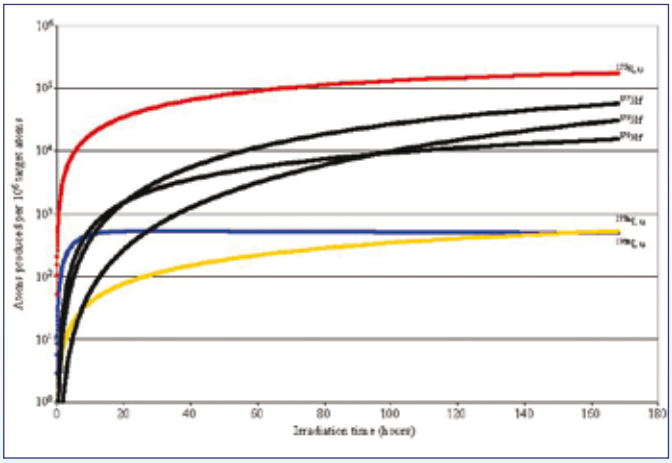

Figure 3. Number of atoms produsedper 10^6 target atoms as function of irradiation time. The ^{177}Lu product (red) clearly is produced in larger amounts. The stable hafnium isotopes (black) are produced in sginificant amounts; only a factor of three between ^{177}Lu and ^{177}Hf. The largest radioactive by-products, ^{177m}Lu and ^{176m}Lu, are shown in blue and yellow, respectively.

Lutetium-177 peptide receptor radionuclide therapy (^{177}Lu-PRRT) is a type of cancer treatment consisting of four components. As the name implies, there is a *peptide* (which targets a specific *receptor*), a *radionuclide*, and a *therapeutic* step. Generally speaking, a radionuclide is chemically attached to a biological targeting agent, injected into a patient, and the energy of the radioactive decay kills tumor cells. The following text further elucidates ^{177}Lu-PRRT.

Octreotate is an amino acid sequence (or peptide) that is closely related to ocreotide, and mimics the naturally occurring somatostatin hormone. This relatively small peptide has a much longer biological half-life (almost two hours) than natural somatostatins. Octreotate serves as a targeting agent to help concentrate the radioactivity in and around the cancer cells. This peptide is often conjugated with a chelator (DOTA) which forms a more stable complex with the lutetium. The chelator helps to ensure the radioactivity is not allowed to move through the body freely. This is the 'peptide' part of ^{177}Lu-PRRT.

Many neuroendocrine tumors strongly over-express receptors for the somatostatin hormone. Since octreotate (and the chelator/radioactivity) also binds very strongly to these receptors, it will accumulate in and on these tumor cells. Tumor cells contain many times the number of somatostatin receptos as healthy cells, and therefore accumulate many times the radioactivity. This is the 'receptor' part of ^{177}Lu-PRRT.

The element lutetium is the 71st element on the periodic table and is the last of the group known as the lanthanoids (or rare earth metals). The radionuclide ^{177}Lu is one of the more than thirty known radioactive isotopes of lutetium. It has a half-life of 6.65 days and its chemistry is very similar to that of other elements with a 3$^+$ oxidation state. The decay characteristics of ^{177}Lu that make it attractive from a therapeutic point of view are the 6.65 day half-life, the maximum beta decay energy of 498 keV, and two rather intense gamma rays. The maximum beta energy corresponds to a tissue penetration depth of about two millimeters. The two gamma rays, 208 keV and 113 keV, are useful for imaging with a gamma camera and can be used for dosimetry purposes.

The Erasmus Medical Center, Rotterdam is one of the world's foremost institutions performing pioneering research and clinical treatment in ^{177}Lu-PRRT. For more information on this therapy at Erasmus MC, please visit their website at http://www.erasmusmc.nl/nucleaire_geneeskunde/prrt/.

Curiously, the number of atoms of ^{177m}Lu produced in a seven day irradiation (enriched ^{176}Lu target in a HFR) is approximately the same as ^{176m}Lu (figure 3). The resulting activity of ^{177m}Lu may be potentially significant because of its decay characteristics. At one week post-irradiation (enriched ^{176}Lu in a HFR), a patient dose of 9.25 GBq (~250 mCi) will contain ~2.35 MBq of ^{177m}Lu. This high-spin isomer has a half-life of 160.44 days (~24 times longer than ^{177}Lu) and decays by two separate routes: 78.3% by β- decay and 21.7% by isomeric transition (IT). The decay scheme of ^{177m}Lu is rather complicated. The relatively intense γ-ray transitions, especially the electric quadrupole (E2) transitions, are accompanied by significant conversion electron and X-ray emission. The dose from the ^{177m}Lu impurity is often neglected when calculating the total patient dose (10-11), because its activity is relatively minor compared to ^{177}Lu. However, if the relatively long-lived ^{177m}Lu radionuclide is allowed to freely roam the body (disconnected from its targeting agent), it would be available for uptake or deposition in healthy tissues. Therefore, it may not be correct to assume a negligible dose due to ^{177m}Lu.

The ^{177m}Lu problem and its potential

Each time a ^{177m}Lu nucleus decays (by either IT or β-) it is accompanied by rather significant conversion electron emission. The loss of inner shell electrons (especially in high atomic number materials) often leads to an Auger cascade; a series of electron emissions that leave the atom in a high charge state. The inevitable loss of valence shell electrons often leads to a rupturing of all chemical bonds. This may result in a separation of the newly formed ^{177}Lu / ^{177m}Hf atom from the biological agent that is responsible for bringing it to its intended target. Depending on the decay / de-excitation route, the Auger cascade will set free one of the following two products: ^{177m}Lu→^{177m}Hf ($t_{½}$=1.08 sec) or ^{177m}Lu→^{177}Lu ($t_{½}$=6.67 day). Within the body, the ^{177m}Hf activity could move freely of its targeting agent before it de-excites to ^{177}Hf. However, given its relatively short half-life, this distance will not be far. In the case of the IT from ^{177m}Lu to ^{177}Lu, the relatively long half-life could result in measureable dose rates to organs where lutetium accumulates.

Despite the potential risk of ^{177m}Lu contained within a typical patient dose, this radionuclide is not without potential. Perhaps in the future a ^{177}Lu generator may be produced from a large stock of ^{177m}Lu. Producing such a device would have several problems to surmount, including production of high specific activity (SA) ^{177m}Lu, identifying an efficient separation technique, and ensuring radionuclide purity of the final product. However, the potential benefits of such a generator would include: the potential for producing very high SA ^{177}Lu, reduced dependency on weekly irradiations, and the possibility for on-site production (as with a ^{99}Mo / ^{99m}Tc generator).

Conclusions

The majority of ^{177}Lu produced for medical use comes from HFR irradiations of enriched ^{176}Lu targets. The preceding discussion of the possible production routes should make the reasoning for this choice apparent. However, further investigation of the potential dose to patients is warranted given the co-production of ^{177m}Lu associated with the direct route. Furthermore, the potential use of ^{177m}Lu, as the ^{177}Lu parent, in a radionuclide generator should also receive additional attention.

References

1. Schlom J, Siler K, Milenic DE et al. Monoclonal Antibody-based Therapy of a Human Tumor Xenograft with a ^{177}Lutetium-labeled Immunoconjugate. Canc Res.1991;51:2889-96
2. Medvedev MG, Mausner LF, Greene GA, Hanson AL Activation of natural Hf and Ta in relation to the production of ^{177}Lu. ApplRadiatIsot.2006;66:1300-6
3. Hermanne A, Takacs S, Goldberg MB, et al. Deuteron-induced reactions on Yb: Measured cross sections and rational for production pathways of carrier-free, medically relevant radionuclides. NuclInstrum Meth Physics Res B. 2006;247:223-31
4. Evaluated Nuclear Data File (ENDF) Retrieval & Plotting. http://www.nndc.bnl.gov/sigma/. National Nuclear Data Center (NNDC), Brookhaven National Laboratory, Upton, New York, USA.
5. Dzysiuk N, Kadenko I, Koning AJ, Yermolenk R. Cross sections for fast-neutron interaction with Lu, Tb, and Ta isotopes. Physical Review C.2010;81:014610
6. Erdtmann, Gerhard. Neutron activation tables. Gerhard ErdtmannVerlag Chemie, Weinheim; New York, USA, 1976.
7. Handbook of Nuclear Activation Data, Technical Reports Series No. 273, IAEA, Vienne, 1987.
8. Roig O, Bélier G, Daugas JM et al. High spin K isomeric target of ^{177m}Lu. Nuclear Instruments and Methods in Physics Research A.2004;521:5-11
9. Bélier G, Roig O, Daugas JM et al.. Thermal neutron cross section for the K isomer ^{177}Lu^{m}. Physical Review C.2006;73:014603.
10. Lewis JS, Wang M, Laforest R et al. Toxicity and dosimetry of ^{177}Lu-DOTA-Y3-Octreotate in a rat model.International Journal of Cancer.2001;94:873-7
11. Schmitt A, Bernhardt P, Nilsson O et al. Biodistribution and dosimetry of ^{177}Lu-labled [DOTA^{0},Tyr^{3}]Octreotate in male nude mice with human small cell lung cancer. Cancer Biotherapy & Radiopharmaceuticals.2003;18:593-9

Making bone inflammation/infection simpler to detect

Scintimun® 1mg

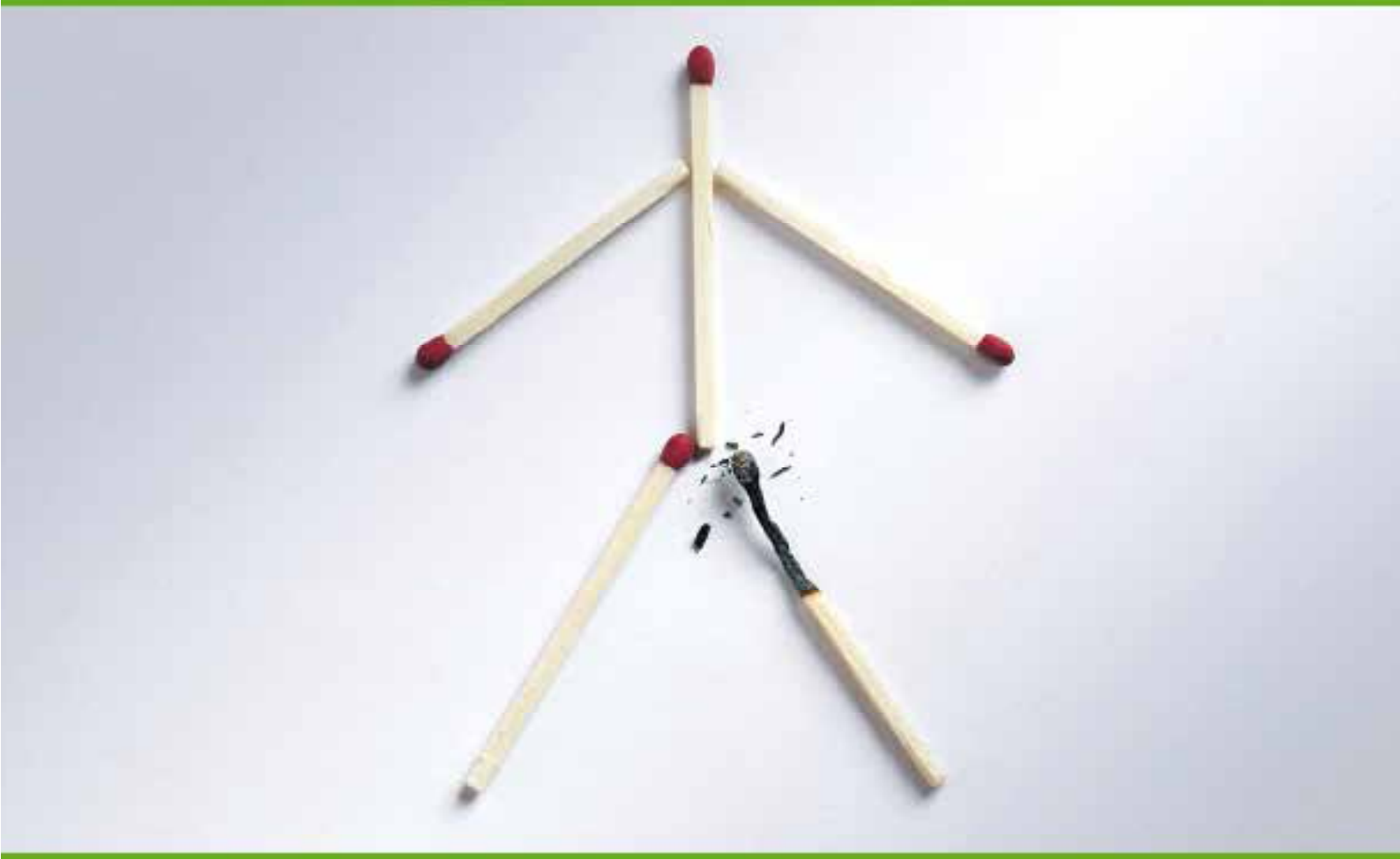

PRESCRIBING INFORMATION: Scintimun 1 mg kit for radiopharmaceutical preparation. Please refer to the full Summary of Product Characteristics (SPC) before prescribing Detailed information on this medicinal product is available on the website of the European Medicines Agency (EMEA) http://www.emea.europa.eu. **PRESENTATION:** Vial containing 1 mg of besilesomab, anti-granulocyte monoclonal antibody (BW 250/183), produced in murine cells. Excipients: contains 2 mg of sorbitol / vial of Scintimun. **DIAGNOSTIC INDICATIONS:** Scintigraphic imaging, in conjunction with other appropriate imaging modalities, for determining the location of inflammation/infection in peripheral bone in adults with suspected osteomyelitis. Scintimun should not be used for the diagnosis of diabetic foot infection. **DOSAGE AND METHOD OF ADMINISTRATION:** Scintimun should be reconstituted with the solvent provided and then radiolabelled with sodium pertechnetate (99mTc) injection in order to obtain a clear and colourless technetium (99mTc) besilesomab injection. In adults, the recommended activity of technetium (99mTc) besilesomab should be between 400 MBq and 800 MBq. This corresponds to the administration of 0.25 to 1 mg of besilesomab. Scintimun is not recommended for use in children below the age of 18 years due to insufficient data on safety and efficacy. Scintimun should be given to sufficiently hydrated patients. In order to obtain images of best quality and to reduce the radiation exposure of the bladder, patients should be encouraged to drink sufficient amounts and to empty their bladder prior to and after the scintigraphic examination. SPECT imaging should start 3 to 6 hours after administration. An additional acquisition 24 hours after initial injection is recommended. Acquisition can be performed using planar imaging. **CONTRAINDICATIONS:** In patients with hypersensitivity to besilesomab, other murine antibodies or any of the excipients, in patients with positive screening test for human anti-mouse antibody (HAMA), and pregnancy. **WARNINGS AND PRECAUTIONS:** This medicinal product is for use in designated nuclear medicine facilities only, and should only be handled by authorised personnel. It should be prepared by the user in a manner which satisfies both radiation safety and pharmaceutical quality requirements. There are currently no criteria to distinguish infection and inflammation by means of Scintimun imaging. Scintimun images should be interpreted in the context of other appropriate anatomical and/or functional imaging examinations. Only limited data is available about binding of technetium (99mTc) besilesomab to Carcino Embryonic Antigen (CEA)-expressing tumors in vivo. In vitro, besilesomab cross-reacts with CEA. False positive findings in patients with CEA-expressing tumours cannot be excluded. False results may be obtained in patients with diseases involving neutrophil defects and in patients with haematological malignancies including myeloma. Scintimun contains sorbitol: therefore patients with rare hereditary problems of fructose intolerance should not be administered this product. Human Anti-Mouse Antibodies (HAMA): Administration of murine monoclonal antibodies can lead to the development of Human Anti-Mouse Antibodies (HAMA). Patients who are HAMA positive may have a greater risk for hypersensitivity reactions. Inquiry on possible previous exposure to murine monoclonal antibodies and a HAMA test should be made prior to administration of Scintimun; a positive response would contraindicate the administration of Scintimun. Repeated use: Scintimun should only be used once in a patient's lifetime. Hypersensitivity reactions: Anaphylactic or anaphylactoid reactions may occur after administration of the medicinal product. Appropriate cardiopulmonary resuscitation facilities and trained personnel should be available for immediate use in the event of an adverse reaction. Since allergic reactions to the murine protein cannot be excluded, cardiovascular treatment, corticosteroids, and antihistamines must be available during administration of the product. **INTERACTIONS:** Active substances which inhibit inflammation or affect the haematopoietic system (such as antibiotics and corticosteroids) may lead to false negative results. Such substances should therefore not be administered together with, or a short time before the injection of Scintimun. **PREGNANCY AND LACTATION:** Contraindicated in pregnancy. Information should be sought about pregnancy from women of child bearing potential. A woman who has missed her period should be assumed to be pregnant. If administration to a breast feeding woman is necessary, breast-feeding should be interrupted for three days. A close contact with the child should also be avoided during the first 12 hours after the injection. **UNDESIRABLE EFFECTS:** Human anti-mouse antibody positive reaction is a very common side effect; hypotension is common. Hypersensitivity including angioedema, urticaria is uncommon. Rare effects include anaphylactic/anaphylactoid reaction, myalgia and arthralgia. Exposure to ionising radiation is linked with cancer induction and a potential for hereditary defects and must be kept as low as reasonably achievable. **DOSIMETRY:** Effective dose from 400 MBq is 6.9 mSv. **OVERDOSE:** Encourage frequent micturition and defecation. **MARKETING AUTHORISATION HOLDER:** CIS bio international, B.P.32, F-91192 Gif-sur-Yvette Cedex, France. **CLASSIFICATION FOR SUPPLY:** subject to restricted medical prescription. **MARKETING AUTHORISATION NUMBERS:** EU/1/04/302/001 and EU/1/04/302/002. **DATE OF REVISION OF TEXT:** 11 January 2010.

PLEASE REPORT ANY ADVERSE EVENTS TO HEALTH AUTHORITIES and/or CIS bio international.

www.iba-worldwide.com

Stralingsbescherming, waar ligt de grens van ALARA, zeker in de gezondheidszorg?

Ir. L van den Berg[1], Dr. M.B.M. Hofman[2]

[1]afdeling Radiologie en Nucleaire Geneeskunde, MeanderMC, Amersfoort
[2]afdeling Fysica en Medische Technologie, VU medisch centrum, Amsterdam

Abstract

van den Berg L, Hofman MBM. Radiation protection, were are the limits of ALARA, especially within healthcare? The use of ionising radiation requires a balance between benefits and health risks. Here, rules are useful to maintain a balance. In the Netherlands, European guidelines are translated into national legislation. This sets limits in the range from 20 mSv/year down to secondary levels of 0.001 mSv/year.
In this manuscript the question is posed whether it is reasonable to set limits that low. Is this still within ALARA?
A background of the current legislation is presented, showing that Dutch legislation sets lower limits than the international guidelines on which they were based. At levels below 1 mSv it becomes practically impossible to empirical show effects of ionising radiation. Secondly, it is shown that even within the Netherlands there are local differences in natural background radiation in the range of 1 mSv/year. Finally, there are indications in literature that risk effects at low doses are questionable. The epidemical data that created the fundament of the linear non-threshold (LNT) model don't show an effect below 60 mSv. And at cellular level there is experimental evidence for hormese effect at low radiation levels. Because of these reasons, we think that the LNT model is inappropriately applied for risk stratification at levels below 1 mSv/year. There is no scientific base for legislation down to the levels of 0.001 mSv. Therefore, such legislation is not within the reasonable part of ALARA. However, it does increase costs of healthcare and may keep useful applications away from the patient.
Tijdschr Nucl Geneesk 2012; 34(2):906-910

Inleiding

Er zijn vele toepassingen van ioniserende straling, zoals in de nucleaire geneeskunde. Naast de baten voor de patiëntenzorg vormen hoge doses ioniserende straling ook een gezondheidrisico. Om dit in balans te houden is goede regelgeving vereist. In Nederland worden bevolking en werkers beschermd door de Kernenergiewet, die binnenkort wordt aangescherpt (1,2). In deze regelgeving worden onder andere limieten gesteld in het bereik van 20 mSv/jaar tot 0,1 mSv/jaar met secundaire niveaus tot 0,001 mSv/jaar. Hiernaast bestaat nog locale wetgeving in de vorm van vergunningen waarin eisen worden gesteld op het niveau van µSv.

De vraag die we in deze notitie willen opwerpen is of deze regelgeving op microsievertniveau wel voldoende basis heeft: is dit zinvol en zitten we hier nog in het 'reasonably' van As Low As Reasonably Achievable (ALARA), of is het schadelijk? Om deze vragen te beantwoorden brengen we eerst in kaart hoe deze limieten in de regelgeving tot stand zijn gekomen. Vervolgens bespreken we de recente inzichten uit de International Commission on Radiological Protection (ICRP) en bekijken we de wetenschappelijke basis van de risicobepaling bij een lage dosis. Daarnaast geven we een enkel voorbeeld waar de huidige regelgeving toe leidt, om te komen tot een conclusie waar de juiste balans volgens ons zou moeten liggen.

Achtergrond van de Nederlandse regelgeving

De huidige Nederlandse regelgeving, de Kernenergiewet en het Besluit Stralingsbescherming uit 2001, is de uitwerking van twee Europese richtlijnen: de 'Euratom Directive 29' uit 1996 en de 'Euratom Directive 43' uit 1997 (1). De eerste, de 'basic safety standard' is ter bescherming van werkers en publiek. De tweede richtlijn heet ook wel de patiëntenrichtlijn. Deze Europese richtlijnen zijn weer gebaseerd op de visie van de ICRP, en specifiek de ICRP rapportages tot en met publicatie 60 uit 1990 (3-5).

De ICRP geeft het beleid van stralingshygiëne sinds de eerste publicaties van 1959 vorm met het concept van rechtvaardiging, ALARA en limieten (3). Voor het vaststellen van limieten neemt de ICRP de 'Linear No Threshold' (LNT) hypothese aan; het feit dat het stochastische risico van ioniserende straling op kankerinductie en erfelijke effecten zich lineair gedraagt ten opzichte van de stralingsdosis, zonder dat er sprake is van een drempeldosis. De limieten voor werkers werden gebaseerd op acceptabele risico's in veilige industrieën door een ongeval [10^{-4} per jaar], 100 mSv over een periode van vijf jaar met een maximum van 50 mSv in één jaar (6). Voor het publiek wordt een stralingsbelasting van gemiddeld 1 mSv/jaar acceptabel geacht (6). Bij deze limieten worden alle bronnen in

ogenschouw genomen, waarbij de ICRP de blootstelling aan meer dan drie bronnen tegelijkertijd onwaarschijnlijk acht.

Het huidige Besluit Stralingsbescherming bevat limieten op verschillende niveaus (van 20 mSv tot 0,001 mSv per jaar) (1). Er wordt onderscheid gemaakt tussen werknemers met een kans op een blootstelling van meer of minder dan 1 mSv/jaar. Met betrekking tot ruimtes is in het huidige besluit de dosisbeperking vastgesteld op 1 mSv/jaar, behalve in een gecontroleerde of bewaakte zone.

Deze limieten zijn vrijwel een één op één vertaling van de ICRP inzichten en Europese regelgeving. Echter de Nederlandse wetgeving (1,2) gaat verder. Naast bovenstaande limieten worden er ook nog extra limieten ingevoerd per mogelijke bron, waarbij er van tien mogelijke bronnen wordt uitgegaan, zodat een terreingrenswaarde van 0,1 mSv/jaar ontstaat. In Nederland is het aantal voor publiek toegankelijke plaatsen waar er bronactiviteit is van twee ondernemers op de vingers van één hand te tellen. Vervolgens wordt onder deze limieten nog expliciete ALARA vereist, en pas onder het secundaire niveau is dat niet meer nodig. Dit secundaire niveau is vastgesteld op 0,001 mSv/jaar voor lozingen in lucht of oppervlaktewater, en op 0,01 mSv/jaar voor externe straling buiten de terreingrens van de ondernemer. Hiermee is er dus een Nederlandse limiet op één duizendste van de Europese regelgeving. Naast nationale regelgeving is er nog een soort locale regelgeving in de vorm van vergunningen, waarin regelmatig vereisten tot op µSv-niveau worden gesteld. In het nieuwe Besluit Stralingsbescherming 2011 blijven deze limieten gehandhaafd, en worden soms verder verlaagd zoals bijvoorbeeld de nieuwe limiet op de terreingrens voor niet-vergunningsplichtige toestellen.

Deze stapsgewijze limitering is niet conform de visie van ICRP, rechtvaardiging, ALARA en limieten. Nu gaat de ondernemer eerst het stralingsniveau zonder maatregelen vaststellen om daarna te inventariseren welke maatregelen leiden tot het stralingsniveau dat past bij de gewenste limiet. Met deze aanpak wordt gelijktijdig voldaan aan het derde criterium, het secundaire niveau. Wel treedt hierdoor vervaging op van het niveau van veiligheid. Is het 1 mSv, 0,1 mSv of 0,01 mSv per jaar? Er ontstaat niet meer veiligheid, maar wel een enorme kostenpost door het invoeren van de beschermingsmaatregelen en het handhaven ervan enerzijds, en onnodig medisch handelen anderzijds. Een voorbeeld van onnodig handelen is het extra flushen van spuiten in de patiënt bij nucleair onderzoek om daarmee de dosis van het afval binnen de vereiste limieten te brengen.

Nieuwe ICPR inzichten

Sinds het ICRP rapport 60 uit 1990, waarop onze huidige stralingsbeschermingswetgeving is gebaseerd, heeft de ICRP nieuwe inzichten verwoord. De risicogetallen genoemd in het ICRP rapport 103 uit 2007 (6) zijn beduidend lager. Het risico wordt uitgedrukt als totaal detriment. In ICRP 60 was het detriment voor volwassenen (werkers) 5,6% per Sv, bestaande uit de kans op overlijden door kanker van 4,8% en op erfelijke schade van 0,8% per Sv. In ICRP 103 is het nieuwe detriment totaal 4,2% per Sv en de erfelijke schade bijna verwaarloosbaar, namelijk 0,1% per Sv (6). Niet alleen is het detriment in getal gereduceerd, ook het is minder ernstig: kanker in plaats van overlijden door kanker. De sterftekans door kanker is door de voortdurende vooruitgang in behandelingsresultaat van diverse kankers continu dalend. Daarom is dit deel van het detriment, de sterftekans door kanker, vervangen door de kans op kanker. Daar de kans op kanker ongeveer 45% bedraagt en de kans op overlijden door kanker circa 30%, is het totale detriment (met de definitie uit rapport 60) niet met 12%, maar met circa 50% gereduceerd. Desondanks heeft de ICRP besloten de limiet voor blootgestelde werkers te handhaven.

Mogelijkheid van aantonen van risico's bij lage doses

Om de afwijking van een dobbelsteen aan te tonen moet je met twee zaken rekening houden: de afwijking moet voldoende groot zijn, en je moet voldoende keren gooien. Dezelfde voorwaarden gelden ook om aan te tonen dat een lage dosis straling carcinogeen is (7). Op basis van het huidige risicogetal (4,2% per Sv voor volwassenen (6) en de huidige kankerincidentie (45%) kan de minimale groepsgrootte worden berekend om de juistheid van het risicogetal te verifiëren met een 95% betrouwbaarheid (7). In figuur 1 is de minimale groepsgrootte hiervoor weergegeven bij een

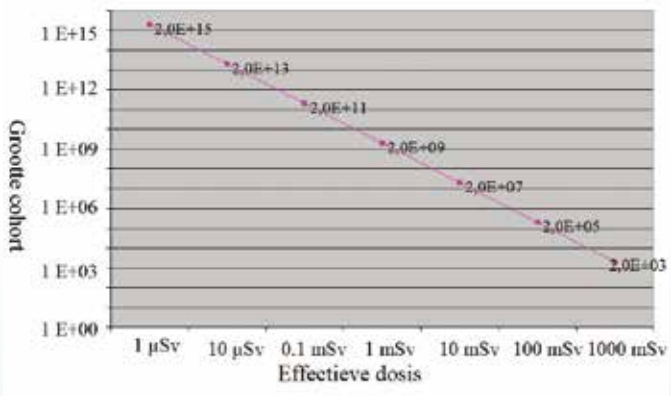

Figuur 1. Noodzakelijke groepsgrootte om een 4,2% per Sv kans op kanker aan te tonen bij een kankerincidentie van 45%, bepaald voor een 95% zekerheidsinterval (7).

bepaalde stralingsbelasting. Hierin is af te lezen dat bij een stralingsbelasting van 100 mSv pas bij meer dan 200.000 blootgestelde personen een statistisch aantoonbare verhoging van de kankerincidentie optreedt. Een derde voorwaarde is dat andere epidemiologische effecten op kanker constant zijn. Gezien de noodzakelijke groepsgrootte is duidelijk dat effecten

als roken of sociale en economische factoren een veel groter effect hebben op de kans op sterfte aan kanker dan een stralingsbelasting van 100 mSv. Als in Nederland elk lid van de bevolking 100 mSv eenmalig oploopt, volgt uit het LNT model dat de natuurlijke kans op overlijden met circa 0,27% toeneemt (4,1% kans op kanker per Sv, twee op de drie mensen met kanker overlijdt door kanker). Dit wordt verdeeld over de latentieperiode (circa vijf tot twintig jaar) waardoor de toename in één jaar niet groter is dan 0,027%. Figuur 2 geeft de spreiding in Nederland van de huidige kans weer, waaruit blijkt dat er regionale verschillen zijn in de orde van 15%. Afhankelijk van de regio ligt de kans om te overlijden aan kanker tussen de 21% en 39%. Het additionele effect (0,027%) ten gevolge van een hoge dosis van 100 mSv aan alle Nederlanders is dus niet waar te nemen.

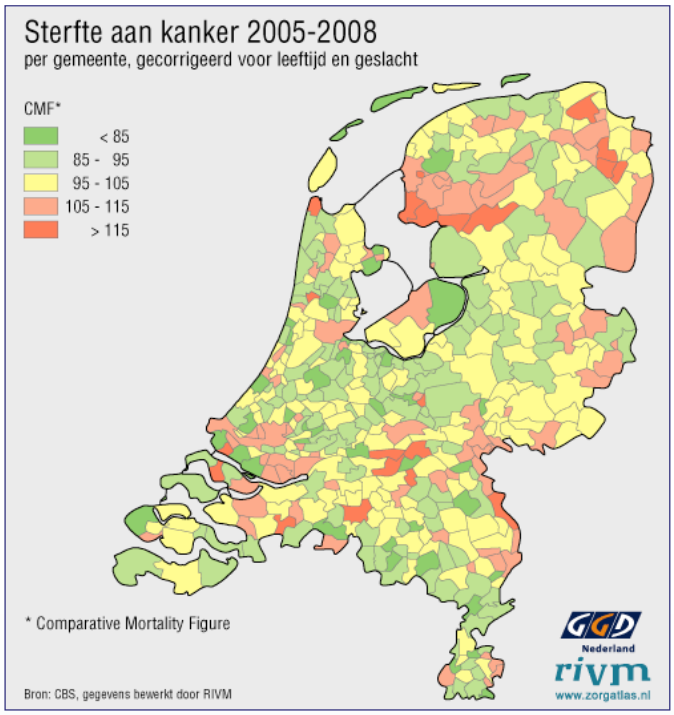

Figuur 2. De sterftekans per regio voor de periode 2005-2008 uit de gezondheidatlas van het RIVM (24). Aangezien de figuur geldt over een periode van vier jaar zijn temporele effecten gedempt.

Uit bovenstaande is duidelijk dat uitsluitend zeer zorgvuldig epidemiologisch onderzoek een verhoging van de kankersterfte door een stralingsbelasting kan aantonen en dat dan uitsluitend voor stralingsbelastingen ruim boven de hoogste limiet van 20 mSv/jaar.

Limieten in vergelijking met achtergrondniveaus

Een andere manier om naar lage stralingsdosis en de bijbehorende gezondheidsrisico's te kijken, is om deze niveaus te vergelijken met de grootte en de variatie van de achtergrondstraling (8-10). De gemiddelde stralingsbelasting voor de Nederlander bedraagt 2,4 mSv/ jaar, waarbij circa 25% een belasting heeft van minder dan 1,8 mSv/jaar en ongeveer 10% een stralingsbelasting van meer dan 3,5 mSv/jaar (8). Verschillen van meer dan 1 mSv/jaar zijn dus normaal. De grondsoort en de bouwkundige aspecten van een woning hebben een belangrijke invloed op die stralingsbelasting. Een limiet lager dan 1 mSv/jaar heeft daarmee vrijwel geen invloed op de daadwerkelijke stralingsbelasting.
In Nederland is de natuurlijke stralingsbelasting gemiddeld 1,9 mSv/jaar. De typische stralingsbelasting voor de wereldbevolking varieert tussen 1 en 10 mSv/jaar en is gemiddeld 2,4 mSv/jaar (11). Maar ook gebieden, zoals Ramsar in Iran, Lake Miri in Sudan en de Chavara-Neendakara kust in India, met stralingsniveaus van 35 mSv/jaar en meer komen voor. Zo'n duidelijke geografische gebonden verhoging van natuurlijke achtergrondstraling biedt de mogelijkheid voor epidemiologisch onderzoek naar de risico's van deze stralingsniveaus. Dit is ook uitgebreid gebeurd (11-13). Hierbij blijkt dat *'alle onderzoekingen over achtergrondstraling altijd hebben opgeleverd dat naarmate de achtergrondstraling hoger is, er minder kanker voorkomt, zonder uitzondering'* (14).

Is het LNT model ook valide voor het werkelijke risico?

Voor de bepaling van de stralingsrisico's in de orde van grootte van een mSv en lager wordt gebruikt gemaakt van extrapolatie van data verkregen bij hogere doses. Hierbij is de aanname van de LNT hypothese essentieel.

Er zijn echter aanwijzingen dat er wel een drempeldosis bestaat (15). Kanker door ioniserende straling ontstaat doordat de reparatie van een dubbelstrengsbreuk van een DNA molecuul door de cel niet juist wordt uitgevoerd. Deze breuken ontstaan vooral door de invloed van radicalen. De cel heeft mechanismen om dit te repareren, en dagelijks worden er circa acht breuken in elke cel gerepareerd. Het ioniserende effect van straling wordt vooral veroorzaakt door verhoogde radicaalvorming. Een eenmalige dosis van 25 mGy leidt tot gemiddeld één extra breuk, dit valt binnen de dagelijkse variatie (15). Weliswaar geeft dit een hogere kans op een gemuteerd DNA, maar anderzijds leidt dit ook tot een hogere activiteit van het reparatiemechanisme van de cel. Dit zou een verklaring zijn van de lagere sterftekans in gebieden met een verhoogd achtergrondniveau van circa 6 mSv/jaar (11-13).

Twee bekende grote epidemiologische onderzoeken naar kankerincidentie door straling die een basis vormen voor de lineaire relatie tussen dosis en kans op kanker laten een drempeldosis zien, en misschien zelfs een positief effect van lage dosis (hormese). De ene groep bestaat uit de Japanse overlevenden van de atoombommen op Hiroshima en Nagasaki (16). In figuur 3 is de mortaliteit vergeleken met die van andere steden in Japan. De grafiek laat zien dat voor 1000 mSv individuele dosis er per 1000 blootgestelden acht extra doden zijn. Opvallend is dat voor doses lager dan 60 mSv het aantal doden lager is dan het gemiddelde van

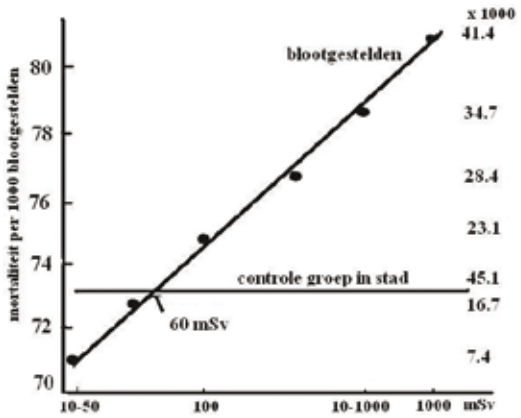

Figuur 3, Cumulatieve kanker mortaliteit van Japanse bom slachtoffers als functie van de dosis. Getallen rechts geven aantal personen per dosis-groep weer, de horizontale lijn geeft de controle groep bestaande uit personen die aanwezig waren op 2,5 tot 10 km van het hypocentum. Uit Luckey (25), op basis van data uit de publicatie van Shimizu et al. 1989 (16).

de controlegroep. Het lijkt alsof een kleine dosis (tussen de 10 en 60 mSv) voor de blootgestelden voordeel heeft. De andere groep bestaat uit Canadese tuberculosepatiënten die regelmatig om diagnostische redenen aan straling werden blootgesteld (17). Ook bij de tuberculosepatiënten lijkt er hormese op te treden rond 120 mSv (17). Het verschil in dosis ten opzichte van de Japanse groep zou te verklaren zijn door de fractionering (18).

Er is wetenschappelijke consensus dat het LNT model correct is voor hoge doses (>200 mSv). Ook is er consensus dat de LNT hypothese een bruikbaar en adequaat instrument is voor een stralingsbeschermingbeleid. Een eerste formulering van het stralingshygiënisch beleid dateert van een periode dat stralingsbelastingen van meer dan 100 mSv niet ongewoon waren. Nu wordt een blootstelling van 20 mSv voor een 'total body' CT gecategoriseerd als een zeer hoge dosis.
Dat de toepassing van de LNT hypothese voor lage doses tot onjuiste conclusies kan leiden, wordt aangetoond bij de grootste kernramp. Schattingen van het aantal kankergevallen ten gevolge van Tsjernobyl variëren enorm door verschil in keuze van de drempelwaarde (19-21). In 1986-1987 waren 350.000 'liquidators' betrokken bij het opruimen van de schade veroorzaakt door de explosie. De gemiddelde stralingsbelasting van deze liquidators was 100 mSv. De kankerincidentie van deze groep bleek niet significant verhoogd ten opzichte van de controlegroep (20).

Consequenties

De huidige lage limieten op stralingshygiëne leiden tot dure beheersmaatregelen, welke niet leiden tot meer veiligheid. Anderzijds is het gevolg van vertaling van het LNT model naar lage dosis dat er een foutieve inschatting wordt gemaakt van de gevolgen van ioniserende straling in z'n algemeenheid of door medisch handelen (22). Ook het RIVM meldt op haar website dat de 2,4 mSv stralingsbelasting leidt tot ongeveer 2000 sterfgevallen per jaar door kanker in Nederland (23).
De IAEA verwerpt deze toepassing van het LNT model voor schattingen van het aantal personen dat kanker krijgen door lage dosis (19). Tenslotte vervagen de lage limieten tot op secundair niveau het begrip waar de reële risico's liggen. De werkelijke veiligheid dient de maat te zijn voor limieten en niet de haalbaarheid. Na een eventuele ramp kan een situatie ontstaan waarbij de huidige regelgeving niet meer reëel is. Als limieten zijn gebaseerd op een reëel veiligheidsniveau is er geen noodzaak om na een eventuele ramp deze limieten bij te stellen, hetgeen onlangs in Fukushima is gebeurd.

Conclusie

Uit bovenstaande overweging komen wij tot de conclusie dat het LNT model ten onrechte wordt toegepast in het kader van risico-inventarisatie voor stralingsniveaus lager dan 20 mSv/jaar. Voor deze stralingsbelasting zal waarschijnlijk nooit een verhoging van kankerinductie kunnen worden aangetoond. Integendeel, er zijn suggesties dat op dit niveau hormese optreedt. Het gebruik van het LNT model is gerechtvaardigd voor een stralingsbeschermingsbeleid, maar niet tot onbeperkt lage doses. Toch gaat de huidige Nederlandse regelgeving verder dan limieten die de ICRP aangeeft.
De regelgevende instanties en inspecties moeten er dan ook bewust van worden gemaakt dat het opnemen van limieten die lager zijn dan 1 mSv/jaar niet meer veiligheid bieden en in strijd zijn met het tweede uitgangspunt van de stralingsbescherming: 'Stralingsbeschermingsmaatregelen moeten in redelijkheid worden toegepast, economische en sociale factoren daarbij in aanmerking genomen'.
Limieten lager dan 1 mSv/jaar zullen gerechtvaardigde toepassingen blokkeren. Gerechtvaardigd betekent dat de opbrengsten hoger zijn dan de kosten. De opbrengsten vertalen zich in kwaliteit van zorg en daarmee in levensjaren of in verbetering van kwaliteit van leven, terwijl de kosten van straling verwaarloosbaar zijn in termen van risico voor de gezondheid. Degene die straling toepast, zoals een ziekenhuis, moet voldoen aan milieueisen van 0,01 of zelfs 0,001 mSv per jaar waarbij de natuurlijke stralingsbelasting in de omgeving meer dan 2 mSv/jaar bedraagt. Wanneer de kosten om te voldoen aan deze wettelijke limieten hoger worden dan de vergoedingen zal een gerechtvaardigde behandeling of gerechtvaardigde diagnostiek met behulp van ioniserende straling niet of slechts beperkt worden uitgevoerd. De bestaande regelgeving toegepast in de gezondheidszorg vermindert daarom de kwaliteit van leven van patiënten en kost hen levensjaren, dit om een niet aantoonbaar en een ons inziens niet bestaand risico uit te sluiten.

Referenties

1. Besluit van 16 juli 2001, houdende vaststelling van het Besluit stralingsbescherming, Staatsblad 16-07-2001. Koninklijk Besluit 397, 2001.

2. Besluit (voorgenomen), houdende vaststelling van het Besluit stralingsbescherming (vereenvoudiging vergunningstelsel en borging deskundigheid alsmede enkele aanpassingen) versie 5 november 2009, zoals voorgelegd aan de leden van de NVS, november 2009.
3. Recommendations of the International Commission on Radiological Protection. ICRP publication 1. Pergamon Press, 1959.
4. Recommendations of the International Commission on Radiological Protection. ICRP publication 26. Annals of the ICRP 1. Pergamon Press, 1977.
5. Recommendations of the International Commission on Radiological Protection. ICRP publication 60. Annals of the ICRP 21. Pergamon Press, 1990.
6. The 2007 recommendations of the International Commission on Radiological Protection. ICPR publication 103. Annals of the ICRP 37. Elsevier, 2007.
7. Gonzalez A. The scope of radiation protection and safety standards. 2005. http://www-ns.iaea.org/downloads/rw/conferences/chernobyl/gonzalez.ppt, 34-40.
8. van der Woude A, de Meijer RJ. Radioactiviteit. Wetenschappelijk Bibliotheek van Natuurwetenschap & Techniek 77. Veen Magazines, 2003.
9. Eleveld H, Tanzi CP, Bijwaard H et al. Emissies en doses door bronnen van ioniserende straling in Nederland. RIVM rapport 861020003, 2004.
10. RIVM. Stralingsbelasting in Nederland. Milieuportaal voor professionals, 2012. http://www.rivm.nl/milieuportaal/onderwerpen/straling-en-EM-velden/ioniserende-straling/
11. Ahmed JU. High levels of natural radiation: Report of an international conference in Ramsar. IAEA bulletin. 1991;2;36-8
12. Wei L, Sugahara T, Tao Z. High levels of natural radiation: radiation doses and health effects. Proceedings of the 4th international conference on high levels of natural radiation. ISBN13: 9780444826305, 1996.
13. Ghiassi-Nejad M, Zakeri F, Assaei RG et al. Long-term immune and cytogenetic effects of high level natural radiation on Ramsar inhabitants in Iran. J Environ Radioact. 2004;74:107-16
14. Citaat van dr. Keverling Buisman, de Nuclear Research & Consultancy Group (NRG) in Petten, geciteerd door Hengel W. Een beetje straling kan geen kwaad, Reformatorisch Dagblad, 25 april 2006.
15. Tubiana M, Feinendegen LE, Yang CC, Kaminski JM. The linear No-Threshold relationship is inconsistent with radiation biologic and experimental data. Radiology. 2009;251:13-22
16. Shimizu Y, Kato H, Schull WJ et al. Studies of the mortality of A-bomb survivors. 9 Mortality 1950 – 1985: Part 1. Comparison of risk coefficients for site-specific cancer mortality based on the DS86 and T65DR shielded kerma and organ doses. Radiat Res. 1989;118:502-24
17. Miller AB, Howe GR, Sherman GJ et al. Mortality from breast cancer after irradiation during fluoroscopic examinations in patients being treated for tuberculosis. N Engl J Med. 1989;321:1285-9
18. Wolff S. The adaptive response in radiobiology: evolving insights and implications, Environ Health Perspect. 1998;106S1:277-83
19. Gonzalez AJ. International harmonization of radiation protection and safety standards: the role of the United Nations System, In: Harmonization of radiation, human life and the ecosystem. Proceedings 10th international congress of the International Radiation Protection Association. 2000;T-10-1,1-20.
20. The Chernobyl Forum. Chernobyl's legacy: Health, environmental and socio-economic impacts. 2nd ed. IAEA, 2005.
21. United Nations Scientific Committee on the effects of Atomic Radiation, Sources and effects of ionizing radiation. UNSCEAR report 2000. J Radiol Prot. 2001;21:83-5
22. Berrington de Gonzalez A, Darby S. Risk of cancer from diagnostic X-rays: estimates for the UK and 14 other countries. Lancet 2004;363:345-51
23. Stralingsdosis per bron, 2008. Compendium voor de leefomgeving. http://www.compendiumvoordeleefomgeving.nl/indicatoren/nl0311-Stralingsdosis-per-bron.html?i=13-95.
24. Zwakhals SLN, Giesbers H, Deuning CM, et al. Kanker totaal per gemeente. in: Volksgezondheid Toekomst Verkenning, Nationale Atlas Volksgezondheid. www.zorgatlas.nl. RIVM, 2010.
25. T.D.Luckey,Radiation Hormesis: the Good, the Bad, and the Ugly, Dose-Response, 2006; 4(3)pag 169-90

Oldelft Benelux Medical Solutions

Mediso AnyScan: de eerste klinische SPECT-CT-PET scanner...

...een unieke oplossing binnen de nucleaire geneeskunde.

Basis configuraties

Upgrade door toevoeging

Upgrade door splitsing

Oldelft Benelux heeft reeds meer dan 80 jaar ervaring in de verkoop en service van diagnostische apparatuur en innovatieve healthcare ICT systemen. Zij heeft zich ontwikkeld van producent van apparatuur naar System Integrator en Service Provider voor ziekenhuizen en zorginstellingen.

Met Mediso levert Oldelft Benelux het hele spectrum aan gamma camera's; van kleine exelloops, tot geavanceerde SPECT-CT-PET combinaties.

Voor meer informatie omtrent de Mediso oplossingen kunt u contact opnemen met uw accountmanager, of stuur een e-mail naar info@oldelftbenelux.nl.

Oldelft Benelux B.V. Witsenstraat 41 3905 KW Veenendaal The Netherlands
T +31 318 583 400 F +31 318 583 401 E info@oldelftbenelux.nl I www.oldelftbenelux.nl

Het verbeteren van de diagnostiek bij de ziekte van Parkinson: de LEAP-DAS studie

Drs. S.R. Suwijn[1], Prof dr. J. Booij[2], Drs. C.V.M. Verschuur[1], Dr. G. Tissingh[3] and Dr. R.M.A. de Bie[1]

[1] *Afdeling Neurologie, Academisch Medisch Centrum, Amsterdam*
[2] *Afdeling Nucleaire Geneeskunde, Academisch Medisch Centrum, Amsterdam*
[3] *Afdeling Neurologie, Atrium Medisch Centrum Parkstad, Heerlen*

De ziekte van Parkinson (zvP) is een neurodegeneratieve aandoening die de motorische, autonome, cognitieve en sensibele systemen aantast. In Nederland lijden ongeveer 50.000 personen aan de zvP en boven de 65 jaar is de prevalentie 1,6% (1). De motorische kernsymptomen worden veroorzaakt door degeneratie van dopamineproducerende neuronen.
De diagnose zvP wordt momenteel gesteld op basis van klinische criteria. De patiënt moet bradykinesie hebben en tenminste twee of meer bijkomende verschijnselen (rigiditeit, asymmetrie en/of rustremor). Echter, in gespecialiseerde centra wordt in 6 tot 25% van de gevallen ten onrechte de diagnose van zvP gesteld. Algemeen neurologen stellen zelfs een verkeerde diagnose tot maximaal 34% van de gevallen (2-5). Een verkeerde diagnose kan zowel vals positief als vals negatief zijn. Dit hoge percentage verkeerde diagnosen in de (niet-)gespecialiseerde centra is zorgwekkend, zeker gezien de impact van het hebben van een neurodegeneratieve ziekte als de zvP. Doordat de zvP een langzaam progressieve ziekte is, kan de onzekerheid als gevolg van een twijfelachtige diagnose meerdere jaren duren.
Dopaminetransporter (DAT) SPECT imaging is een betrouwbaar hulpmiddel om onderscheid te maken tussen parkinsonisme veroorzaakt door een neurodegeneratieve ziekte en reversibel parkinsonisme/non-parkinsonisme bij patiënten met een klinische diagnose van de zvP (6-10).
Bij patiënten met (vermoeden op) een neurodegeneratieve ziekte zijn soms bij het neurologisch onderzoek kenmerkende verschijnselen te vinden. Tot op heden is geen prospectieve studie uitgevoerd die de eventuele waarde van deze kenmerken met betrekking tot de accuratesse van de klinische diagnose heeft onderzocht. Daarom zijn de auteurs van dit artikel, binnen de Levodopa in EArly Parkinson's disease (LEAP-studie) (zie kader) gestart met een dubbelblind diagnostisch onderzoek (figuur 1) naar de diagnostische nauwkeurigheid van de verschillende parameters van een uitgebreid neurologisch onderzoek bij aanvang van de ziekte (index test) in vergelijking met de resultaten van de DAT SPECT bij aanvang van de ziekte (referentie test). In totaal 150 van de 446 deelnemers aan de LEAP-studie krijgen een uitgebreid neurologisch onderzoek dat zal worden opgenomen op video. Een expertcommissie, bestaande uit zes bewegingsstoornissen neurologen zal de video's analyseren. Vervolgens krijgen deze 150 patiënten, die dus deelnemen aan de LEAP-DAS substudie, een ^{123}I-FP-CIT (N-ω-(fluoropropyl)-2β-carbomethoxy-3β-(4-iodophenyl)nortropane)

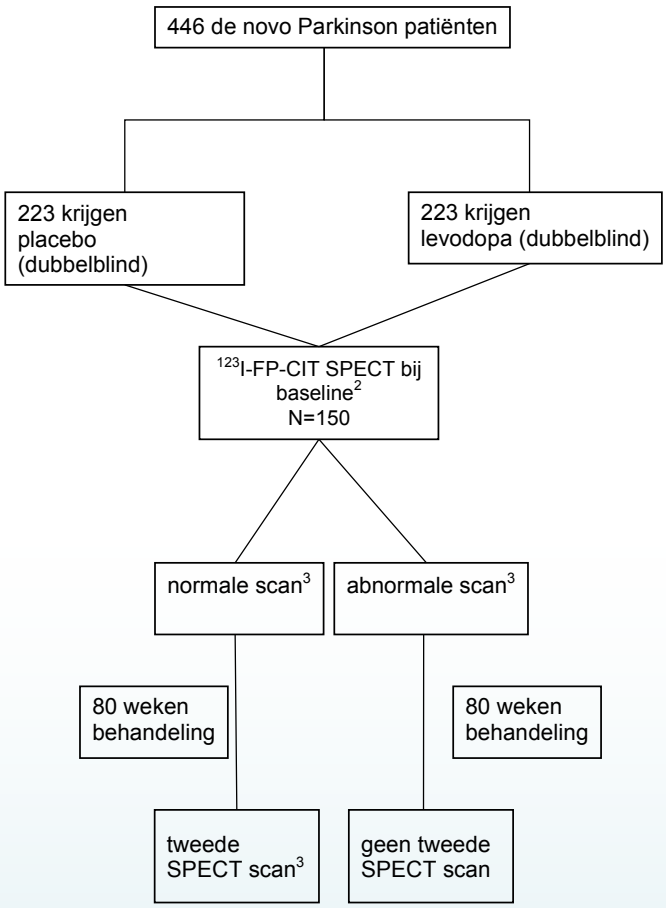

Figuur 1. Opzet LEAP-DAS studie[1]

[1]de LEAP-DAS studie wordt gefinancierd door GE Healthcare
[2]omdat het om een dubbelblinde studie gaat, krijgt de aanvrager geen uitslag van de SPECT studie
[3]visuele beoordeling tijdens consensus beoordeling

Design LEAP-studie
Het doel van de LEAP-studie is te onderzoeken wat het lange termijn effect is van levodopa, het meest gebruikte en efficiëntste medicijn bij de zvP. De LEAP-studie is een gerandomiseerd delayed start, dubbelblind en placebo-gecontroleerd multi-center onderzoek. Patiënten met nieuw gediagnosticeerde zvP zonder beperkingen in het dagelijks leven kunnen deelnemen aan het onderzoek. In de eerste fase krijgen patiënten 40 weken levodopa/carbidopa 100/25 mg 3dd (de vroege behandelgroep) of placebo 3dd (de late behandelgroep). Daarna krijgen alle patiënten 40 weken levodopa/carbidopa 100/25 mg 3dd. Volgens onze steekproefgrootte-schatting zijn in totaal 446 patiënten nodig om een relevant verschil tussen de twee groepen te vinden (www.leapamc.nl). Deze studie wordt gefinancierd door ZonMw en het Internationaal Parkinson Fonds.

SPECT scan voordat medicatie wordt gestart (figuur 1). Alle gemaakte scans worden centraal visueel beoordeeld en gezien het dubbelblinde design van zowel de LEAP als de LEAP-DAS studie worden deze resultaten niet teruggekoppeld naar de behandelend neuroloog. Alle patiënten met een normale scan bij baseline worden aan het eind van de LEAP-studie (80 weken) opnieuw onderzocht door middel van een ^{123}I-FP-CIT SPECT scan. De resultaten van het expertpanel en de DAT SPECT resultaten zullen vergeleken worden met behulp van 2x2 tabellen. De patiënten zullen gevolgd worden voor nog eens drie jaar, waarna een nieuwe video wordt gemaakt en de videobeoordeling wordt vervolgens herhaald, echter zal het expertpanel een definitieve diagnose geven waarbij het beschikking heeft over alle medisch relevante informatie. De eerste resultaten worden verwacht aan het einde van 2015.

Referenties

1. de Rijk MC, Tzourio C, Breteler MM et al. Prevalence of parkinsonism and Parkinson's disease in Europe: the EUROPARKINSON Collaborative Study. European Community Concerted Action on the Epidemiology of Parkinson's disease. J Neurol Neurosurg Psychiatry. 1997;62:10-5
2. Hughes AJ, Daniel SE, Lees AJ. Improved accuracy of clinical diagnosis of Lewy body Parkinson's disease. Neurology. 2001;57:1497-9
3. Hughes AJ, Daniel SE, Ben-Shlomo Y, Lees AJ. The accuracy of diagnosis of parkinsonian syndromes in a specialist movement disorder service. Brain. 2002;125:861-70
4. Jankovic J, Rajput AH, McDermott MP, Perl DP. The evolution of diagnosis in early Parkinson disease. Parkinson Study Group. Arch Neurol. 2000;57:369-72
5. Litvan I, MacIntyre A, Goetz CG et al. Accuracy of the clinical diagnoses of Lewy body disease, Parkinson disease, and dementia with Lewy bodies: a clinicopathologic study. Arch Neurol. 1998 ;55:969-78
6. Chouker M, Tatsch K, Linke R, Pogarell O, Hahn K, Schwarz J. Striatal dopamine transporter binding in early to moderately advanced Parkinson's disease: monitoring of disease progression over 2 years. Nucl Med Commun. 2001;22:721-5
7. Fahn S, Oakes D, Shoulson I et al. Levodopa and the progression of Parkinson's disease. N Engl J Med. 2004;351:2498-508
8. Marek K, Innis R, van Dyck C et al. [123I]beta-CIT SPECT imaging assessment of the rate of Parkinson's disease progression. Neurology. 2001;57:2089-94
9. Pirker W, Djamshidian S, Asenbaum S et al. Progression of dopaminergic degeneration in Parkinson's disease and atypical parkinsonism: a longitudinal beta-CIT SPECT study. Mov Disord. 2002 ;17:45-53
10. Staffen W, Mair A, Unterrainer J, Trinka E, Ladurner G. Measuring the progression of idiopathic Parkinson's disease with [123I] beta-CIT SPECT. J Neural Transm. 2000;107:543-52

SIEMENS

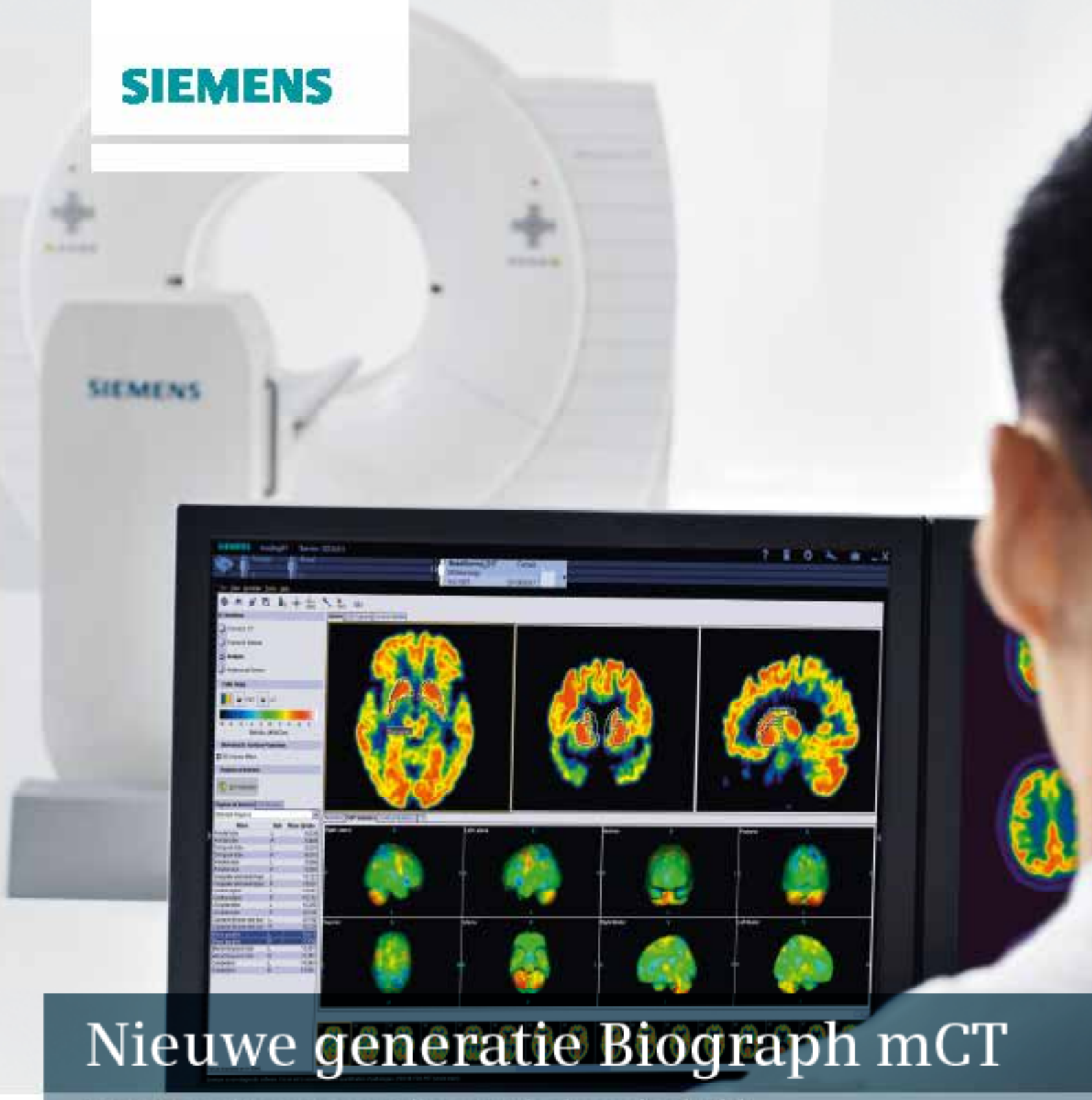

Nieuwe generatie Biograph mCT

PET-CT met nog meer diagnostische zekerheid

Siemens Healthcare introduceert de nieuwste generatie Biograph mCT: een PET-CT scanner die de exacte meting van metabolische processen en datakwantificering mogelijk maakt, inclusief de beoordeling van neurologische aandoeningen, tumoruitval en de doorbloeding van het hart (perfusie). De nieuwe Biograph mCT is voorzien van een uniek OptiselHD (High-Definition) detectorsysteem, met een fijne volumetrische resolutie van maar liefst 87 mm³. Andere innovatieve technologieën die zijn toegepast zijn Time of Flight (TOF) en HD (High-Definition) PET, voor mooie, nauwkeurige beeldvorming bij een minimale stralingsdosis. Met Siemens Quanti•QC kan de dagelijkse normalisatie van het systeem 's nachts plaatsvinden en wordt het systeem exact gijkt. Zo worden elke dag optimale, consistente prestaties geleverd voor betrouwbare en reproduceerbare onderzoeksresultaten.

www.siemens.nl/healthcare

Dr. mr. O.J.N. Bloemen

11 februari 2011
Academisch Medisch Centrum, Universiteit van Amsterdam

Promotores:
Prof.dr. D.H. Linszen
Prof.dr. J. Booij

Co-promotor:
Dr. T.A.M.J. van Amelsvoort

Brain markers of psychosis and autism

Achtergrond

In dit proefschrift hebben we onderzoek gedaan naar mogelijke afwijkingen in neurotransmissiesystemen en structurele hersenafwijkingen bij schizofrenie en naar autisme spectrum stoornissen (ASS). Schizofrenie, een stoornis die gekenmerkt wordt door terugkerende psychotische episoden, wordt doorgaans voorafgegaan door een prodromale periode met milde positieve psychotische en negatieve symptomen, aspecifieke symptomen en een daling in psychosociaal functioneren. Met diagnostische instrumenten is het mogelijk om patiënten te diagnosticeren met een ultra hoog risico (UHR) om een psychose te ontwikkelen, waarvan tien tot veertig procent daadwerkelijk ook psychotisch worden. Autisme wordt gekenmerkt door kwalitatieve en kwantitatieve beperkingen in sociaal functioneren en stereotiep gedrag, en is geassocieerd met een hogere kans op het ontwikkelen van een psychose. Psychose is geassocieerd met een veranderde transmissie van dopamine van glutamaat in de hersenen.

Methoden

Wij gebruikten ^{123}I-IBZM single photon emission computed tomography (SPECT) gecombineerd met acute dopaminedepletie om bij UHR patiënten de bezetting van dopamine $D_{2/3}$ receptoren met endogeen dopamine te vergelijken met gezonde controles. Acute depletie van dopamine werd bewerkstelligd door het geneesmiddel alfa-methyl-para-tyrosine (AMPT) toe te dienen. Dit leidt tot een acute, maar omkeerbare, daling van de dopamineproductie. Met deze methode (een IBZM scan voor toediening van AMPT en een scan vlak na toediening; het verschil reflecteert de bezetting van dopamine $D_{2/3}$ receptoren met endogeen dopamine) kan een inschatting worden gemaakt van de dopamineconcentratie in de hersenen. Bovendien onderzochten we de relatie tussen glutamaat in de linker hippocampus (gemeten met proton magnetic resonance spectroscopy (1H-MRS)) en de bezetting van dopamine D_2 receptoren met endogeen dopamine in UHR patiënten en gezonde controles. Verder onderzochten wij met diffusion tensor magnetic resonance imaging (DT-MRI) UHR patiënten die later een psychose kregen en in een andere studie patiënten met het syndroom van Asperger. Verder onderzochten wij structurele afwijkingen bij autistische patiënten die een comorbide psychose ontwikkelden. Bij alle klinische beoordelingen van de deelnemers is gebruik gemaakt van gestandaardiseerde meetschalen en een intelligentietest.

Resultaten

Een belangrijke bevinding was dat er mogelijk een subgroep van UHR patiënten is met reeds bestaande afwijkingen in de dopaminerge neurotransmissie. Deze subgroep wordt gekarakteriseerd door hoge scores op schalen voor positieve symptomen, en heeft een verhoogde bezetting van dopaminereceptoren door endogeen dopamine vergeleken met de subgroep met lage scores voor positieve symptomen en vergeleken met gezonde controles. Wij vonden geen aanwijzingen voor een relatie tussen glutamaat en postsynaptische $D_{2/3}$ receptorbeschikbaarheid en bezetting door endogeen dopamine, maar vonden wel dat UHR patiënten, vergeleken met controles, een significant lagere glutamaatconcentratie in de hippocampus hadden. Verder vonden wij dat UHR patiënten die later een psychose ontwikkelden specifieke wittestof-integriteitverschillen hadden in de hersenen in vergelijking met UHR patiënten die geen psychose ontwikkelden en met controles. Volwassen patiënten met het syndroom van Asperger bleken ook verminderde integriteit van wittestof te hebben. Daarnaast zijn bij autistische patiënten die een psychose ontwikkelden structurele afwijkingen in de hersenen te vinden.

Conclusies en overwegingen

Dit proefschrift bevat resultaten van onderzoeken die de hypothese van verstoringen in neurotransmissiesystemen bij UHR patiënten ondersteunen. De resultaten ondersteunen daarnaast een dimensionele kijk op het voorkomen van psychose, waarbij meer positieve symptomen samengaan met verhoogde concentraties van dopamine in de hersenen. Verder gaat het optreden van psychose bij UHR patiënten en bij patiënten met autisme gepaard met specifieke, maar relatief milde, structurele afwijkingen in de hersenen. Het lijkt er op dat de hersenen van UHR patiënten en autistische patiënten niet veel (structurele) veranderingen nodig hebben om een psychose te laten doen ontstaan.

PROEFSCHRIFT

Dr. T.H. Oude Munnink

5 oktober 2011
Rijksuniversiteit Groningen

Promotores:
Prof.dr. E.G.E. de Vries
Prof.dr. R.A.J.O. Dierckx

Co-promotores:
Dr. M.N. Lub-de Hooge
Dr. A.H. Brouwers
Dr. C.P. Schröder

PET imaging with ^{89}zirconium labeled antibodies to guide cancer therapy

The development of antitumor agents that target specific dysregulated processes in tumors is expanding rapidly. One class of these new drugs are antibodies. Molecular imaging, for example with PET scans, might well contribute in the development and implementation of new antitumor antibodies. This thesis aimed at evaluating the role of molecular imaging with ^{89}zirconium (^{89}Zr) labeled antibodies in the guidance of targeted anticancer agents, with a focus on breast cancer.

Antibodies targeted at three relevant proteins were radiolabeled with ^{89}Zr: human epidermal growth factor receptor-2 (HER2), vascular endothelial growth factor (VEGF) and transforming growth factor-β (TGF-β). PET scans were made with these radioactive antibodies to measure the molecular effects of new antitumor drugs and to explore the pharmacokinetics, organ distribution and tumor uptake of the antibodies.

A HER2-PET feasibility study was performed in metastatic breast cancer patients to determine the optimal conditions of ^{89}Zr-trastuzumab antibody dose and timing. HER2 positive metastatic breast cancer patients received a dose of 37 MBq ^{89}Zr-trastuzumab at three trastuzumab protein doses (10 or 50 mg when trastuzumab naive and 10 mg while on trastuzumab treatment) and underwent two or more PET scans around day two and five post tracer injection. The best time point to assess ^{89}Zr-trastuzumab tumor uptake was four to five days post injection. Trastuzumab naive patients required 50 mg ^{89}Zr-trastuzumab and patients on trastuzumab treatment 10 mg. Accumulation of ^{89}Zr-trastuzumab occurred in most known tumor lesions and some unknown lesions. ^{89}Zr-trastuzumab PET at appropriate antibody dose allowed visualisation and quantification of uptake in HER2 positive lesions in metastatic breast cancer patients.

The TGF-β antibody fresolimumab was labeled with ^{89}Zr and preclinically validated. The pro-invasive and -metastatic TGF-β is a potential drug target for the treatment of cancer, especially in case of highly invasive and metastatic tumors such as glioblastomas and metastatic breast cancer. Tumor uptake and organ distribution of ^{89}Zr-fresolimumab was assessed in a human TGF-β transfected chinese hamster ovary (CHO) xenograft model, a human breast cancer MDA-MB-231 xenograft and metastatic model. ^{89}Zr-fresolimumab PET is currently being evaluated in glioblastoma patients.

One of the therapies for which molecular imaging could serve as an early biomarker is HSP90 inhibition. The HSP90 inhibitor NVP-AUY922 downregulates the expression of many oncogenic HSP90 client proteins (including HER2), and inhibits angiogenesis by downregulating hypoxia inducible factor 1α (HIF-1α) resulting in decreased VEGF excretion. HER2-PET imaging in SKOV3 xenograft bearing mice showed a mean reduction of 41 percent in ^{89}Zr-trastuzumab tumor uptake after NVP-AUY922 treatment. Similarly, VEGF-PET showed that NVP-AUY922 treatment decreased ^{89}Zr-bevacizumab uptake with 44 percent in A2780 xenografts. This technique is currently evaluated in a phase II clinical trial for its role as an early biomarker for HSP90 inhibition effect in patients with metastatic breast cancer.

This thesis is an example of the possible applications of molecular imaging with antibodies during cancer drug development. Currently, this technique is used in the development of several new antitumor drugs, both in preclinical studies as well as in clinical studies. The research for this thesis was supported by a grant from the Dutch Cancer Society.

Dr. I. Farinha Antunes

25 januari 2012
Rijksuniversiteit Groningen

Promotores:
Prof. dr. R.A.J.O. Dierckx
Prof. dr. H.J. Haisma
Prof. dr. P.H. Elsinga

Co-promotor:
Dr. E.F.J. de Vries

Development and evaluation of PET tracers for imaging β-glucuronidase activity in cancer and inflammation

The prime obstacle in achieving an effective treatment in cancer or in certain inflammatory diseases is the eradication of the disease without harming healthy tissue in the patient. This lack of efficacy is mainly due to the physiological similarities between healthy and affected cells which prevent the selective incorporation of the cytotoxic drugs into the affected cells. With this in mind, a new concept was introduced called Prodrug therapy, where the drug is modified to a less reactive/cytotoxic prodrug that is converted to the active drug by an enzyme that is highly present at the target site. β-glucuronidase could be an attractive target for this prodrug approach, since in various tumor types, infection, rheumatoid arthritis and neurological disorders, high levels of β-glucuronidase are found in the interstitial space, unlike in healthy cells where it is only found in lysosomes. Selective prodrugs for β-glucuronidase are usually glucuronide conjugates which are relatively nontoxic due to the hydrophilic nature of the glucuronide group, preventing them from entering cells and, thus, from being activated by lysosomal β-glucuronidase in healthy cells. However, in target tissues where the enzyme is expressed extracellularly, the prodrug will be converted to the toxic parent drug, which can subsequently exert its therapeutic effect at the target site only.

When prodrug therapy is based on elevated activity of β-glucuronidase at the target site, the localisation and magnitude of expression of extracellular β-glucuronidase are probably the most important factors that determine the target-specificity of the release of the active drug from the glucuronide prodrug. The variability in the activity of β-glucuronidase between different tissues as well as between different individuals is high. Thus, imaging of β-glucuronidase activity by positron emission tomography (PET) to monitor and evaluate β-glucuronidase based prodrug therapy has become desirable.

Driven by the lack of PET tracers suitable to monitor extracellular β-glucuronidase activity, the aim of this study was to develop PET tracers for evaluation of β-glucuronidase expression in different animal models for various disorders.

The glucuronide PET tracers developed in this project, ^{18}F-FEAnGA and ^{18}F-FEAnGA-Me, were first evaluated *in vitro* to confirm whether they would be cleaved in the presence of β-glucuronidase. Then, their *in vivo* evaluation in mice and rat bearing different types of tumors was performed. The tracers were also tested in a sterile inflammation and the one we found more suitable, ^{18}F-FEAnGA, was also tested in a neuroinflammation model.

We were able to conclude that ^{18}F-FEAnGA had better pharmacokinetics than ^{18}F-FEAnGA-Me. ^{18}F-FEAnGA can detect the extracellular β-glucuronidase not only in tumors, but also in inflammatory lesions, suggesting that glucuronide-based prodrug therapy might also be applicable in inflammatory disorders. In the last *in vivo* evaluation in tumor bearing rats, we were able to provide a proof of principle that a single dose of cytostatic drug can increase the release of β-glucuronidase inside the tumor and that ^{18}F-FEAnGA is a suitable PET tracer to monitor this process (figure 1). This study may open the way to a two-step chemotherapy-prodrug approach, in which tumors are treated with a single dose of a cytostatic drug to increase the levels of β-glucuronidase before starting prodrug treatment, in order to increase the prodrug therapy efficacy.

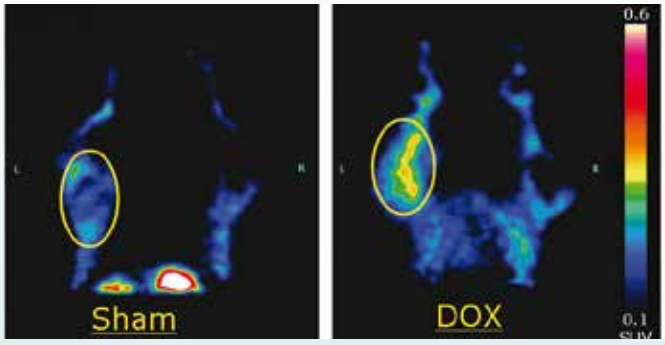

Figure 1. Coronal microPET image of a rat bearing a C6 glioma: treated with doxorubicin (DOX, right side) and a sham rat treated with phosphate buffered saline (PBS, left side).

Brain metastasis in an adolescent with neuroblastoma stage IV

Drs. S.A. van der Haar, Prof.dr. B.L.F. van Eck-Smit

Department of Nuclear Medicine, Academic Medical Centre, University of Amsterdam

Abstract

van der Haar SA, van Eck-Smit FLB. Brain metastasis in an adolescent with neuroblastoma stage IV. We report a case of neuroblastoma with metastases in the brain. Brain metastases occur rarely in patients with neuroblastoma. Additional MIBG SPECT/CT images of the head should be considered if clinical signs exceed the usual symptoms of malaise. Early recognition of neurologic involvement is essential for optimal treatment of these severely ill patients.

Tijdschr Nucl Geneesk 2012; 34(2):918-919

Case report

A 16-year old adolescent was transferred to the Emma Children's Hospital for the evaluation of complaints of painful extremities, night sweating, pruritus and weight loss of ten kilograms in 21 months. Except for an extremely low BMI of 15 and painful extremities, no abnormalities were reported at physical examination. Chest X-ray was normal. Ultrasound of the abdomen showed hepatosplenomegaly and enlarged lymph nodes at the hepatic hilus. From one of the abdominal lymph nodes a biopsy was taken.

As lymphoma was one of the most probable differential diagnoses ^{18}F-FDG PET/CT was performed. This investigation showed ^{18}F-FDG accumulation in enlarged lymph nodes at the hepatic hilus and aortacaval, as well as focal uptake in the bone marrow proximally in the left femur. These findings were in concordance with the suspicion for lymphoma.

Surprisingly, histopathological examination of the abdominal lymph node showed poorly differentiated malignancy with neuro-endocrine signs; despite of the age of the patient suspect of neuroblastoma. This diagnosis was confirmed by the results of bone marrow biopsies, performed as part of the staging workup. Groups of cells, larger than normal lymphocytes and arranged in the characteristic Homer-Wright rosettes were found. ^{123}I-MIBG scintigraphy was performed to confirm the diagnosis of neuroblastoma and for staging purposes. Whole body ^{123}I-MIBG scintigraphy showed intense uptake in the right adrenal region, corresponding with the primary tumor and multiple osteomedullary foci involving the skull, appendicular and axial skeleton. According to the International Neuroblastoma Staging System (1) stage IV neuroblastoma (NB), originating from the right adrenal with diffuse bone (marrow) involvement was concluded. After adequate thyroid protection, radionuclide therapy with 7400 MBq I-131-metaiodobenzylguanidine (^{131}I-MIBG) as induction therapy (2,3) was started. Before and during ^{131}I-MIBG therapy there were severe complaints of nausea and vomiting. These complaints persisted despite optimal anti-emetic medication. Post therapy scintigraphy two days after the infusion of ^{131}I-MIBG showed homogenous uptake of the radiopharmaceutical in the primary tumor and diffuse bone marrow involvement. Furthermore prominent inhomogenous MIBG accumulation in the neurocranium was noted (figure 1).

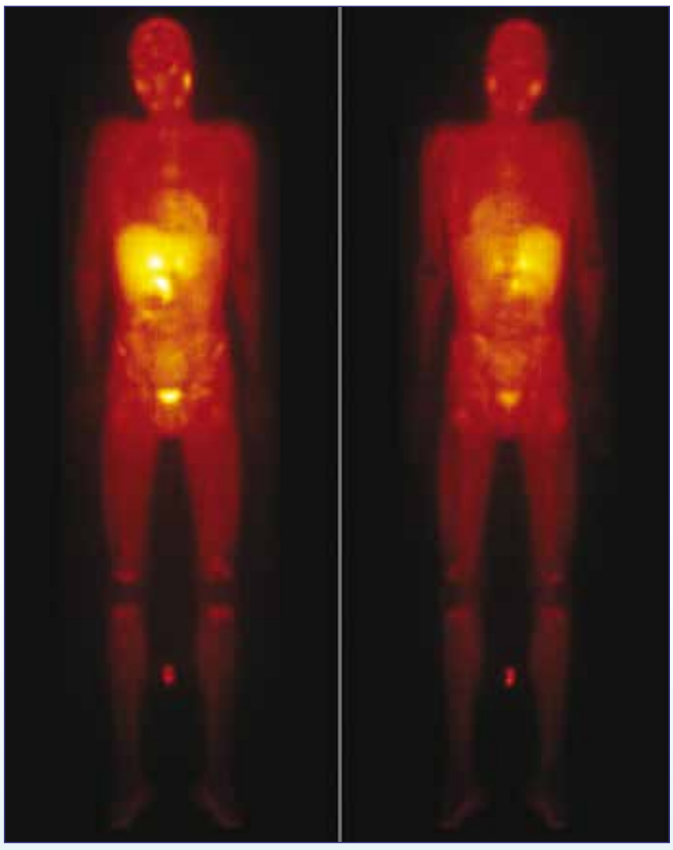

Figure 1. ^{131}I-MIBG whole body scintigraphy two days after therapy in a 16-year old adolescent diagnosed with stadium IV neuroblastoma. Intense ^{131}I- MIBG uptake in the right adrenal region with extensive bone marrow metastasis in the appendicular and axial skeleton. Inhomogeneous ^{131}I-MIBG uptake in the skull/neurocranium.

Because of persistent discomfort, and malaise (pain, vertigo, nausea), a SPECT/CT was not performed the same day. Whole body scintigraphy seven days after the infusion of ^{131}I-MIBG showed unchanged uptake of MIBG in the abdomen and a decrease in activity in the bone marrow. Complementary SPECT/CT images of the brain showed only slightly increased and irregular MIBG uptake in the cerebellum.
On suspicion of pathologic MIBG accumulation in skull and brain and the persistent nausea of the patient a MRI of the brain was performed. MR imaging of the brain confirmed diffuse metastatic involvement of the dura with epidural metastasis of the right cerebellum and invasion in the right cerebellar hemisphere. In retrospect, decreased FDG uptake was already visible in the same region on the ^{18}F-FDG PET/CT images (figure 2).

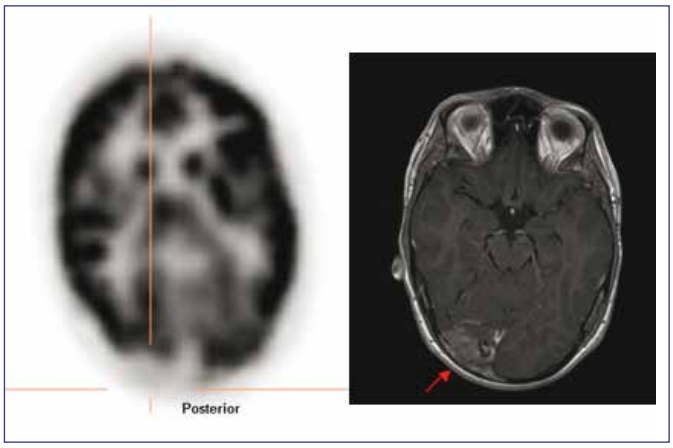

*Figure 2. ^{18}F-FDG PET/CT scan with asymmetric uptake in the brain. Decreased metabolic activity in the right cerebellum. On the left: MRI-brain shows diffuse metastasis of the neurocranium with involvement of the dura with epidural metastasis of the right cerebellum and invasion in the right cerebellar hemisphere (*arrow*).*

Discussion

Neuroblastoma, a malignancy of the autonomic nervous system, is the most common extracranial solid tumour in childhood. The median age at diagnosis is 17 months (4). If the tumour is first detected after the age of one year, metastases are already present in the majority of patients. Previous studies have demonstrated that despite aggressive multimodality therapy chances to reach complete remission are low in older patients with advanced neuroblastoma (5). Neuroblastoma first presenting after the age of ten years is rare. Prognosis for these patients is extremely poor (6).
Moreover, true parenchymal brain metastasis is an uncommon feature of the disease. Paulino et al (7) reported that parenchymal brain metastasis in children with the diagnosis of neuroblastoma (excluding primary braintumors and tumors directly extending from the skull or dura mater) occur in 8% (9/113). Among the European Neuroblastoma Study Group (ENSG) the incidence of hematogenous cranial metastasis was comparable; 5% (44/950) and 4.4% (19/429) according to literature review (8).

Conclusion

Central nervous system metastases rarely occur in patients with neuroblastoma. Realising that brain localisation of neuroblastoma may occur, additional MIBG SPECT/CT images of the head should be considered if clinical signs exceed the usual symptoms of malaise. Early recognition of neurologic involvement is essential for optimal treatment of these severely ill patients.

References

1. Brodeur GM, Pritchard J, Berthold F et al. Revisions of the international criteria for neuroblastoma diagnosis, staging, and response to treatment. J Clin Oncol. 1993;11:1466–77
2. Kraker J, Hoefnagel KA, Verschuur AC et al. Iodine-131-metaiodobenzylguanidine as initial induction therapy in stage 4 neuroblastoma patients over 1 year of age. European Journal of Cancer. 2008; 44:551-6
3. Polishchuk AL, Dubois SG, Haas-Kogan D, Hawkins R, Matthay KK. Response, survival, and toxicity after iodine-131-metaiodobenzylguanidine therapy for neuroblastoma in preadolescents, adolescents, and adults. Cancer. 2011;117:4286-93
4. London WB, Castleberry RP, Matthay KK et al. Evidence for an age cutoff greater than 365 days for neuroblastoma risk group stratification in the Children's Oncology Group. J Clin Oncol. 2005;23:6459-65
5. Maris J, Hogarty M, Bagatell R, Cohn S. Neuroblastoma. Lancet. 2007;369:2106-20
6. Refaat M, Idriss S, Blaszkowsky L. Case report: an unusual case of adrenal neuroblastoma in pregnancy. Oncologist. 2008;13:152-6
7. Paulino AC, Nguyen TX. Brain metastasis in children with sarcoma, neuroblastoma, and Wilms' tumor. International Journal of Radiation Oncology Biology Physics. 2003; 57:177-83
8. Kebudi R, Ayan I, Görgün O et al. Brain metastasis in pediatric extracranial solid tumors: survey and literature review. J Neuro-Oncology 2005;71:43-8

Lung perfusion in a patient with Scimitar syndrome

Drs. R.E.L. Hezemans, Dr. H.J. Verberne, Prof.dr. J. Booij

Department of Nuclear Medicine, Academic Medical Center, University of Amsterdam

Abstract

Hezemans REL, Verberne HJ, Booij J. Lung perfusion in a patient with Scimitar syndrome. We present the case of a 34-year old pregnant female with Scimitar syndrome of the right lung in combination with an anomaly in arterial blood supply of the lower right lung lobe through vessels of the abdominal aorta. This rare congenital syndrome is characterised by an anomalous pulmonary venous drainage of the right or left lung, mostly in the inferior vena cava. Lung hypoplasia with a secondary dextroposition of the heart is commonly associated with this syndrome. In our patient, pulmonary perfusion scintigraphy was performed in order to quantify the contribution of the right lung to the total lung perfusion. Due to the anomalous arterial blood supply the perfusion scintigram showed no visualisation of the right lower lobe. Therefore, when reading lung perfusion images in these patients one should be aware that the contribution of a separate lung to the total lung perfusion may be underestimated.

Tijdschr Nucl Geneesk 2012; 34(2):920-921

Case report

The scimitar syndrome is called after an anomalous vein shaped as a Turkish sword 'scimitar'. It constitutes 0.5 to 1.0 percent of all congenital heart diseases and has an incidence of three per 100,000 life births (1). This congenital syndrome is characterised by a partial or complete anomalous pulmonary venous drainage of the right or left lung, mostly in the inferior vena cava. Lung hypoplasia with a secondary dextroposition of the heart is commonly associated with this syndrome. Symptoms or signs, like tachypnea, recurrent pneumonia or signs of heart failure can start during infancy or beyond, but some patients may be completely asymptomatic (2). Surgery is indicated when systemic shunting is advanced or malformation is associated with congenital heart defects. We present the case of a 34-year old pregnant female with a known history of closure of a patent ductus Botalli in her early childhood, a dextroposition of the heart and a hypoplastic right lung. The patient was referred by her gynaecologist, to evaluate if her cardiologic status required additional perinatal care. Besides recurrent respiratory infections during childhood, there were no other complaints. Recent magnetic resonance imaging (MRI) revealed anomalous drainage of the right upper and mid lobe veins into the inferior vena cava.

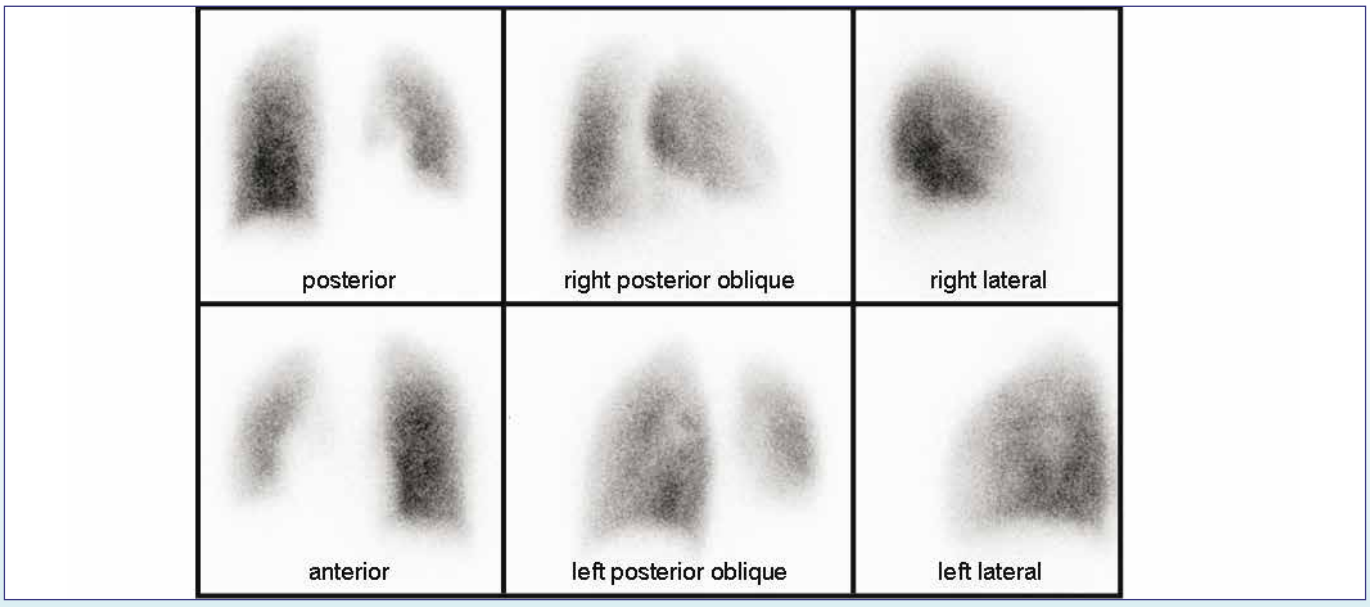

Figure 1. Perfusion scintigraphy with visualisation of the left lung and the hypoplastic upper and lower lobes of the right lung. The right posterior oblique view shows absent perfusion in the right lower lobe. The dextroposition of the heart is seen best on the anterior view.

The left pulmonary veins had a normal course. The arterial blood supply of the right upper lobe consisted of an aberrant vessel from the celiac trunk. Based on the MRI findings the diagnosis Scimitar syndrome was made.
A pulmonary perfusion scintigraphy, with ^{99m}Tc-microspheres (^{99m}Tc-MAA), was performed in order to quantify the contribution of the right lung to the total lung perfusion. ^{99m}Tc-MAA was injected in the cephalic vein. The images (figure 1) showed a homogenous perfusion of both the left lung and hypoplastic right upper and middle lobes. In addition these images gave an indication of cardiomegaly in the right hemi-thorax (dextroposition of the heart). There was no visualisation of the right lower lobe. In addition, the images showed a more intense perfusion of the left lung compared to the right lobes (upper and middle lobes). Semi-quantification of the pulmonary perfusion confirmed the visual interpretation with a contribution of 30 percent of the total lung perfusion for the right lobes (upper and middle lobe) versus 70 percent for the left lung.
As the ^{99m}Tc-MAA was injected in the cephalic vein, the microspheres were trapped in the circulation of the left lung and right upper and lower lobes, before reaching the right lower lobe through the celiac trunk. Therefore the right lobe was not visualised and the total contribution of the right lung to the total lung perfusion could not be calculated. Other injection techniques to overcome this problem were technically not possible. Therefore the contribution of the right lung to the total lung perfusion is probably slightly underestimated.
Anomaly in vascular supply of the lower lobe of the right lung through vessels of the abdominal aorta is seen more often (3). Therefore, when reading lung perfusion images in these patients one should be aware that the contribution of a separate lung to the total lung perfusion may be underestimated.

References

1. Midyat L, Demir E, Memnune A et al. Eponym; Scimitar syndrome. Eur J Pediatr. 2010;169:1171-7
2. Kramer U, Dörnberger V, Fenchel M et al. Scimitar syndrome: morphological diagnosis and assessment of hemodynamic significance by magnetic resonance imaging. Eur Radiol. 2003;13(suppl. 4):L147-50
3. Gupta M, Vaughan DJ, Zimmerman J et al. Partial anomalous pulmonary venous connection. http://emedicine.medscape.com/article/897686-overview

Tijdschrift voor Nucleaire Geneeskunde
ISSN 1381-4842, nr. 2, juni 2012
Uitgever

KLOOSTERHOF
ACQUISITIE SERVICES - UITGEVERIJ

Kloosterhof acquisitie services - uitgeverij
Napoleonsweg 128a
6086 AJ Neer
T 0475 59 71 51
F 0475 59 71 53
E info@kloosterhof.nl
I www.kloosterhof.nl

Hoofdredacteur
prof. dr. J. Booij
j.booij@amc.uva.nl

Redactie
mw. drs. B. Bosveld
mw. drs. F. Celik
dr. J. van Dalen
dr. E.M.W. van de Garde
drs. A.W.J.M. Glaudemans
mw. dr.C.J. Hoekstra
dr. P. Laverman
A. Reniers
dr. H.J. Verberne
dr. O. de Winter

Bureauredactie
Yvonne van Pol-Houben
T 0475 60 09 44
E nucleaire@kloosterhof.nl

Advertentie-exploitatie
Kloosterhof Neer B.V.
acquisitie services – uitgeverij
Eric Vullers
T 0475 597151
E. eric@kloosterhof.nl

Vormgeving
Kloosterhof Vormgeving
Marie-José Verstappen
Sandra Geraedts

Adviesraad
Prof.dr. F.J. Beekman
Prof.dr. O.C. Boerman
Prof.dr. J. Booij
Prof.dr. E.F.I. Comans
Prof.dr. R.A.J.O. Dierckx
Prof.dr. A.A.M.S. van Dongen
Prof.dr. B.L.F. van Eck-Smit
Prof.dr. P.H. Elsinga
Prof.dr.ir. M.de Jong
Prof.dr.I. Goethals
Prof.dr. O.S. Hoekstra
Prof.dr. E.P. Krenning
Prof.dr. A.A. Lammertsma
Prof.dr. L. Mortelmans
Prof.dr. W.J.G. Oyen
Prof.dr. A.M.J. Paans
Prof.dr. P.P. van Rijk
Prof.dr. G.J.J. Teule
Dr. R.A. Valdés Olmos

Abonnementen
Leden en donateurs van de aangesloten beroepsverenigingen ontvangen het Tijdschrift voor Nucleaire Geneeskunde kosteloos. Voor anderen geldt een abonnementsprijs van € 45,00 per jaar; studenten betalen € 29,00 per jaar (incl. BTW en verzendkosten). Opgave en informatie over abonnementen en losse nummers (€ 13,50) bij Kloosterhof acquisitie services - uitgeverij,
telefoon 0475 59 71 51.

Verschijningsdata, jaargang 34
Nummer 2 26 juni 2012
Nummer 3 25 september 2012
Nummer 4 27 december 2012

Verschijningsdata, jaargang 35
Nummer 1 26 maart 2013
Nummer 2 25 juni 2013

Aanleveren kopij, jaargang 34
Nummer 3 1 juli 2012
Nummer 4 1 oktober 2012

Aanleveren kopij, jaargang 35
Nummer 1 1 januari 2013
Nummer 2 1 april 2013

Cursus- en Congresagenda

WMIC 2012
5 - 8 September, 2012. Dublin, Ireland. www.wmicmeeting.org

ASNC 2012
6 - 9 September, 2012. Baltimore, USA. www.asnc.org

EANM Advanced Technologist PET/CT Course
8 - 9 September, 2012. Vienna, Austria. www.eanm.org

Nucleaire Dagen Neurologie
13 - 14 September, 2012. Nieuwegein, The Netherlands. www.nvng.nl

EANM Advanced Dosimetry Course
13 - 14 September, 2012. Vienna, Austria. www.eanm.org

EANM Basic Learning Course on PET/CT in Oncology
20 September, 2012. Vienna, Austria. www.eanm.org

ICIS 2012: International Cancer Imaging Society Meeting and 12th Annual Teaching Course
4 - 6 October, 2012. Oxford, UK. www.eanm.org

4th International Workshop on PET in Lymphoma
4 - 5 October, 2012. Menton, France. www.eanm.org

Symposium 'Radiation dosimetry: balance between patient safety and cure'
5 Oktober, 2012. Leiden, The Netherlands. www.stralingsdosimetrie.nl

EANM'12
27 - 31 October, 2012. Milan, Italy. www.eanm.org

5th Annual Barcelona PET-CT and MRI-PET Practical Course
8 - 9 November, 2012. Barcelona, Spain. www.barcelonapet-ct.com

Nucleaire Dagen Radiofarmacie
15 - 16 November, 2012. Nijmegen, The Netherlands. www.nvng.nl

EANM-ESTRO Educational Seminar on PET in Radiation Oncology
23 - 24 November, 2012. Vienna, Austria. www.eanm.org

ICRT 2012: 7th International Conference on Radiopharmaceutical Therapy
25 - 29 November, 2012. Levi, Finland. www.eanm.org

Joint International Oncology Congress 5th Symposium on Cancer Metastasis and the Lymphovascular System and the 8th International Sentinel Node Society Congress
29 November - 1 December, 2012. Los Angeles, USA. www.sn-cancermets.org

EANM Advanced Learning Course on PET/CT in Oncology
29 November - 1 December, 2012. Vienna, Austria. www.eanm.org

Adreswijzigingen

Regelmatig komt het voor dat wijziging in het bezorgadres voor het Tijdschrift voor Nucleaire Geneeskunde op de verkeerde plaats worden doorgegeven. Adreswijzigingen moeten altijd aan de betreffende verenigingssecretariaten worden doorgegeven. Dus voor de medisch nucleair werkers bij de NVMBR, en voor de leden van de NVNG en het Belgisch Genootschap voor Nucleaire Geneeskunde aan hun respectievelijke secretariaten.
De verenigingssecretariaten zorgen voor het doorgeven van de wijzigingen aan de Tijdschrift adresadministratie.
Alleen adreswijzigingen van betaalde abonnementen moeten met ingang van 1 januari 2011 rechtstreeks aan de abonnementenadministratie van Kloosterhof Neer B.V. worden doorgegeven: Kloosterhof Neer B.V., t.a.v. administratie TvNG, Napoleonsweg 128a | 6086 AJ Neer of per E-mail: nucleaire@kloosterhof.nl

The power of one workstation:
everything at your fingertips.

Process, read and report, all from a single workstation. Consolidating Nuclear Medicine images and data across a wide range of modalities and departments and integrating them within a single IT platform delivering increased convenience. From order entry and process management through reporting and distribution of all Nuclear Medicine results and reports.

Insight. **Delivered.**

Learn about Agfa HealthCare at
www.agfahealthcare.com

AGFA HealthCare

GE Healthcare

Improving Heart Failure Risk Assessment

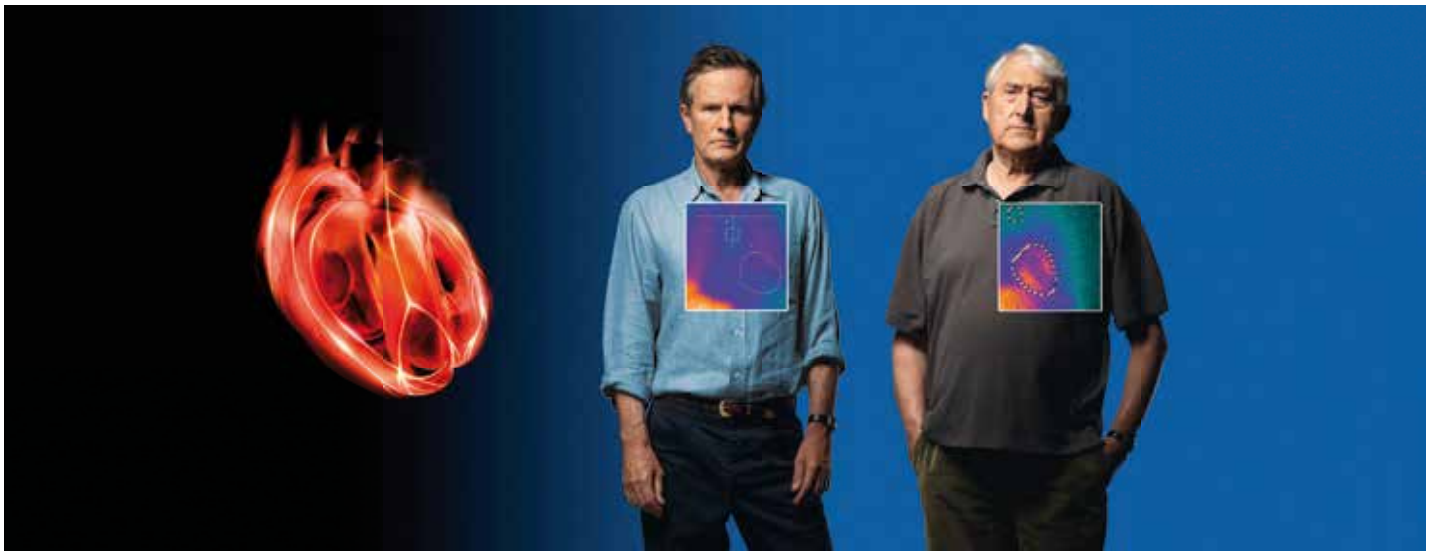

AdreView is a diagnostic agent providing a powerful prognostic insight into heart failure[1]

- Assesses cardiac sympathetic innervation[1]
- Helps predict patients who are at greater or lower risk of heart failure progression, arrhythmias & cardiac death[1]
- Provides a Negative Predictive Value (NPV) of 96% for arrhythmia likelihood & an NPV of 98% for cardiac death likelihood over 2 years[1]
- Provides superior prognostic information in combination with LVEF or BNP compared to LVEF or BNP alone[1]
- Improves heart failure patients' risk assessment and may help clinicians' management decisions[1]

GE imagination at work

AdreView™ Iobenguane I 123 Injection

AdreView is authorised for marketing in the following European countries: Germany, France, Spain, Italy, the United Kingdom, Denmark, Norway, The Netherlands and Belgium.

PRESCRIBING INFORMATION AdreView, Iobenguane (^{123}I) Injection 74 MBq/ml solution for injection
Please refer to full national Summary of Product Characteristics (SPC) before prescribing. Indications and approvals may vary in different countries. Further information available on request.
PRESENTATION Vials containing 74 MBq/ml [^{123}I]Iobenguane at calibration date and hour. Available pack size: 37 to 740 MBq. **DIAGNOSTIC INDICATIONS** • Assessment of sympathetic innervation of the myocardium as a prognostic indicator of risk for progression of symptomatic heart failure, potentially fatal arrhythmic events, or cardiac death in patients with NYHA class II or class III heart failure and LV dysfunction. • Diagnostic scintigraphic localisation of tumours originating in tissue that embryologically stems from the neural crest. These are pheochromocytomas, paragangliomas, chemodectomas and ganglioneuromas. • Detection, staging and follow-up on therapy of neuroblastomas. • Evaluation of the uptake of iobenguane. The sensitivity to diagnostic visualisation is different for the listed pathological entities. The sensitivity is approximately 90% for the detection of pheochromocytoma and neuroblastoma, 70% in case of carcinoid and only 35% in case of medullary thyroid carcinoma (MTC). • Functional studies of the adrenal medulla (hyperplasia). **DOSAGE AND METHOD OF ADMINISTRATION** Cardiology: For adults the recommended dosage is 370MBq. Children under 6 months: 4 MBq per kg body weight (max. 40 MBq), the product must not be given to premature babies or neonates. Children between 6 months and 2 years: 4 MBq per kg body weight (min. 40 MBq). Children over 2 years: a fraction of the adult dosage should be chosen, dependent on body weight (see SPC for scheme). No special dosage scheme required for elderly patients. Oncology: For adults the recommended dosage is 80-200 MBq, higher activities may be justifiable. For children see cardiology. No special dosage scheme required for elderly patients. Administer dose by slow intravenous injection or infusion over several minutes. **CONTRAINDICATIONS** Hypersensitivity to the active substance or to any of the excipients. The product contains benzyl alcohol 10.4 mg/ml and must not be given to premature babies or neonates **WARNINGS AND PRECAUTIONS** Drugs known or expected to reduce the iobenguane(123-I) uptake should be stopped before administration of AdreView (usually 4 biological half-lives). At least 1 hour before the AdreView dose administer a thyroid blockading agent (Potassium Iodide Oral Solution or Lugol's Solution equivalent to 100 mg iodine or potassium perchlorate 400 mg). Ensure emergency cardiac and anti-hypertensive treatments are readily available. In theory, iobenguane uptake in the chromaffin granules may induce a hypertensive crisis due to noradrenaline secretion; the likelihood of such an occurrence is believed to be extremely low. Consider assessing pulse and blood pressure before and shortly after AdreView administration and initiate appropriate anti-hypertensive treatment if needed. This medicinal product contains benzyl alcohol. Benzyl alcohol may cause toxic reactions and anaphylactoid reactions in infants and children up to 3 years old. **INTERACTIONS** Nifedipine (a Ca-channel blocker) is reported to prolong retention of iobenguane. Decreased uptake was observed under therapeutic regimens involving the administration of antihypertensives that deplete norepinephrine stores or reuptake (reserpine, labetalol), calcium-channel blockers (diltiazem, nifedipine, verapamil), tricyclic antidepressives that inhibit norepinephrine transporter function (amitryptiline and derivatives, imipramine and derivatives), sympathomimetic agents (present in nasal decongestants, such as phenylephrine, ephedrine, pseudoephedrine or phenylpropanolamine), cocaine and phenothiazine. These drugs should be stopped before administration of [123I]iobenguane (usually for four biological half-lives to allow complete washout). **PREGNANCY AND LACTATION** Only imperative investigation should be carried out during pregnancy when likely benefit exceeds the risk to mother and foetus. Radionuclide procedures carried out on pregnant women also involve radiation doses to the foetus. Any woman who has missed a period should be assumed to be pregnant until proven otherwise. If uncertain, radiation exposure should be kept to the minimum needed for clinical information. Consider alternative techniques. If administration to a breast feeding woman is necessary, breast-feeding should be interrupted for three days and the expressed feeds discarded. Breast-feeding can be restarted when the level in the milk will not result in a radiation dose to a child greater than 1 mSv. **UNDESIRABLE EFFECTS** In rare cases the following undesirable effects have occurred: blushes, urticaria, nausea, cold chills and other symptoms of anaphylactoid reactions. When the drug is administered too fast palpitations, dyspnoea, heat sensations, transient hypertension and abdominal cramps may occur during or immediately after administration. Within one hour these symptoms disappear. Exposure to ionising radiation is linked with cancer induction and a potential for development of hereditary defects. For diagnostic nuclear medicine investigations the current evidence suggests that these adverse effects will occur with low frequency because of the low radiation doses incurred. **DOSIMETRY** The effective dose equivalent resulting from an administered activity amount of 200 MBq is 2.6 mSv in adults. The effective dose equivalent resulting from an administered activity amount of 370 MBq is 4.8 mSv in adults. **OVERDOSE** The effect of an overdose of iobenguane is due to the release of adrenaline. This effect is of short duration and requires supportive measures aimed at lowering the blood pressure. Prompt injection of phentolamine followed by propanolol is needed. Maintain a high urine flow to reduce the influence of radiation. **CLASSIFICATION FOR SUPPLY** Subject to medical prescription (POM).**MARKETING AUTHORISATION HOLDERS.** DE: GE Healthcare Buchler GmbH & Co. KG, 18974.00.00. DK: GE Healtcare B.V., DK R. 1013. FR: GE Healthcare SA, NL 18599. NL: GE Healthcare B.V., RVG 57689. NO: GE Healthcare B.V., MTnr. 94-191. **DATE OF REVISION OF TEXT** 9 August 2010 .

GE Healthcare Limited, Amersham Place, Little Chalfont, Buckinghamshire, England HP7 9NA
www.gehealthcare.com

References: 1. Jacobson AF *et al.* Myocardial Iodine-123 *Meta*-Iodobenzylguanidine Imaging and Cardiac Events in Heart Failure. Results of the Prospective ADMIRE-HF (AdreView Myocardial Imaging for Risk Evaluation in Heart Failure) Study. J Am Coll Cardiol 2010;55.

10-2010 JB4260/OS INT'L ENGLISH